Mitigating PAPR in Cooperative Wireless Networks with Frequency Selective Channels and Relay Selection

by

Masoud M. Eddaghel

A thesis submitted in partial fulfilment of the requirements for the award of the degree of Doctor of Philosophy (PhD)

April 2014

Advanced Signal Processing Group,
School of Electronic, Electrical and System Engineering,
Loughborough University, Loughborough,
Leicestershire, UK, LE11 3TU

I dedicate this thesis to the souls of my parents, my wife, my loving children and my sisters and brothers.

Abstract

The focus of this thesis is peak-to-average power ratio (PAPR) reduction in cooperative wireless networks which exploit orthogonal frequency division multiplexing in transmission. To reduce the PAPR clipping is employed at the source node. The first contribution focuses upon an amplify-and-forward (AF) type network with four relay nodes which exploits distributed closed loop extended orthogonal space frequency block coding to improve end-to-end performance. Oversampling and filtering are used at the source node to reduce out-of-band interference and the iterative amplitude reconstruction decoding technique is used at the destination node to mitigate in-band distortion which is introduced by the clipping process. In addition, by exploiting quantized group feedback and phase rotation at two of the relay nodes, the system achieves full cooperative diversity in addition to array gain.

The second contribution area is outage probability analysis in the context of multi-relay selection in a cooperative AF network with frequency selective fading channels. The gains of time domain multi-path fading channels with L paths are modeled with an Erlang distribution. General closed form expressions for the lower and upper bounds of outage probability are derived for arbitrary channel length L as a function of end-to-end signal to noise ratio. This analysis is then extended for the case when single relay selection from an arbitrary number of relay

nodes M is performed. The spatial and temporal cooperative diversity gain is then analysed. In addition, exact form of outage probability for multi-path channel length $L = 2$ and selecting the best single relay from an arbitrary number of relay nodes M is obtained. Moreover, selecting a pair of relays when $L = 2$ or 3 is additionally analysed.

Finally, the third contribution context is outage probability analysis of a cooperative AF network with single and two relay pair selection from M available relay nodes together with clipping at the source node, which is explicitly modelled. MATLAB and Maple software based simulations are employed throughout the thesis to support the analytical results and assess the performance of algorithms and methods.

Contents

Statement of Originality

The contributions of this thesis are mainly related to peak-to-average power ratio (PAPR) reduction techniques within cooperative relaying networks exploiting orthogonal frequency division multiplexing (OFDM) based transmission and outage probability analysis of two-hop multi-path networks in the context of multi-relay selection scheme. The novelty of the contributions is supported by the following international journals and conference papers.

In Chapter 4, PAPR reduction after clipping at the source node in a distributed decode-and-forward and amplify-and-forward type cooperative schemes using extended orthogonal space frequency block coding (EO-SFBC) transmission with an iterative amplitude reconstruction (IAR) decoding technique is considered. The related works are:

1. **M. Eddaghel** and J. Chambers, "Comparison of distributed space frequency block coding schemes in broadband multi-node cooperative relay networks with PAPR reduction", in Proc. IEEE DSP, Corfu, Greece, July. 2011.

2. **M. Eddaghel** and J. Chambers, "PAPR reduction in distributed closed loop extended orthogonal space frequency block coding with quantized two-bit group feedback for broadband multi-node cooperative communications", in Proc. IEEE IWCMC, Istanbul,

Turkey, July. 2011.

3. **M. Eddaghel** and J. Chambers, "PAPR Reduction in Distributed Amplify-and-Forward Type Closed Loop Extended Orthogonal Space Frequency Block Coding with One-bit Group Feedback for Cooperative Communications", in Proc. IEEE EW, Poznan, Poland, April. 2012.

The contribution of Chapter 5 is end-to-end performance analysis of a cooperative communication system transmitted over multi-path channels with best single, best two relay pair selection and AF two-hop relaying. These works have been presented in:

4. **M. Eddaghel**, U. N. Mannai, G. J. Chen, J. A. Chambers, "Outage probability analysis of an amplify-and-forward cooperative communication system with multi-path channels and max-min relay selection," Communications, IET, vol.7, no.5, pp. 408-416, 2013.

5. U.N. Mannai, **M. Eddaghel**, F.A.M. Bribesh and J.A. Chambers, "Outage Probability Analysis of a Multi-Path Cooperative Communication Scheme Based on Single Relay Selection and Amplify-and-Forward Relaying", in Proc. IEEE SoftCOM, Split, Croatia, Sep. 2012.

6. **M. Eddaghel**, U. N. Mannai and J. A. Chambers, "Outage Probability Analysis of a Multi-Path Cooperative Communication Scheme Based on Single Relay Selection", in Proc. IEEE MIC CSC, Istanbul, Turkey, Oct. 2012.

The contribution of Chapter 6 is a theoretical analysis of the outage probability of a clipped OFDM signal transmitted over a multi-path

fading channel of length L and an arbitrary number of relay nodes M with best single and best two relay selection. In both cases, the clipping process is modeled as an aggregate of an attenuated signal component and clipping noise. The novelty of the work is supported by the following publication:

7. **M. Eddaghel**, U. Mannai, and J. Chambers, "Outage probability analysis of an AF Cooperative Multi-Relay Network with Best Relay Selection and Clipped OFDM Transmission", in the tenth International Symposium on Wireless Communication Systems (ISWCS), Ilmenau, Germany, August 2013.

Acknowledgements

I would like to express my gratitude to my supervisor Professor Jonathon A. Chambers for his kind interest, generous support and constant advice during my PhD study. I have benefited tremendously from his rare insight, his ample intuition and his exceptional knowledge. Therefore, I wish that I will have more opportunities to cooperate with him in the future.

I am also grateful to all my friends in the Advanced Signal Processing Group for providing a stable and cooperative environment within the Advanced Signal Processing Group. Also I would like to express appreciation for all the administrative assistance given to me throughout my study at Loughborough University by administrative staff.

Finally, I would like to remember my parents for their support in all stages of my study. I also can not forget when they encouraged me to travel and read for my PhD; therefore, I am happy to achieve what they wished for and also I pray they receive mercy from Allah (God). Also I would like to express my sincere heartfelt thanks, appreciations and gratefulness to all my family members, especially my wife and my children. I would like to dedicate this thesis to my parents.

Masoud Eddaghel

April, 2014

List of Acronyms

3G	Third Generation
3GPP	3rd Generation Partnership Project
4G	Fourth Generation
ADC	Analog-to-Digital Converter
AF	Amplify-and-Forward
AWGN	Additive White Gaussian Noise
BER	Bit Error Rate
BPSK	Binary Phase Shift Keying
CDF	Cumulative Distribution Function
CDMA	Code Division Multiple Access
CP	Cyclic Prefix
CSI	Channel State Information
DAC	Digital-to-Analog Converter
DF	Decode-and-Forward
DFT	Discrete Fourier Transform

DSTBC	Distributed Space-Time Block Coding
EO-SFBC	Extended Orthogonal Space-Frequency Block Coding
EO-STBC	Extended Orthogonal Space-Time Block Coding
FDMA	Frequency Division Multiple Access
FEC	Forward Error Correction
FFT	Fast Fourier Transform
i.i.d.	independent identically distributed
IAR	Iterative Amplitude Reconstruction
ICI	Inter-Carrier-Interference
IDFT	Inverse Discrete Fourier Transform
IFFT	Inverse Fast Fourier Transform
MAP	Maximum A-Posteriori decoder
MIMO	Multiple-Input Multiple-Output
MISO	Multi-Input Single-Output
ML	Maximum Likelihood
MMSE	Minimum Mean Square Error
MRRC	Maximal-Ratio Receiver Combining
OFDM	Orthogonal Frequency Division Multiplexing
OOB	Out-of-Band Interference
PAPR	Peak-to-Average Power Ratio

PDF	Probability Density Function
QAM	Quadrature Amplitude Modulation
QPSK	Quadrature Phase Shift Keying
RF	Radio Frequency
SFBCs	Space-frequency Block Codes
SIMO	Single-Input Multiple-Output
SISO	Single-Input Single-Output
SNR	Signal-to-Noise Ratio
STBCs	Space-Time Block Codes
STC	Space-Time Coding
TDMA	Time Division Multiple Access
WiFi	Wireless Fidelity
WiMax	Worldwide Inter-operability for Microwave Access

List of Symbols

Scalar variables are denoted by plain lower-case letters, (e.g., x), vectors by bold-face lower-case letters, (e.g., $\mathbf{x}$), and matrices by upper-case bold-face letters, (e.g., $\mathbf{X}$). Some frequently used notations are as follows:

M_t	Number of transmit antennas
M_r	Number of receiver antennas
T_s	Symbol duration
S	Code matrix of STBC
t	time symbol periods
$(.)^H$	Hermitian conjugate operator
$(.)^*$	Conjugate operator
$(.)^T$	Transpose operator
$\|.\|$	Absolute value of a complex number
α	Conventional channel gain
β	Channel dependent interference
$\Re(.)$	Real part of a complex number

N_s	Number of information symbols and
$E\{.\}$	Statistical expectation
$\|.\|$	Euclidean norm
$arg\ \ a_1...a_n$	Argument of $a_1...a_n$
$f_\gamma(\gamma)$	Probability density function
$F_\gamma(\gamma)$	Cumulative distribution function
$\oplus$	The modulo two addition
$angle(.)$	Phase angle
m	Relay number
M	Total number of available relays
$DFT(.)$	Discrete Fourier Transform operator
$FFT(.)$	Fast Fourier Transform operator
$IFFT(.)$	Inverse Fast Fourier Transform operator
$IDFT(.)$	Inverse Discrete Fourier Transform operator
$\circ$	The Hadamard product
$CN(0, N_0)$	Circularly symmetric complex Gaussian distribution with zero mean and N_0 is noise variance
E_s	Average energy per symbol
$max(.)$	Maximum value
$min(.)$	Minimum value

$argmax$	The argument which maximizes the expression
$argmin$	The argument which minimizes the expression
$\Gamma(.)$	Gamma function
$\Gamma(.,.)$	Incomplete Gamma function
$K(0,.)$	Modified Bessel function of the first order
$K(1,.)$	Modified Bessel function of the second order
$C_A(.)$	The clipping operation
μ	The clipping ratio
J	Oversampling factor
N	Number of subcarrier in OFDM frame
L	Number of multi-paths
λ	Diagonal matrix

List of Figures

List of Tables

Chapter 1

INTRODUCTION

Demand for improving the performance of wireless communications has been rapidly increasing worldwide. In particular, there is a need for higher data rate (capacity), larger coverage area and increased quality of service (reliability). At the physical layer it may not be possible to achieve these targets simply by increasing the power or the bandwidth (BW) due to constraints on operators [4] and [5]. To improve performance orthogonal frequency division multiplexing (OFDM) has drawn significant interest in broadband wireless communications, due primarily to its high bandwidth efficiency and robustness to multipath fading channels. Nonetheless, this technology has shortcomings. High peak-to-average power ratio (PAPR) is an inherent drawback of OFDM systems and mitigating this in cooperative wireless systems is the major focus of this thesis.

1.1 OFDM System

In recent years orthogonal frequency division multiplexing (OFDM) has emerged as a successful air-interface technique. In the context of wired environments, OFDM techniques are also known as discrete multi-tone (DMT) [6] transmissions and are employed in the American national standards institute's (ANSI's) asymmetric digital sub-

scriber line (ADSL) [7] technology. In wireless scenarios, OFDM has been advocated by many European standards, such as digital audio broadcasting (DAB), digital video broadcasting for terrestrial television (DVB-T) [8], digital video broadcasting for handheld terminals (DVB-H), wireless local area networks (WLANs) and broadband radio access networks (BRANs). Furthermore, OFDM has been ratified as a standard or has been considered as a candidate standard by a number of standardization groups of the institute of electrical and electronics engineers (IEEE), such as the 802.11 system wireless fidelity (WiFi) system standard, and the 802.16 WiMAX standard families [9]. Also, it is adopted for fourth generation (4G) mobile wireless systems and 3GPP long-term evolution (LTE) and LTE-advanced.

OFDM has some key advantages over other widely used wireless access techniques, such as time-division multiple access (TDMA), frequency division multiple access (FDMA) and code-division multiple access (CDMA) [9]. The main merit of OFDM is the fact that the radio channel is divided into many narrowband, low-rate, frequency-non-selective subchannels or subcarriers, so that multiple symbols can be transmitted in parallel, while maintaining a high spectral efficiency due to the subchannels being at the minimum possible separation to avoid co-channel interference.

However, besides its significant advantages, OFDM also has a few disadvantages. One problem is the associated increased PAPR in comparison with single-carrier systems, requiring a large linear range for the OFDM transmitter's output amplifier. In addition, OFDM is sensitive to carrier frequency offset, and synchronization in general, which may result in inter-carrier-interference (ICI) [8], but this is not a focus

of this thesis.

Combining OFDM with a MIMO system can simultaneously improve the system performance. Therefore, a MIMO system will be presented in the next subsection.

1.2 MIMO System

According to the number of transmit antennas M_t and the number of receive antennas M_r, wireless systems can be classified as single-input single-output (SISO), single-input multiple-output (SIMO), multiple-input single-output (MISO) and multiple-input multiple-output (MIMO) systems as in Fig. 1.1. MIMO technology theoretically offers several benefits which help to achieve such significant performance gains without additional bandwidth or transmit power. In particular, some significant advantages will be presented, such as array gain, temporal and spatial diversity gain and spatial multiplexing gain. These gains are described in brief, see [10] and [11] for more details, as:

- **Array gain** is significantly improving the average SNR at the receiver; which can be achieved by using multiple-antennas at the transmitter and/or receiver, as well as a correlative combination technique. Array gain improves resistance to noise, thereby improving the coverage and the range of a wireless network.

- **Diversity gain** mitigates fading, which wireless transmission commonly suffers from, by providing additional independent copies of the same information via independent shadowing and fading channels. With an increasing number of independent copies, the probability that at least one of the copies is not experiencing

a deep fade increases, thereby improving the quality and reliability of reception. The diversity order is equal to the product of the number of antennas at the source and destination nodes $D_g = M_t \times M_r$, if the channel between each transmit-receive antenna pair fades independently from the others.

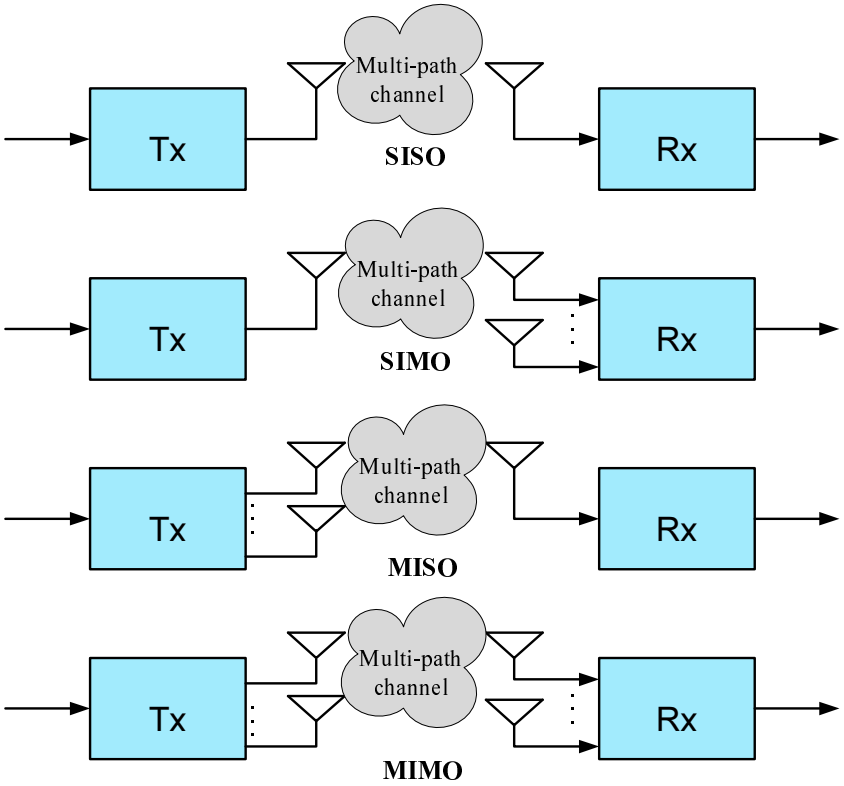

Figure 1.1. Illustration of transmitters (Tx) and receivers (Rx) with different antenna configurations.

- **Spatial multiplexing gain** is an increase in data rate, which means the capacity of a MIMO wireless network can linearly increase with the maximum spatial multiplexing order $min(M_t, M_r)$.

In general, it may not be possible to exploit simultaneously all the benefits of a MIMO system due to conflicting demands on the spa-

tial degrees of freedom (i.e. there are diversity and multiplexing gain trade-offs). However, using some combination of the benefits across a wireless network will result in improved capacity, coverage and reliability. Nonetheless, the requirement of multiple-antenna terminals increases the system complexity and the separation between the antennas increases the terminal size. Also, MIMO systems suffer from the effect of path loss and shadowing, where the path loss is referred to as the signal attenuation between the source and destination nodes due to propagation distance; while shadowing is signal fading due to objects obstructing the propagation path between the source and destination nodes [12]. In addition, estimating the MIMO channel for a high number of transmit and receive antennas becomes extremely challenging [9].

1.3 Cooperative MIMO-OFDM System

To avoid some of the drawbacks and gain the same benefits of MIMO systems, a cooperative relay system has been used. Cooperative techniques in wireless networks are used to form virtual MIMO systems from separated single antenna terminals [13]. One of the main advantages of cooperative communications is the ability to achieve spatial diversity gains without employing multiple antennas on each terminal [14]. In this system, the transmission reliability can be achieved by a cooperative diversity gain, which is an effective gain to combat the detrimental effects of severe fading in the wireless channel [15]. As in Figure 1.2 the copies of the same information can be forwarded to the destination node by intermediate relays $R_m, m = 1, 2, 3, 4$ between the source node S and destination node D with independent channels, because of diversity gain. Therefore, diversity gain can be obtained due to the number

of independent channels in the cooperative relay network, which depends on the number of the relay nodes and the environment [16].

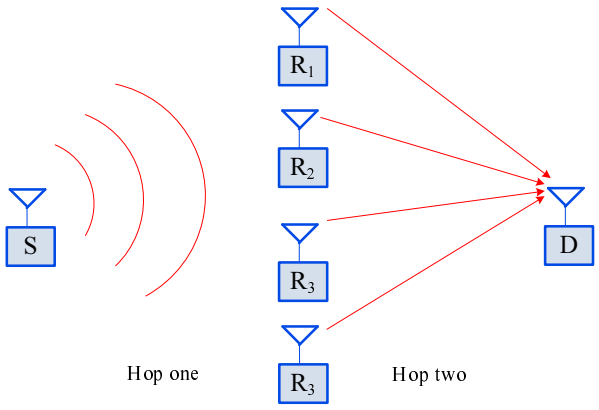

Figure 1.2. The cooperative MIMO-OFDM system with one source node, four relay nodes and destination node.

In the next subsection, another important issue in an OFDM system will be considered, which is PAPR reduction.

1.3.1 PAPR reduction in a cooperative MIMO-OFDM system

In multinode cooperative communications based on MIMO-OFDM system techniques PAPR becomes even more important since there are multiple transmit antennas each of which would require its own radio frequency (RF) power amplifier and digital-to-analog converter (DAC). As a result of the PAPR drawback, the system requires more bits to cover a potentially broad dynamic range as well a large linear range for the RF power amplifier which can be expensive. However, in exploiting a commercial DAC and RF power amplifier may lead to unwanted out-of-band interference and in-band distortion as a consequence of intermodulation effects induced by a nonlinear power amplifier. There-

fore, the PAPR reduction issue becomes an important research topic in these systems.

This thesis concentrates upon the straightforward approach for reducing OFDM peaks in such systems, which is clipping. This is a simple PAPR reduction method which can be easily implemented, although it introduces several undesired effects such as introducing out-of-band interference. Fortunately, it is possible to perform clipping before the RF power amplifier, most desirably in the digital domain. The advantage of this method is that distortion may be controlled by applying advanced digital signal processing (DSP). By considering the time domain samples output from the inverse fast Fourier transform (IFFT), the discrete-time PAPR is defined as the peak power within one IFFT block (one OFDM symbol) normalized by the average signal power [17] and [18]

$$PAPR(x[n]) = \frac{\max\limits_{0 \leq n \leq N-1} |x[n]|^2}{E\{|x[n]|^2\}}, \tag{1.3.1}$$

where $x[n], n = 0, 1, ..., N-1$ are the time samples of an OFDM symbol and $max\{\cdot\}$ and $E\{\cdot\}$ denote respectively the maximum value and statistical expectation operation.

The RF power amplifier and digital-to-analog converters within wireless communication systems are power limited and only perform effectively when signals passed through them are within the dynamic range which is linear. To accommodate high PAPR signals, these devices must have a large dynamic linearity which can result in the need for expensive devices and high power consumption which means low

efficiency. Otherwise, they are then forced to operate in a nonlinear region creating in-band distortion which induces increasing BER within the in-band transmission and out-of-band noise which causes adjacent channel interference. To avoid the non-linearity effect, the input signal has to be backed-off to the linear region of the RF power amplifier. Figure 1.3 shows a typical input-output power response for an RF power amplifier, with the associated input and output back-off regions which are shorted to input back-off (IBO) and out-back-off (OBO), respectively.

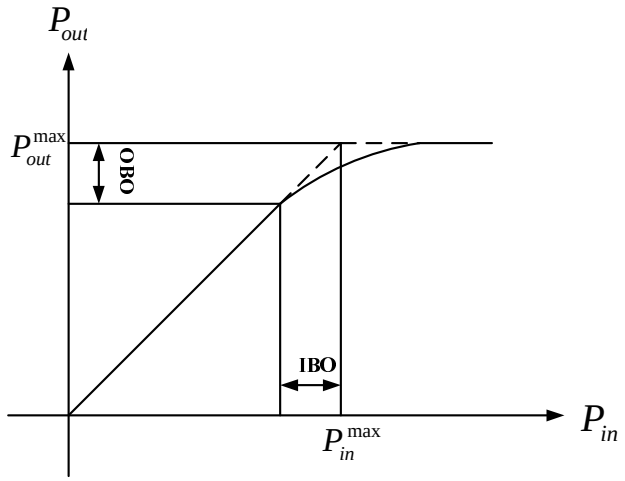

Figure 1.3. A typical input-output power response for an RF power amplifier.

In the next subsection, another important method will be presented to improve performance and reduce system complexity, which is relay selection scheme.

1.4 Relay Selection and Performance Analysis of a Cooperative Multinode Network

Cooperative diversity has been recently proposed as a way to form virtual antenna arrays that provide large spatial diversity gain in fading wireless environments. However, in cooperative wireless networks, the relay nodes have different locations so each transmitted signal from the source node to the destination node must pass through different paths causing different attenuations within the signals received at the destination which results in reducing the overall system performance. Therefore, to avoid or minimize this effect, a relay selection scheme is used to select the highest quality paths. In other words, the main objective of the relay selection scheme is to achieve higher bandwidth efficiency while guaranteeing the same diversity order as in a conventional cooperative scheme.

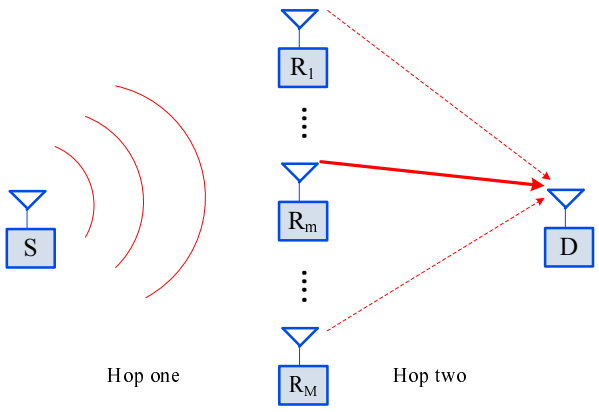

Figure 1.4. The cooperative MIMO-OFDM system with the best relay selection scheme.

The space frequency block coding technique is exploited in order to benefit from the advantages of a cooperative MIMO-OFDM system.

Space frequency block coding (SFBC) is applied within each OFDM block to exploit the spatial and frequency diversities. Also it is a synonymous term often used in place of multipath diversity or temporal diversity gain [19]. As in [20], [21] and [22], the performance criteria for a SFB coded MIMO-OFDM system and the maximum achievable cooperative (temporal and spatial) diversity gain is equivalent to $L \times M_s \times M_r \times M_d$, where M_s, M_r and M_d are the number of single antenna sources, relay nodes and destination node, respectively, and L is the number of delay paths in frequency selective fading channels [22]. The maximum achievable temporal diversity is given by $Dg = min(N, L)$, however, the length of the OFDM frame is always greater than the channel length ($N > L$). Therefore, the maximum temporal diversity order is equal to L, which is the total number of independent fading paths from the source to relay nodes or from the relays to the destination node [14].

Performance analysis assessment, cooperative multirelay wireless networks suffer from the effects of path loss and shadowing, which have important implications on the system performance. In wireless systems there is typically a target minimum received power level, below which performance becomes unacceptable (e.g. the voice quality in a cellular system is too poor to understand). Therefore, there are two performance evaluation criteria for wireless communication systems at the physical layer; firstly, the probability of error, which is defined relative to either symbol or bit errors, secondly, the outage probability, which is defined as the probability that the instantaneous SNR falls below a given threshold

$$P_{out} = \int_0^{\gamma} f_{\gamma}(\gamma) d\gamma = F_{\gamma}(\gamma), \tag{1.4.1}$$

where $f_{\gamma}(\gamma)$ is the probability density function (PDF) and $F_{\gamma}(\gamma)$ is the cumulative distribution function (CDF) of the SNR.

1.5 Motivations

The work presented in this thesis has been motivated by the contributions of [3] and [5] on distributed SFBCs as applied to cooperative MIMO-OFDM systems considering PAPR reduction and iterative amplitude reconstruction (IAR) decoding techniques; [23], [24] and [25] cooperative multi-node network schemes. Therefore, on the basis of this foundation work the aims of this thesis are listed in the next subsection.

1.5.1 Aims

The aims of this thesis are to:

- Consider PAPR reduction by clipping at the source node for cooperative MIMO-OFDM system by implementing conventional open-loop space frequency block coding (SFBC) and closed-loop EO-SFBC at the relay nodes which allow two and four relays to communicate cooperatively with a common destination over frequency selective fading channels. An iterative amplitude reconstruction (IAR) decoding technique is used to recover the distortion which is introduced by the clipping process at the source node.

- Model multi-path fading channels in an amplify-and-forward cooperative MIMO-OFDM type transmission.
- Propose the use of relay selection techniques to improve cooperative communication over frequency-selective channels.
- Evaluate the improvement of the network performance over frequency selective fading channels with relay selection through outage probability analysis.
- Evaluate the effect of the clipping process at the source node on the network performance over frequency selective fading channels with relay selection through outage probability analysis.

1.5.2 Objectives

At the end of the study the objectives are to have

- Demonstrated that the PAPR reduction by clipping at the source node and IAR decoding for cooperative relay systems can improve the system performance and provide cooperative diversity gain.
- Performed different types of outage probability analyses for cooperative relaying communication system transmitting over frequency selective fading channels.
- Published the research findings in international conferences and journals.

In the next subsection, the structure of the thesis will be presented.

1.6 Structure of the Thesis

To simplify the understanding of this thesis and its contributions, its structure is summarized as follows:

In Chapter 1, a general introduction to wireless communication systems including the basic concepts of MIMO and OFDM systems is provided. Furthermore, short description of the PAPR problem in a virtual MIMO-OFDM system was given. In addition, a relay selection technique is also presented.

In Chapter 2, a brief overview of a MIMO-OFDM system is provided. Then details of SISO-OFDM based transmission including transmission and receiver stages such as a convolutional encoder, interleaving, an appropriate modulation technique and a Viterbi decoder scheme are given. Then, a description of conventional MIMO and cooperative MIMO systems are presented. In addition, SFBC is used to exploit the benefit of the combination of SISO-OFDM with a MIMO system virtually. Finally, simulations and a summary are given.

In Chapter 3, an introduction and a brief overview of PAPR mitigation methods including definition and statistical properties of PAPR techniques are presented. Then, a simple approach to limit the amplitude peaks in an OFDM waveform is described. In addition to this, oversampling and filtering after clipping are studied to reduce the harmful effects induced by the clipping process. Finally, simulations and a summary are given.

In Chapter 4, a brief introduction of PAPR reduction by clipping the OFDM signal at the source node of a distributed cooperative virtual MIMO-OFDM wireless network is described. Then, the system model of distributed open loop EO-SFBC at the relaying nodes includ-

ing broadcasting and relaying phases, together with the IAR decoding technique are presented. In addition, feedback techniques which are needed to achieve full spatial diversity and array gains, such as two and one-bit feedback schemes and the proposed group feedback, are explained. Finally, simulations are presented.

In Chapter 5, end-to-end performance analysis of cooperative amplify and forward network over frequency selective fading channels with a multi-relay selection scheme is provided. Then, outage probability analysis of selecting the best single and pair of relays from M available relays over limited number of multipath channel length $L = 2$ and $L = 3$ are studied. Moreover, the spatial and temporal cooperative diversity order of the network is considered. Further analysis of exact outage probability analysis for specific channel length $L = 2$ is considered. In addition, general closed formulas of single relay selection scheme of upper and lower bonds SNRs for an arbitrary channel length L and also an arbitrary number M of relay nodes is obtained. Finally, simulation results and a summary are provided.

In Chapter 6, PAPR reduction by clipping the OFDM signal at the source node of a cooperative amplify and forward network over frequency selective fading channels in multi-relay selection scheme is provided. Then, outage probability analysis based on CDF of the upper bound SNR with various clipping ratios (μ) is studied. Also, the outage probability analysis of selecting one relay and selecting the best two relay pairs from M Relays are explained. Then, simulations are represented and conclusions are drawn.

In Chapter 7, this thesis is concluded by summarizing its contributions and also suggesting some future possible research directions.

Chapter 2

BASIC SYSTEM AND RELATED LITERATURE REVIEW

2.1 An Overview

In wired communications channels, a physical connection, such as a copper wire or fiber-optic cable, guides the signal from the transmitter to the receiver, and generally has well defined effect on system performance. However, in point-to-point wireless communication systems, the transmission over wireless channels is generally subject to many more errors, for example due to severe multi-path fading channels which thereby results in more severe effect on the quality and reliability of wireless communication. This means the transmitted signal, from a potentially moving device, reaches the receiver node via a possibly infinite number of time varying wave propagation paths, due to reflections and refraction on different structures in the environment. To reduce the effects of such a multi-path fading channel, orthogonal frequency division multiplexing (OFDM) is used. OFDM is a digital multicarrier transmission technique that distributes the digi-

tally encoded symbols over N subcarrier frequencies in order to reduce the symbol clock rate to achieve robustness against long echoes in a multi-path fading channel [26], [13] and [27]. By introducing a cyclic prefix (CP) with length exceeding the maximum excess delay of the multi-path propagation channel, inter-symbol-interference (ISI) can be avoided. Moreover, the frequency selective fading channel may severely attenuate the data symbols transmitted on one or several subcarriers, which leads to bit errors [28]. Therefore, it may be essential to employ forward error correction (FEC) codes, in order to deal with the burst symbol errors due to deep fading. However, FEC coding leads to reduction in the overall data rate. Practical OFDM systems are coded with popular FEC codes such as the Reed-Solomon (RS) code, convolutional code, trellis-coded modulation (TCM), concatenated code, turbo code, and LDPC code [29]. The FEC codes can achieve error corrections only as far as the errors are within their error-correcting capability. Also in practice, interleaving is often employed to convert the burst errors into random errors [11].

High reliability wireless communication systems can be achieved by exploiting a multiple-input, multiple-output (MIMO) technique, which is capable of employing both transmitter and receiver diversity, thereby maintaining reliable communications in a multi-path environment. A MIMO system can potentially be combined with an OFDM system in order to combine the advantages of both systems. Furthermore, to reduce the complexity of a MIMO-OFDM system cooperative communication can be exploited and also space frequency block coding (SFBC) can be used to distribute channel symbols across space (transmit antennas) and frequency (OFDM tones) within one OFDM block [13].

2.1.1 The chapter organization

The chapter began with a brief overview of a MIMO-OFDM system. In section two, explanations of OFDM based transmission, a convolutional encoder, a Viterbi decoder, interleaving and an appropriate modulation technique are given. Then, the benefits of the combination of conventional MIMO with an OFDM system will be presented and finally, a cooperative relaying network will also be studied. In addition, SFBC is explained in order to exploit the benefit of the combination of SISO-OFDM with MIMO system virtually. Finally, simulation results and a summary are presented.

2.2 OFDM Based Transmission

Single-input single-output (SISO) OFDM is a block modulation technique where a block of N information symbols is modulated onto N parallel subcarriers having frequency separation $1/T$, where T is the data block duration. An OFDM implementation is basically performed by using an inverse discrete Fourier transform (IDFT) at the modulator and a discrete Fourier transform (DFT) at the demodulator. Fortunately, the OFDM modulator and demodulator can be implemented as an inverse fast Fourier transform (IFFT) and fast Fourier transform (FFT), respectively, which are fast signal processing transforms [30]. In fact, IFFT and FFT algorithms are efficient methods to compute the IDFT and DFT, respectively, in addition to providing further reductions in computation complexity especially when the transform size N is large and typically a power of two. For example, the FFT needs $N \log(N)$ arithmetical operations compared with the DFT which requires N^2 arithmetical operations to achieve the same result. At the trans-

mitter of the OFDM system, a sequence of QPSK symbols or 16-QAM symbols stream, is converted into size N parallel streams, then modulated onto N subcarriers via a size $N - IFFT$. The IFFT converts the input parallel data, which are complex data in the frequency domain, into a time domain signal, whilst maintaining the orthogonality. However, the major disadvantage of OFDM is the high PAPR because an OFDM signal is a superposition of N sinusoids modulated by possibly coded data symbols. The peak power can theoretically be up to N times larger than the average power level [31]. Moreover, in order to mitigate the inter symbol interference (ISI) in OFDM which is induced by the multipath channel during the signal propagation, a cyclic prefix (CP) is used. As such, at the transmitter, a CP with length not less than the channel delay spread is added to the OFDM block after the IFFT. At the receiver side, this extension of the CP is removed before applying the FFT process. Mathematically, a linear convolution of the transmitted OFDM signal and the channel is converted to a circular convolution in the case of applying the CP. So, the effects of the ISI are easily and completely eliminated [32].

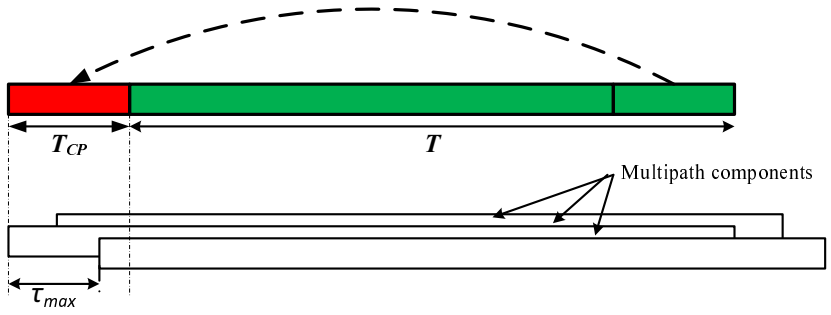

Figure 2.1. Cyclic prefix extension of the original OFDM symbol.

Fig.2.1 illustrates the effect of the CP at the receiver side, a certain

position within the cyclic prefix is chosen as the sampling starting point, which satisfies the criterion $\tau_{max} < T_{CP}$ where τ_{max} is the worst-case multi-path spread. For example, in Fig.2.1, this condition is satisfied, which means there is no ISI since the previous symbol will only have effect over samples within $[0, \tau_{max}]$.

The output data go through a parallel-to-serial converter and than to a digital-to-analog converter (DAC). The analog signal is than amplified and converted to the radio frequency (RF) signal and transmitted by antennas into the channel.

At the receiver side, the FFT converts the time-domain signal into the frequency domain to recover the information that was originally sent. The size N FFT efficiently implements a bank of filters each matched to the N possible subcarriers.

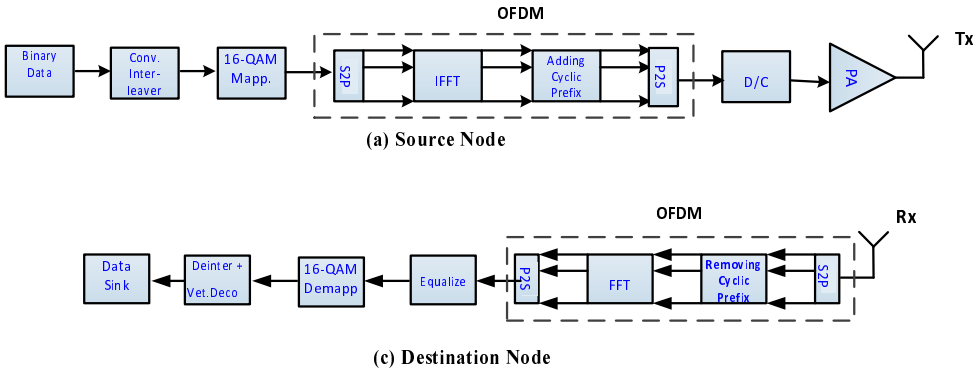

Figure 2.2. Block diagram of source node and destination node of a point-to-point coded SISO-OFDM communication system.

Then, the FFT output is then converted into a single serial data stream, and fed into Viterbi decoding. The individual coding operations are considered next in more detail.

2.2.1 Convolutional encoder

The channel coder adds redundant information to the stream of input symbols in a way that allows errors which are induced by the channel to be corrected or detected. Channel coding is an inherent part of an OFDM system. By using channel coding high coding gain can be achieved, especially useful for fading channels. Convolutional codes represent one technique within the general class of error-correcting codes [33] and [34] which are used widely in many wireless applications such as mobile communications, and satellite communications in order to achieve reliable and efficient transmission over various channel conditions. Convolutional codes are commonly specified by three parameters which are required output data, current input data and the constraint length of the code where the ratio of the number of input data bits to the number of output data bits is the code rate. As an example, a convolutional encoder is depicted in Figure 2.3, the information bits u are shifted into a register of length $q = 2$, such as a register with two binary memory elements u_{-1} and u_{-2} [18] and [35]. The output sequence results from multiplexing the two sequences denoted by $\mathbf{a}_1$ and $\mathbf{a}_2$. Each output bit is generated by modulo two addition of the current input bit and some symbols of the register contents. For instance, the information sequence $\mathbf{u} = (1, 1, 0, 1)$ will be encoded to $\mathbf{a}_1 = (1, 0, 0, 0, 1, 1)$ and $\mathbf{a}_2 = (1, 1, 1, 0, 0, 1)$. The generated code sequence after multiplexing of $\mathbf{a}_1$ and $\mathbf{a}_2$ is $\mathbf{a} = (1, 1, 1, 0, 0, 0, 1, 0, 1, 1)$. The two coding polynomial of this particular encoder are $\mathbf{g}_1 = (1, 1, 1)$ and $\mathbf{g}_2 = (1, 0, 1)$. These generator coding polynomial are helpful for calculating the output sequences for an arbitrary input sequence [36] and [37]

$$\begin{aligned} \mathbf{a}_1 &= \mathbf{u} \oplus \mathbf{g}_1 \\ \mathbf{a}_2 &= \mathbf{u} \oplus \mathbf{g}_2, \end{aligned} \tag{2.2.1}$$

where $\oplus$ denotes the modulo two addition used to form the outputs.

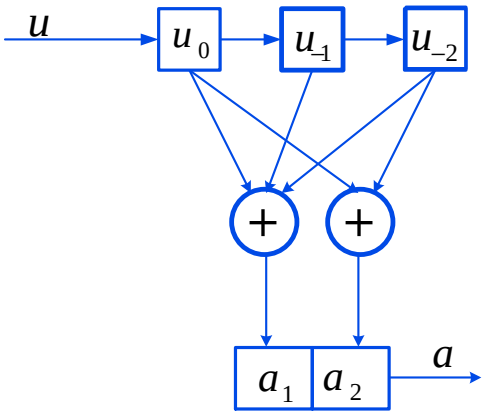

Figure 2.3. Convolutional encoder consists of current state (u_0), two memory states (u_{-1}, u_{-2}) and the code block consists of two bits ($a = a_1, a_2$).

The code rate is $R = \frac{k}{n}$, where k and n denote the number of encoder inputs and outputs respectively. The state diagram of a convolutional encoder describes the operation of the encoder and is also helpful later in decoding algorithms. The state diagram is a graph that has 2^q nodes representing the encoder states as in Figure 2.4. The easiest way to determine the state diagram is to first determine the state table as shown below which contains a input, actual state, output and next state

From the state table which has been shown in Table 2.1 the state diagram can be directly obtained.

Input	Actual State		Output		Next State	
u	u_{-1}	u_{-2}	a_1	a_2	u_{-1}	u_{-2}
0	0	0	0	0	0	0
0	0	1	1	1	0	0
0	1	0	1	0	0	1
0	1	1	0	1	0	1
1	0	0	1	1	1	0
1	0	1	0	0	1	0
1	1	0	0	1	1	1
1	1	1	1	0	1	1

Table 2.1. State table for the memory length two convolutional encoder.

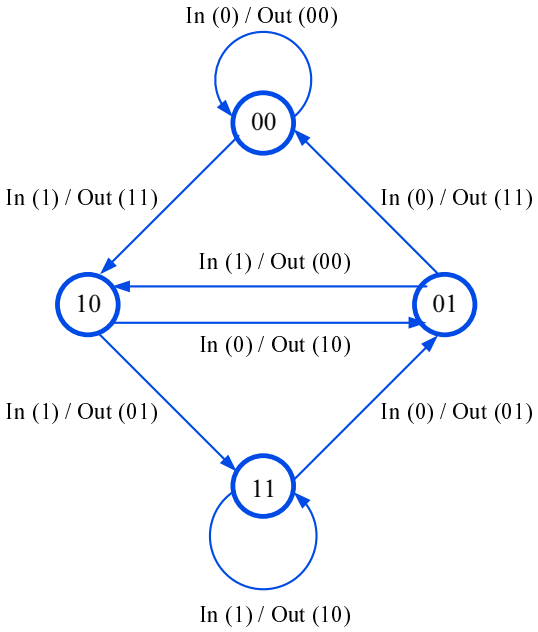

Figure 2.4. State diagram of convolutional encoder with memory length (q = 2) which has 2^q nodes. The branches along the state diagram indicate input/output values based on Table 2.1.

In order to obtain a terminated code sequence, the encoding is started in the all-zero encoder state and it is ensured that, after the encoding process, all memory elements contain zeros again. In the case of an encoder without feedback this can be done by adding q zero bits to the information sequence. The termination operation leads to low error

probabilities for the last bits in a sequence. However, the termination process decreases slightly the data rate [36].

2.2.2 Code interleaving

Interleaving is applied in order to make the fading gains affecting the symbols independent. In other words, by permuting the order of the transmitted elementary signals, interleaving consists of making the channel approximately memoryless [38]. In real channels, however, error bursts might occur such as in fading channels in wireless communication systems. With the help of code interleaving, an existing error-correcting channel code can be adapted such that error bursts up to a given length can also be corrected. The code interleaving to interleaving depth t is obtained as follows; assume that t code words $\mathbf{a}_1,\ \mathbf{a}_2,\ \ldots,\ \mathbf{a}_t$, with $\mathbf{a}_j = (a_{j,0},\ a_{j,1},\ \ldots,\ a_{j,n-1})$, are arranged as rows in the $t \times n$ matrix

$$\begin{bmatrix} a_{1,0} & a_{1,1} & \cdot & a_{1,n-1} \\ a_{2,0} & a_{2,1} & \cdot & a_{2,n-1} \\ \cdot & \cdot & \cdot & \cdot \\ a_{t,0} & a_{t,1} & \cdot & a_{t,n-1} \end{bmatrix}. \tag{2.2.2}$$

The resulting code word $\mathbf{a}$ of length nt of the interleaved code is generated by reading the symbols off the matrix column-wise.

$$\mathbf{a} = a_{1,0}\ a_{2,0}\ \ldots\ a_{t,0}\ a_{1,1}\ a_{2,1}\ \ldots\ a_{t,1}\ \ldots\ a_{1,n-1}\ a_{2,n-1}\ \ldots\ a_{t,n-1}. \tag{2.2.3}$$

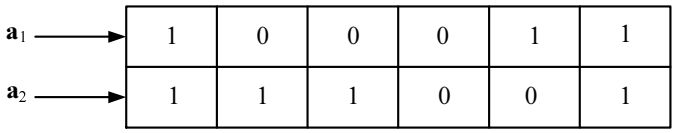

Figure 2.5. Interleaver table for convolutional code example.

The output of the previous convolutional code example can be illustrated in Figure 2.5. As a result, the interleaved convolutional code output according to the above figure is $\mathbf{a} = (11,\ 01,\ 01,\ 00,\ 10,\ 11)$. The binary data which are encoded by the convolutional coding technique and interleaved, are fed into the constellation mapper which will be explained in the next subsection.

2.2.3 Mapping to digital modulation technique

The interleaved coded data which enter into the digital modulation technique which are employed in the OFDM system are usually based on quadrature amplitude modulation (QAM) with 2^d constellation points, where d is the number of bits transmitted per modulated symbol and $\mathbb{M} = 2^d$ is the number of constellation points. Typically, constellation mappings are based on Gray mapping, where adjacent constellation points differ by only one bit as in Figure 2.6 [39].

In this section, it has seen that the encoder of a convolutional code can be considered as a finite-state machine that is characterized by a state diagram. Alternatively, a convolutional encoder may be represented by a trellis diagram. In the next subsection, explanation of the Viterbi algorithm which is used to find the code word with minimum distance to the received sequence in a trellis is given.

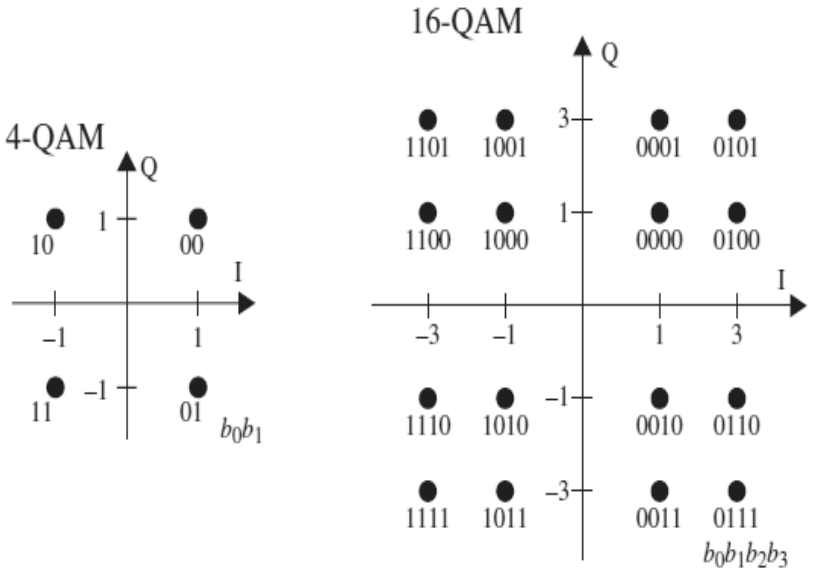

Figure 2.6. Constellation mappings of 4-QAM and 16-QAM modulation techniques.

2.2.4 Viterbi decoder

The encoding of convolutional codes has been considered, therefore, the most popular decoding procedure, the Viterbi algorithm, which is based on a graphical representation of the convolutional code, the trellis diagram, is studied. A trellis is a directed graph, where the nodes represent encoder states. In contrast to the state diagram, the trellis has a time axis, i.e. the i^{th} level of the trellis corresponds to all possible encoder states at time i. The trellis of a convolutional code has a very regular structure. It can be constructed from the trellis module, which is simply a state diagram as in Figure 2.4.

The Viterbi algorithm is based on a procedure to find the code word with minimum distance to the received sequence in a trellis. However, the Viterbi algorithm can be described in some steps. Firstly, starting at the zero state (left) of the trellis diagram. Secondly, calculating the

number of matches of the output and the corresponding received bits for any possible path (every arrow in the trellis diagram) to the next stage. Thirdly, for every state on every stage only the maximum number of matches is used for the further calculations. All other numbers are cancelled (thus the paths that belong to these numbers are also cancelled). Finally, the path with the highest number of matches is used and retraced to the beginning of the trellis diagram as in Figure 2.7 [36]. The information sequence $\mathbf{u} = (1, 1, 0, 1, 0, 0)$ and the transmitted encoded signal $\mathbf{a} = (11, 01, 01, 00, 10, 11)$, so the received signal which is affected by noise is $\mathbf{a}' = (10, 01, 01, 01, 10, 11)$.

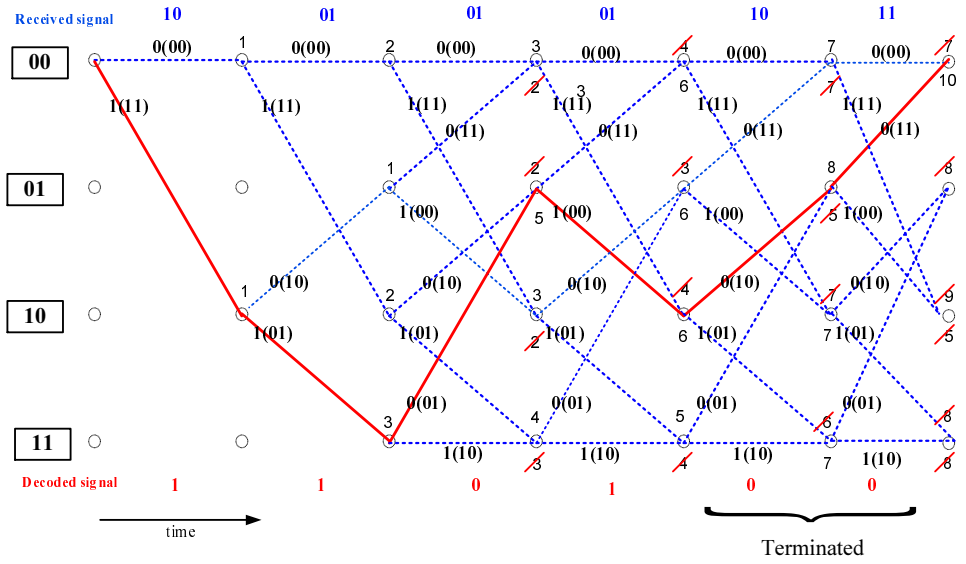

Figure 2.7. Trellis diagram showing the process of Viterbi decoding. Starting at the zero state (left) of the trellis diagram. Calculating the the number of matches of the output and the corresponding received bits for any possible path (every segments in the trellis diagram) to the next stage and only the maximum number of matches is used for the further use. Finally, the path with the highest number of matches is used and retraced to the beginning of the trellis diagram.

From the Trellis diagram can be seen that, the received sequence

$\mathbf{a}' = (10\ \ 01\ \ 01\ \ 01\ \ 10\ \ 11)$ which contains some errors, can be decoded as $1 \quad 1 \quad 0 \quad 1 \quad 0 \quad 0$. In this example, 2 bit errors are corrected, at 2^{nd} digit and 8^{th} digit which results in the decoded sequence being identical to the transmitted information bits.

In this section, it has been seen that an OFDM system has the advantage of converting a wideband frequency selective fading channel into a large number of narrow band flat-fading sub-channels. Therefore, channel fading can be mitigated by a simple one tap equalizer [39].

In the next section, MIMO techniques and also combination of MIMO and OFDM, will be studied. These techniques result in high speed wireless communication systems by adopting the benefits from both technologies.

2.3 Cooperative MIMO-OFDM System

The most important parameters of the quality of a wireless link are transmission rate, the transmission range and the transmission reliability. In conventional communication systems, the increase in transmission rate may reduce the transmission range and reliability. In contrast, increasing coverage area will introduce cost in transmission rate and reliability, and vice versa; strong transmission reliability will be achieved by reducing the transmission rate and range [9]. Therefore, combining MIMO with an OFDM system can simultaneously improve the transmission rate, coverage and the transmission reliability [40]. However, although this combined MIMO with OFDM system can achieve these three crucial advantages, the system will still be complex, and suffer from the effect of path loss and shadowing and the channel estimation is challenging. In addition, PAPR becomes even more important

in MIMO-OFDM systems because there are multiple transmit antennas each of which would require its own DAC and RF power amplifier [41]. In the next subsection, a cooperative relaying system based on an OFDM transmission technique will be studied in order to mitigate some disadvantages of MIMO systems.

2.3.1 Cooperative relaying system based on MIMO-OFDM transmission

To avoid some of the drawbacks and gain the same benefits of MIMO systems, a cooperative relay system has been used. Cooperative techniques in wireless networks are used to form virtual MIMO systems from separated single antenna terminals [13]. One of the main advantages of cooperative communications is the ability to achieve spatial diversity gains without employing multiple antennas on each terminal [14]. In this system, the transmission reliability can be achieved by a cooperative diversity gain, which is an effective gain to combat the detrimental effects of severe fading in the wireless channel [15]. The copies of the same information can be forwarded to the destination node by intermediate relays between the source and destination with independent channels, because of diversity gain. Therefore, diversity gain can be obtained due to the number of independent channels in the cooperative relay network, which depends on the number of the relay nodes and the environment [16]. For example, in a frequency-flat channel, the maximum diversity gain $D_g = M_s \times M_r \times M_d$, where M_s, M_r and M_d are the number of single antenna source nodes, relay nodes and destination nodes, respectively. Increased diversity gain leads to improvements in the system performance such as the probability of er-

ror P_e or the outage probability P_{out}. The diversity gain indicates how fast the probability of error decreases with an increase in the signal strength typically measured by SNR [42]. Generally, the diversity gain or diversity order, D_g, in terms of error probability P_e and outage probability P_{out} can be seen as in [43]. In addition, the available spatial and temporal cooperative diversity order of the cooperative network can be derived as in [23]. In a multi-path environment, fading has detrimental effect on the error rate performance, therefore, exploiting spatial and temporal cooperative diversity to overcome such fading is beneficial, in terms of error probability and outage probability as given by [23] and [43]

$$D_g = -\lim_{SNR\to\infty} \frac{\log_2 P_e(SNR)}{\log_2 SNR} \tag{2.3.1}$$

and

$$D_g = -\lim_{SNR\to\infty} \frac{\log_2 P_{out}(R)}{\log_2 SNR}, \tag{2.3.2}$$

where $P_{out}(R)$ denotes the probability and the target rate $R = rlog_2(SNR)$, where r is referred to the multiplexing gain and is equal to the number of independent channels over which different information can be sent. In a system with M_r transmit and M_d receive antennas, the maximum number of independent channels under favorable propagation conditions is $r = min(M_r, M_d)$ [14], [43].

Cooperative relay systems potentially offer advantages such as high transmission reliability, high date rate transmission, and large coverage

area. Cooperative virtual MIMO-OFDM systems mitigate some disadvantages of conventional MIMO-OFDM system such as reducing system complexity, effect of path loss and shadowing and also the channel estimation complexity. However, cooperative relay systems introduce some other problems such as interference, which potentially causes the system performance to deteriorate and asynchronization, due to using large number of relay nodes, being in different locations and timing delay between each other, however, this problem will not considered in this work. Another drawback of the system is PAPR which is considered in this thesis. The PAPR reduction in a cooperative relaying network is performed by using a clipping technique in this thesis, which is a simple method. In the next subsection, the space frequency block coding technique is exploited in order to benefit from the advantages of combination of both the virtual MIMO and the OFDM systems.

2.3.2 SFBC of cooperative relaying OFDM system

The Alamouti space time block coding (STBC) technique is a simple and effective scheme for two transmit antenna elements which can be built virtually by relay nodes in cooperative networks and a single receive antenna achieving diversity order of two. This is performed in two phases; in the first phase the source node broadcast the data symbols to the relay nodes; then, in the second phase, two data symbols are transmitted simultaneously from the two transmit antennas. In general, STBC provides a simple transmit diversity scheme with order two in a flat fading channel. However, frequency selective fading channels destroy the orthogonality of the received signals, which is critical to the operation of diversity systems. Therefore, STBC is often only effective

over flat fading channels, such as indoor wireless networks or low data rate systems [44]. For future wireless broadband systems, an OFDM system provides an essentially flat fading channel for each subcarrier so that orthogonal space time transmitter diversity can be applied, even for channels with large delay spreads. OFDM also offers the possibility of coding in the frequency dimension in a form of space frequency block coding (SFBC). In this case, the two symbols are sent on two different frequencies, for example, on different subcarriers in an OFDM system as in [45], [46], [47] and [48].

An example conventional MIMO system with two transmit and two receive antennas is considered. Both the transmit antennas and the receive antennas are spaced sufficiently far apart so that the transmission paths can be assumed to be independent. There are four independently faded signal paths between the transmitter and the receiver, suggesting that the maximum diversity gain that can be achieved is four as in Fig. 2.8 (a). In multi-relay cooperative systems, as shown in Fig. 2.8 (b), the relays can be viewed as a distributed antenna array and be used to perform many conventional MIMO transmission schemes. Also this diversity gain can be achieved by a MISO system structure which contains four transmit antennas and one receive antenna. Moreover, this structure can be built naturally in a multinode wireless communication environment, which is commonly called a virtual antenna array or virtual MIMO system [14] and [43]. The $\mathbf{h}_{m,1,L}$ and $\mathbf{h}_{m,2,L}$ are the channel impulse response with L^{th} number of multi-paths.

Although a virtual MIMO-OFDM system has some problems such as it needs feedback to achieve full diversity gain, it still is a more

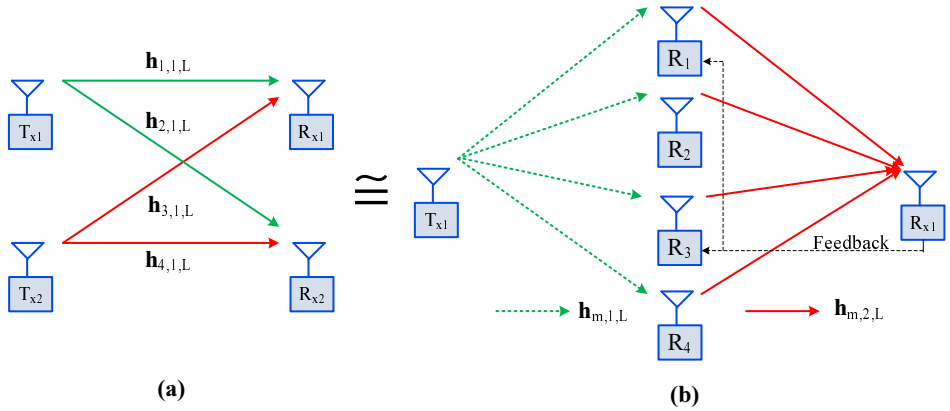

Figure 2.8. (a) Conventional MIMO-OFDM system (2,2) with diversity gain of four. (b) Multinode cooperative virtual MIMO-OFDM system (4,1) which needs a feedback scheme to achieve almost the same diversity gain as a conventional MIMO-OFDM system.

attractive scheme than conventional MIMO-OFDM, that is because the spatial links between different nodes in the network fade independently, again because of the distributed nature of the formed virtual array, which leads to full spatial diversity gain. In this chapter, the performance of the conventional MIMO-OFDM system ($2T_x,\ 2R_x$) and ($4T_x,\ 1R_x$) will be compared.

2.3.3 DF distributed Alamouti SFBC-OFDM scheme

The source node S first modulates its information bits and divides the modulated signals into pairs with size N. The symbol $X[k]$, $k = 0, 1, \cdots, N-1$, denotes the k^{th} sample of the OFDM symbol, where N is the number of OFDM subcarriers. After that, each N symbols as a block are modulated by inverse fast Fourier transform (IFFT). And then each modulated block is appended with a cyclic prefix (CP). Then, the source node broadcasts the OFDM symbols to the relay nodes. Then, the

received signals at the relay nodes are given by

$$\mathbf{y}_{SR_m} = \sqrt{P_s}\mathbf{H}_{m,1,L}\mathbf{x} + \mathbf{w}_{R_m} \qquad m = 1, 2 \tag{2.3.3}$$

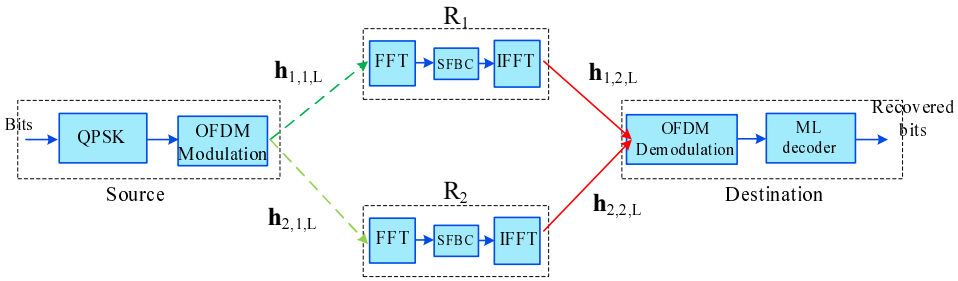

Figure 2.9. Wireless relay system architecture with two relay nodes. For simplicity, it is assumed that the original data are fully recovered at the relay nodes, which means no effect of the channel between source and relays (represented as dash line).

where $\sqrt{P_s}$ represents the average input power of OFDM signal, $\mathbf{H}_{m,1,L}$ represent convolution matrices formed from the coefficients of the source-to-relay channels and $\mathbf{w}_{R_m}$ is an additive white Gaussian noise (AWGN) vector. The channel impulse response (CIR) for the first and second hop is given by a vector, $\mathbf{h}_{m,i,L} = [h_{1,i,L},\ h_{2,i,L},\ h_{3,i,L},\ h_{4,i,L}]^T$ where L denotes the channel length, $m = 1, 2$ which is number of relay nodes and $i = 1, 2$ is a hop one and two. Then, the relay nodes removes the cyclic prefix (CP) and then transforms the OFDM signals into the frequency domain by FFT and decodes them to form the SFBC vector

$$\begin{aligned} \mathbf{Y}_{SR_m} &= \sqrt{P_s}\mathbf{F}\mathbf{H}_{m,1,L}\mathbf{F}^H\mathbf{X} + \mathbf{W}_{R_m} \\ \mathbf{Y}_{SR_m} &= \sqrt{P_s}\mathbf{\Lambda}_{m,1,L}\mathbf{X} + \mathbf{W}_{R_m}, \end{aligned} \tag{2.3.4}$$

where $\mathbf{\Lambda}_{m,1,L} = \mathbf{F}\mathbf{H}_{m,1,L}\mathbf{F}^H$ is the frequency domain representation of the source to relays and $\mathbf{F}$ is a normalized DFT matrix. For convenience, as $\mathbf{\Lambda}_{m,1,L}$ is diagonal, a vector $\lambda_{m,1,L} = diag(\mathbf{\Lambda}_{m,1,L})$ is defined [3]. The elements of $\lambda_{m,1,L}[k]$, $k = 0, 1, ..., N-1$, denote the required channel gains. The decode-and-forward (DF) mode has been assumed which is capable of fully recovering the original data sequence at the relay nodes with sufficient error correction coding [14] and [49]. The SFBC encoder generates the effective code matrices across two relay nodes and over two adjacent subcarriers, $k = 2v, 2v+1$, $v = 0, 1, ..., N/2-1$

$$\mathbf{C}[v] = \begin{bmatrix} X[2v] & -X^*[2v+1] \\ X[2v+1] & X^*[2v] \end{bmatrix}. \tag{2.3.5}$$

Then, the SFB coded vectors at the two relay nodes are given as

$$\begin{aligned} \mathbf{Y}_{R_1} &= [X[0] \quad X[1] \quad X[2] \quad X[3] \quad . \quad . \quad . \quad X[N-1]]^T \\ \mathbf{Y}_{R_2} &= [-X^*[1] \quad X^*[0] \quad -X^*[3] \quad X^*[2] \quad . \quad . \quad . \quad X^*[N-2]]^T, \end{aligned} \tag{2.3.6}$$

where $(\cdot)^*$ denoted complex conjugate. During the block, $\mathbf{Y}_{R_1}$ is transmitted from the first relay node R_1, while $\mathbf{Y}_{R_2}$ is transmitted simultaneously from the second relay node R_2 as in Fig. 2.9. The equivalent channel matrix corresponding to the code used over two transmitters

is given by:

$$\mathbf{C}_e[v] = \begin{bmatrix} \lambda_{1,2,L}[2v] & -\lambda_{2,2,L}[2v+1] \\ \lambda^*_{2,2,L}[2v] & \lambda^*_{1,2,L}[2v+1] \end{bmatrix}, \tag{2.3.7}$$

where $\lambda_{1,2,L}[2v]$ and $\lambda_{2,2,L}[2v+1]$ are the channel coefficients modeled by independent zero-mean complex Gaussian random variables with 0.5 variance per dimension. The signal at the receiver is given by

$$\begin{bmatrix} R[2v] \\ R^*[2v+1] \end{bmatrix} = \mathbf{C}_e[v] \begin{bmatrix} X[2v] \\ X^*[2v+1] \end{bmatrix} + \begin{bmatrix} Z[2v] \\ Z^*[2v+1] \end{bmatrix}. \tag{2.3.8}$$

Assuming that the channel impulse responses are known or can be estimated accurately at the receiver, the space-frequency decoder constructs the decision estimate vector $\widehat{\mathbf{X}}$ as

$$\begin{bmatrix} \widehat{X}[2v] \\ \widehat{X}[2v+1] \end{bmatrix} = \Delta[v] \begin{bmatrix} X[2v] \\ X[2v+1] \end{bmatrix} + \begin{bmatrix} \widetilde{Z}[2v] \\ \widetilde{Z}[2v+1] \end{bmatrix}, \tag{2.3.9}$$

where $\widetilde{(\cdot)}$ denotes a quantity processed by $\mathbf{C}_e[v]^H$. It can be shown that for an orthogonal block code, all the off-diagonal terms of $\Delta[v] = \mathbf{C}_e[v]^H \mathbf{C}_e[v]$ will be zero. To fulfil that, the complex channel gains between adjacent subcarriers are approximately constant $\lambda_{1,2,L}[2v] \approx \lambda_{2,2,L}[2v+1]$

$$\Delta[v] = \begin{bmatrix} |\lambda_{1,2,L}[2v]|^2 + |\lambda_{2,2,L}[2v]|^2 & 0 \\ 0 & |\lambda_{1,2,L}[2v]|^2 + |\lambda_{2,2,L}[2v]|^2 \end{bmatrix}, \tag{2.3.10}$$

$$\begin{aligned} \widehat{X}[2v] &= [\Delta[v]]_{1,1} X_1[2v] + \widetilde{Z}[2v] \\ \widehat{X}[2v+1] &= [\Delta[v]]_{2,2} X_2[2v+1] + \widetilde{Z}[2v+1], \end{aligned} \tag{2.3.11}$$

where $\widetilde{Z}[2v] = \lambda^*_{1,2,L}[2v]Z[2v] + \lambda_{2,2,L}[2v]Z^*[2v+1]$ and $\widetilde{Z}[2v+1] = \lambda_{1,2,L}[2v]Z^*[2v+1] + \lambda^*_{2,2,L}[2v]Z[2v]$. The SFBC-ODFM transmitter diversity scheme is similar in form to that of the optimal two-branch maximal ratio combining (MRC) receiver diversity system [44] and is exactly the same as that of the STBC-OFDM transmitter diversity system [50]. Simulation of BER of SISO-OFDM and cooperative Alamouti SFBC-OFDM system will be presented in the next section.

2.4 Simulations Results

In the simulation, a comparison of the BER for SISO-OFDM, the Alamouti SFBC-OFDM and EO-SFBC-OFDM system is given. The main parameters used in the system are an uncoded QPSK OFDM signal with 1024 subcarriers and the SFBC encoding is applied in the relays. Additionally, all links are assumed to be quasi-static frequency selective channels.

In Fig. 2.10 it is confirmed that the performances of the EO-SFBC-OFDM (4,1) scheme is close to the conventional MIMO-OFDM system

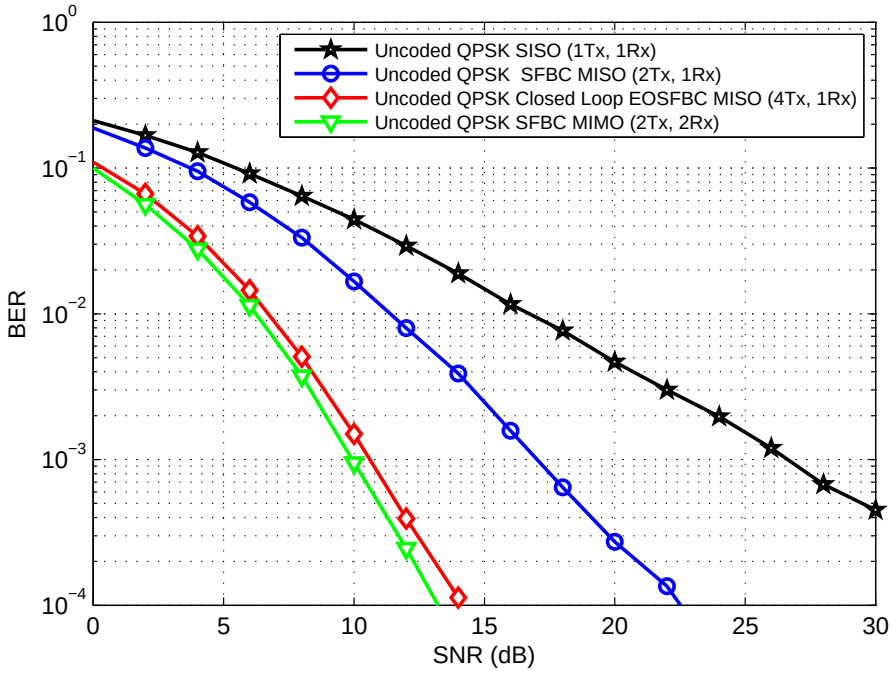

Figure 2.10. Comparison of BER performance of uncoded SISO-OFDM point-to-point wireless system as in Fig. 2.2, Alamouti scheme as in Fig. 2.9, conventional MIMO-OFDM system as in (a) Fig. 2.8 and multinode virtual MIMO-OFDM system as in (b) Fig. 2.8.

(2,2) performance. At 10^{-4} the difference between both schemes is approximately 0.8 dB, this is because there are two AWGN sources in the conventional MIMO-OFDM scheme at the receiver side, which can be combined, whereas in the EO-SFBC-OFDM scheme there is just one AWGN source at the receiver which always effects the system performance. Both schemes have better performance compared with the Alamouti SFBC-OFDM scheme (2,1) and point-to-point SISO-OFDM system (1,1). For example, at a BER of 10^{-3}, the conventional Alamouti SFBC-OFDM and EO-SFBC-OFDM schemes require approximately 10 dB and 10.8 dB (Eb/No), respectively, while the

Alamouti SFBC-OFDM scheme (2,1) and SISO-OFDM schemes require approximately 17 dB and 27 dB, respectively. In other words, exploiting the EO-SFBC-OFDM (4,1) technique at four relay nodes results in significant performance improvement, which is approximately 16 dB compared with point-to-point SISO-OFDM system.

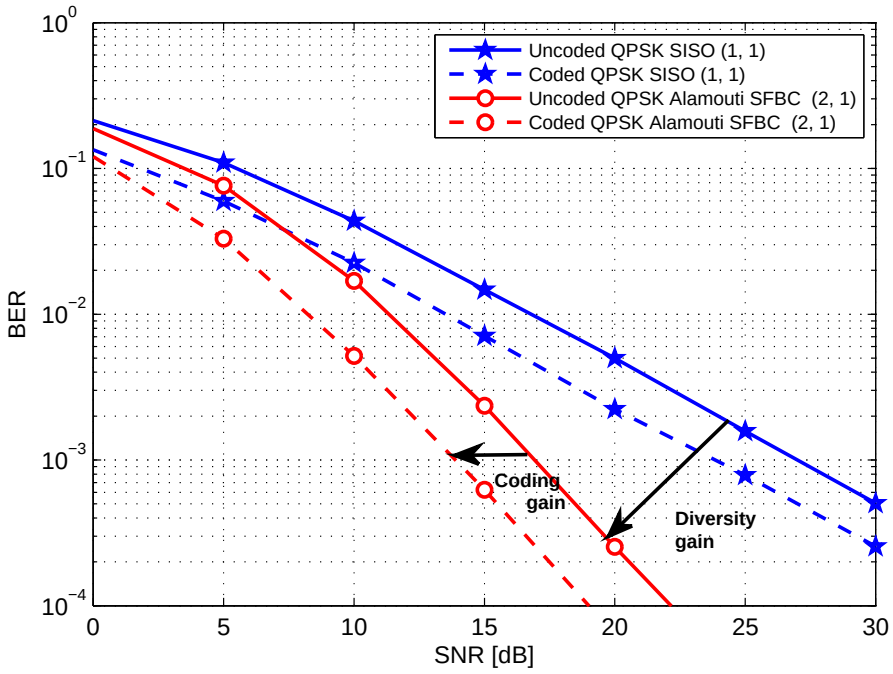

Figure 2.11. The comparison of uncoded and coded of the SISO-OFDM and Alamouti SFBC-OFDM (2,1) schemes. The effect of the coding gain and diversity gain on bit error rate performance.

In Fig. 2.11 it is confirmed that the coding gain in both cases improves the performance by approximately 3 dB at all SNR values (low and high values), whereas the effect of spatial diversity gain at higher SNR is much better than at low SNR values, as expected due to its asymptotic definition.

2.5 Summary

MIMO technology theoretically offers several benefits which help to achieve significant performance gains e.g. array gain, spatial diversity gain and spatial multiplexing gain without additional bandwidth or transmit power. Spatial diversity gain increases the magnitude of the slope of the BER curve, whereas coding gain generally just shifts the error rate curve to the left. Moreover, in a multipath environment, combining MIMO and OFDM improves the quality of a wireless link such as transmission rate, transmission range and the transmission reliability. However, there are some disadvantages in this system such as the system is still complex, also it suffers from the effect of path loss and shadowing and the channel estimation is challenging. Therefore, exploiting a cooperative relay network (virtual MIMO-OFDM system) mitigates some of these drawbacks. Moreover, to minimize further these effects, a relay selection scheme is used to select the highest quality paths. As a result, a cooperative relay network system potentially offers close performance to the conventional MIMO-OFDM system, if the number of transmit and receive antennas in both schemes are equal. Therefore, a cooperative relay network system provides significant improvement in the system performance compared with a SISO-OFDM system. In addition, simplifying the system and performance improvement is expected by using relays selection scheme. In the next chapter, PAPR reduction by clipping method will be studied, as the basis for mitigating the PAPR problem in cooperative transmission, the focus of this thesis.

Chapter 3

ANALYSIS OF PAPR IN OFDM TRANSMISSION AND MITIGATION WITH CLIPPING

3.1 Introduction

The orthogonal frequency division multiplexing (OFDM) technique has received much attention in recent years because it has many advantages such as bandwidth efficiency and robustness to multi-path fading channels. However, this technique can have high peak values in the time domain since many subcarrier components are added via an IFFT operation. Therefore, OFDM systems are known to have a high peak-to-average power ratio (PAPR). An OFDM signal is a superposition of N usually statistically independent sinusoidal subchannels modulated by possibly coded data symbols. It can constructively sum up to high peaks which theoretically can be up to the number of OFDM subcarriers N in magnitude. As a result, there are two different problems. The first one is related to the analog-to-digital converter (ADC) and digital-

to-analog converter (DAC), which must be equipped with a sufficient number of bits to cover a potentially broad dynamic range. The second problem is that the transmitted signal may suffer significant spectral spreading and in-band distortion as a consequence of intermodulation effects induced by a non-linear radio frequency (RF) power amplifier. One possible method to overcome the RF power amplifier problem is the use of a large power backoff which allows the amplifier to operate in its linear region. However, this results in considerable power efficiency penalty, which translates into expensive transmitter equipment and reduced battery lifetime at the user's terminal [18] and [28]. Therefore, it is thus of interest to look for some efficient schemes for PAPR reduction techniques.

3.1.1 The motivation

In this chapter, among many PAPR reduction methods [18], [39], deliberate amplitude clipping is studied. This technique is one of the most simplest and effective solutions for OFDM PAPR reduction when the number of OFDM subcarriers is large. Clipping, however, causes distortion that degrades the system performance and introduces out-of-band interference, therefore, oversampling of the digital signal may be used to overcome interference and improve PAPR. In addition, PAPR reduction is considered in a coded SISO-OFDM system and a distributed space frequency block coding cooperative transmission scheme. In this system, the PAPR reduction technique is based on amplitude clipping at the source node, the relay nodes apply space frequency block coding (SFBC) and a conventional decoding technique at the destination node.

3.1.2 The chapter organization

The chapter begins with an introduction and a brief overview of PAPR mitigation methods including definition and statistical properties of PAPR. Then a simple approach to limit the amplitude peaks in an OFDM waveform is described. In addition to this, oversampling and filtering after clipping is studied to reduce the harmful effects induced by the clipping process. Finally, simulation results are presented and conclusions are drawn.

3.2 An Overview of PAPR Mitigation Methods for MIMO-OFDM

In MIMO-OFDM systems PAPR becomes even more important since there are multiple transmit antennas each of which would require its own RF power amplifier and DAC. A number of solutions to the PAPR problem of OFDM have been proposed in [18], [28], [29] and [51]. These approaches can be essentially divided into two classes. The first one is characterized by the fact that, although the PAPR of the transmit signal is reduced, the signal remains undistorted. While this costs bandwidth efficiency, the BER remains unchanged. Therefore, such methods are called distortionless PAPR reduction techniques and include the selective mapping approach, optimization techniques such as the partial transmit sequence approach and algebraic coding techniques [18]. The other class distorts the transmitted signal by clipping the signal peaks, increasing the BER and adding out-of-band noise. This work exploits the second simpler approach to limit the amplitude peaks in an OFDM waveform i.e. to clip deliberately the signal before amplification. This operation is normally accomplished at baseband using an envelope limiter. However, in general amplitude clipping gives rise

to in-band distortion as well as out-of-band leakage. To overcome the out-of-band problem, oversampling before clipping and then filtering can be used [18]. In this chapter the effect of the clipping process will be illustrated when the conventional decoding technique is used.

3.2.1 PAPR definition

The OFDM symbol in the time domain is generated as an N subcarrier symbol by adding the weighted subcarrier components represented as [39]:

$$x(t) = \frac{1}{\sqrt{N}} \sum_{k=0}^{N-1} c_k e^{j2\pi k f_c t} \quad 0 \leq t \leq N-1, \tag{3.2.1}$$

where c_k is the complex symbol transmitted on the k^{th} subcarrier, f_c denotes the subcarrier spacing and $T = \frac{1}{f_c}$ is the data block duration without cyclic prefix. The PAPR might be defined over the radio frequency signal $x_{RF}(t)$ rather than over the baseband signal x(t) [18]. In general PAPR should be measured with respect to the continuous time signal. However, since this approach would lead to some mathematical complications, in practice to overcome this difficulty, the baseband modulation is applied in the digital domain using an oversampled version of x(t) which is given by

$$x[n] = \frac{1}{\sqrt{N}} \sum_{k=0}^{N-1} c_k e^{j2\pi k n / JN} \quad , \; n \in [0, JN-1], \tag{3.2.2}$$

where J is a suitable integer which is commonly referred to as oversampling factor. By considering the time domain samples output from the IFFT, the discrete-time PAPR is defined as

$$PAPR(x[n]) = \frac{\max\limits_{0 \leq n \leq N-1} |x[n]|^2}{E\{|x[n]|^2\}}, \tag{3.2.3}$$

where max and $E\{\cdot\}$ denote the maximum value and statistical expectation operation, respectively. Statistical properties of PAPR will be considered in the next subsection.

3.2.2 Statistical properties of PAPR

The statistical properties of the PAPR are normally given in terms of the corresponding complementary cumulative distribution function (CCDF). The CCDF of the PAPR denotes the probability that the PAPR of a data block exceeds a given threshold [52]. The most interest is to find the probability that the signal power is out of the linear range of the RF power amplifier. The input samples of the N-point IFFT are assumed independent with finite magnitudes which are uniformly distributed for quadrature phase shift keying (QPSK) and quadrature amplitude modulation (QAM) constellation [29]. From the central limit theorem, it is known that the real and imaginary parts of the time-domain samples $x[n]$ can reasonably be approximated as statistically independent Gaussian random variables with zero-mean and 0.5 variance [18], [53] and [54]. Assuming that the average power of $x[n]$ is equal to one, that is, $E\{|x[n]|^2\} = 1$, then the probability density function (PDF) of the magnitudes of complex samples, are inde-

pendent and identically distributed (i.i.d.) Rayleigh random variables normalized by their own average power P_{in}, which have the following probability density functions [53], [54]:

$$f_X(x) = \frac{2x}{P_{in}} e^{-x^2/P_{in}}. \tag{3.2.4}$$

The probability that at least one value of the whole OFDM symbol exceeds a certain threshold level γ can be given by:

$$\begin{aligned} Pr\{|x[n]| > \gamma\} &= 1 - Pr\{\max_{0 \le n \le N-1} |x[n]| \le \gamma\} \\ &= 1 - (Pr\{|x[n]| \le \gamma\})^N \\ &= 1 - (1 - e^{-\frac{\gamma^2}{\sigma_x^2}})^N \\ &= 1 - (1 - e^{-\gamma})^N, \end{aligned} \tag{3.2.5}$$

where $|x[n]|$ is the magnitude of the OFDM symbol, $P_{in} = \sigma_x^2 = 1$ is the average input power of the samples $x[n]$. Figure 3.1 shows the theoretical and simulated CCDFs of the PAPR of a nonclipped QPSK-OFDM signal with different number of subcarriers i.e. $N = 16$, $N = 32$, $N = 64$, $N = 128$ and $N = 1024$.

This figure compares the analytical result of equation (3.2.5) with the simulated CCDF of a QPSK-OFDM signal for different numbers of subcarriers. It is clearly seen that the probability that the signal power exceeds a given threshold increases with the number of subcarriers N. Moreover, for large values of N, equation (3.2.5) provides a reasonable approximation of the true CCDF. The analytical and simulated results become closer when the number of subcarriers is greater than 64 ($N \geq$

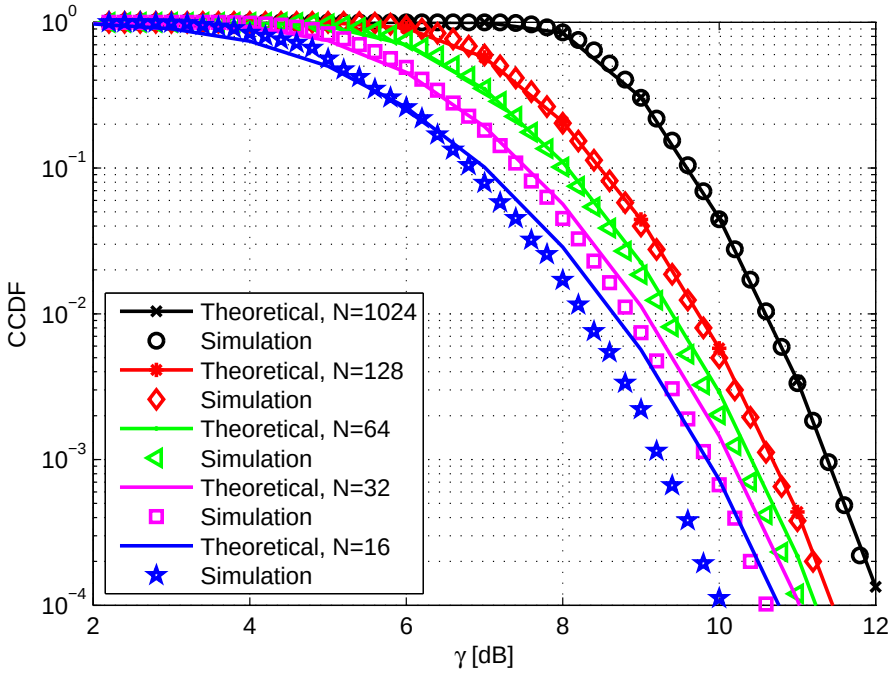

Figure 3.1. Theoretical and simulated CCDF of the PAPR for a nonclipped QPSK-OFDM signal with different number of subcarriers. The theoretical results are shown in line style and the simulation results as points.

64).

It is clear that the PAPR is a major problem in a system which is based on the OFDM technique; therefore, effective PAPR-mitigation techniques are essential to enable the use of efficient non-linear power amplifiers without incurring severe spectral spreading and/or in-band distortion. However, in MIMO-OFDM systems it becomes even more important since there are multiple transmit antennas each of which would require its own RF power amplifier and DAC. A simpler approach to limit the amplitude peaks in an OFDM waveform is described in the subsequent sections.

3.3 Amplitude Clipping

The simplest approach to reduce the PAPR in an OFDM waveform is to deliberately clip the signal before amplification. This operation is normally accomplished at baseband using an envelope limiter. As in Figure 3.2, discontinuities at the clipping instants lead to theoretically infinite bandwidth. This leads to, out-of-band interference which affects signals in adjacent bands and also induces in-band distortion that results in attenuated signal component and clipping noise [52].

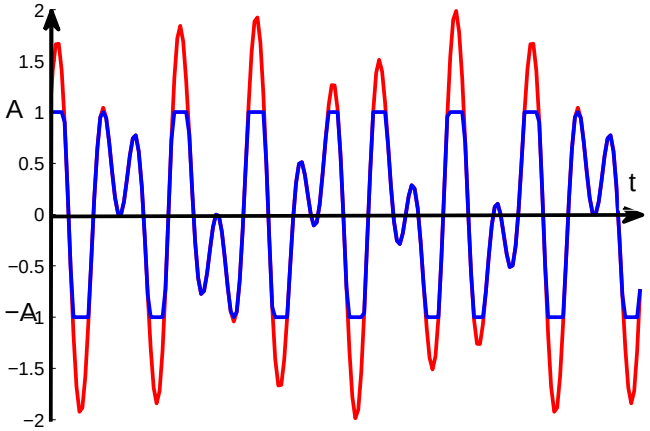

Figure 3.2. The effect of clipping on the transmitted signal.

As a result in transmission, in-band distortion degrades the bit-error-rate (BER) performance while the out-of-band energy reduces the spectral efficiency of the communication system. Oversampling and filtering after clipping can reduce out-of-band radiation, but may also produce some slight peak regrowth in the filtered signal. The oversampling, clipping and filtering processes, will be explained in the next subsection.

3.3.1 Oversampling, clipping and filtering processes

To overcome the out-of-band interference problem which is introduced by the clipping process, oversampling and filtering are used. In practical applications oversampling and filtering are performed digitally before the DAC [52]. The term $X[k]$, $k = 0, 1, \cdots, N-1$, denotes the k^{th} sample of the OFDM symbol duration, where N is the number of OFDM subcarriers, an oversampling factor $J > 1$ can be used, and is achieved by extending $\mathbf{X}$ with $(J-1)N$ zeros.

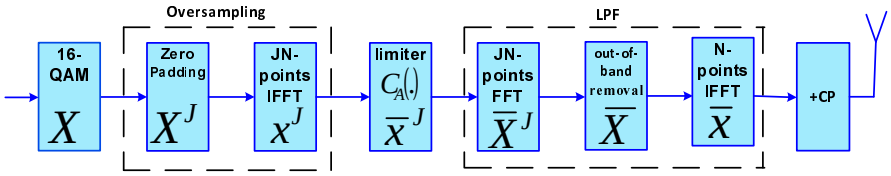

Figure 3.3. Structure of coded clipped source node with J oversampling factor and filtering operation on the transmitter of an OFDM system.

Figure 3.3 shows a block diagram of the coded clipped OFDM system with oversampling and filtering operations. The OFDM block is represented as $\mathbf{X} = [X[0], X[1], \cdots, X[N-1]]^T$, then the OFDM block, $\mathbf{X}$, is oversampled by padding with $(J-1)N$ zeros which yields $\mathbf{X}^J$. Then it can be efficiently generated as the IFFT of the zero-padded data block $\mathbf{x}^J = IFFT(\mathbf{X}^J)$:

$$\begin{aligned} \mathbf{x}^J &= \{[x(0), x(1), \cdots, x(N/2-1), 0, 0, \cdots, 0, 0, \\ &\quad x(JN/2), x(JN/2+1) \cdots, x(JN-1)]^T\}. \end{aligned} \tag{3.3.1}$$

Each oversampled OFDM sample of $\mathbf{x}^J$ is then clipped by an envelope limiter. Then, the clipped elements of $\mathbf{x}^J$ are given as:

$$\begin{aligned}\overline{x}[n]^J &= \mathcal{C}_A(x[n]^J) \\ &= \begin{cases} x[n]^J & |x[n]^J| \leq A \\ Ae^{\arg\{x[n]^J\}} & |x[n]^J| > A \end{cases} \qquad n = 0, 1, \cdot\cdot, JN-1,\end{aligned} \tag{3.3.2}$$

where $\mathcal{C}_A(\cdot)$ denotes the clipping operation with the clipping amplitude A. A clipping ratio (μ) is defined as

$$\mu = \frac{A}{\sqrt{P_{in}}}, \tag{3.3.3}$$

where P_{in} is the average input power of the nonclipped samples $\mathbf{x}^J$. According to the Bussgang theorem [55], [56] and [57], the output memoryless nonlinear (envelope limiter device as in equation (3.3.2)) can be modeled as in equation (3.3.4) which is an aggregate of the original signal which is scaled by factor ξ and clipping noise $\mathbf{d}_{dis}$ as in [3] and [5]

$$\overline{\mathbf{x}} = \xi\ \mathbf{x} + \mathbf{d}_{dis}. \tag{3.3.4}$$

Consequently, the attenuation factor (ξ) is a function of the clipping ratio and is given as $\xi = 1 - e^{-\mu^2} + \frac{\sqrt{\pi}\mu}{2} erfc(\mu)$ [58]. As a result, if the number of subcarriers increases and the clipping ratio value decreases, then, the clipping noise $\mathbf{d}_{dis}$ will be close to complex Gaussian random variables with zero mean and variance $\sigma_d^2 = P_{in}(1 - e^{-\mu^2} - \xi)$ [58] and [59]. Moreover, the clipping process leads to a certain reduction of the output power which can be given as

$$P_{out} = (1 - e^{-\mu^2})P_{in}. \tag{3.3.5}$$

It is clearly seen from equation (3.3.5), $P_{out} = P_{in}$ when the μ tends to ∞ which corresponds to a nonclipped system. In contrast, when μ is zero the output is zero which means the signal is totally distorted by the clipping process.

Then, the clipped samples which are $\overline{\mathbf{x}}^J = [\overline{x}[0], \overline{x}[1], \cdots, \overline{x}[JN-1]]$, pass through a low-pass filter (LPF) as indicated in Figure 3.3. However, the oversampled approach has the advantage of reducing the in-band distortion and leads to slight peak regrowth, but definitely generates out-of-band interference. Therefore, using an LPF is the best technique to remove the out-of-band energy. According to Figure 3.3 the oversampled sequence is transformed in the frequency domain through an FFT operation which produces the following vector of length JN

$$\begin{aligned}\overline{\mathbf{X}}^J = \ & \{[\overline{X}[0], \overline{X}[1], \cdots, \overline{X}[N-1], \overline{X}[N], \\ & \overline{X}[N+1] \cdots, \overline{X}[JN-1]]^T\}. \end{aligned} \tag{3.3.6}$$

Next, out-of-band energy is suppressed by discarding $(J-1)N$ elements from the middle of $\overline{\mathbf{X}}^J$ (out-of-band components) while leaving just N elements unaltered (in-band components). This yields a vector of N modified frequency-domain samples

$$\overline{\mathbf{X}} = [\overline{X}[0], \overline{X}[1], \cdots, \overline{X}[N-1]]^T, \tag{3.3.7}$$

where $\overline{\mathbf{X}}$ is in fact a distorted version of the original data block $\mathbf{X}$. The

vector $\overline{\mathbf{X}}$ is then transformed back in the time domain through an N-point IFFT, which yields the N modified time-domain samples. Then, in practice, the DAC would then convert the signal to analogue form and an RF radio frequency amplifier would be used before the source node broadcasts this data block to all relay nodes.

3.4 Simulation Results

3.4.1 CCDF of the PAPR of the clipped OFDM signal

As in Fig 3.3 the main parameters of the clipped OFDM source node which is used in the proposed system are 1024 subcarriers, a 1/2-rate convolutional code with a constraint length of three, 16-QAM modulation constellation and oversampling and filtering processes.

Figure 3.4 shows the CCDF of the PAPR for a clipped 16-QAM-OFDM signal with $N = 1024$ subcarriers, $\mu = 1$ and oversampling factor is $J = 1$, 2, 4 or 8 compared with nonclipped 16QAM-OFDM signal $\mu = \infty$ with identical subcarriers. Clipping at Nyquist rate oversampling ($J = 1$) reduces the PAPR by approximately 4 dB compared with the nonclipped system. Moreover, approximately 3dB improvement of PAPR is achieved when the oversampling factor is four ($J = 4$). However, the oversampling process becomes less significant when the factor is greater than four ($J > 4$). This confirms that filtering the oversampled and clipped OFDM signal produces much less peak regrowth compared with clipping at the Nyquist rate. Next, the simulation results of clipped SISO-OFDM system and a clipped cooperative decode-and-forward SFBC-OFDM Alamouti scheme network are presented; in both systems the clipping operation is applied at the source

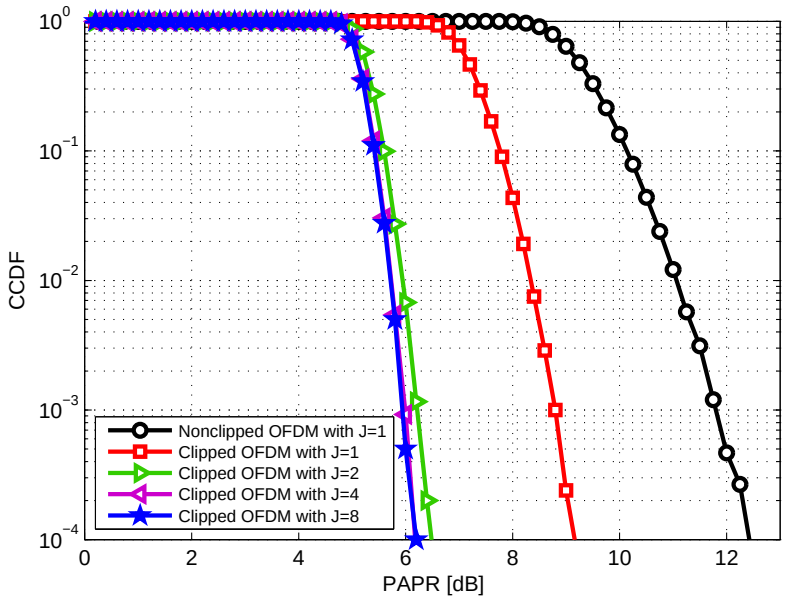

Figure 3.4. CCDF of the PAPR for a nonclipped 16-QAM-OFDM signal and clipped signals with different oversampling factors. The figure confirms that the oversampling process becomes less effective when $J > 4$, as the PAPR is no longer reduced.

node. The simulation of the end-to-end BER as a function of E_b/N_o is presented.

3.4.2 Evaluation of PAPR reduction by clipping method of point-to-point SISO-OFDM and cooperative SFBC-OFDM network

The evaluation of the PAPR reduction by clipping process for two different systems is considered. The first one is a point-to-point SISO-OFDM scheme which is depicted in Fig 3.5 part (A) and the second is a cooperative SFBC-OFDM system which is illustrated in Fig 3.5 part (B). Both systems, include one source node, one destination node with

Viterbi decoder, and the clipping process is performed at the source node. Also the source node of both systems contains a 16-QAM modulation constellation which is coded by a 1/2-rate convolutional code with a constraint length of three, 1024 OFDM subcarriers, oversampling with $J = 4$ factor, envelope limiter, low-pass-filter as in Fig 3.3. In the second system, it is assumed that the destination is beyond the range of the source and, thus, receives signals only from the relays and an ideal DF scheme is used that is capable of fully recovering the original data sequence at the relays. In a cooperative SFBC-OFDM system, the cooperation is performed in two phases. In phase one, the source node broadcasts the clipped data to the two half-duplex single antenna relay nodes R_i, $i = 1, 2$ and then stops sending during the second stage. In the second phase, the two relay nodes generate space frequency block coding of the received signals and then retransmits them to the destination node. In both systems, the channel between any two terminals is assumed to be quasi-static frequency selective Rayleigh fading.

Fig. 3.6 illustrates clearly that the cooperative decode-and-forward SFBC-OFDM system offers better performance compared with the SISO-OFDM system. This is because the spatial diversity gain of the former system is two $D_g = 2$ whereas the diversity gain of the latter system is one $D_g = 1$. It is clear that the clipping process affects the BER performance of both systems, clearly, at the deep clipping ratio. For example, when the clipping ratio $\mu = 0.8$ the BER performance of both schemes is approximately identical which is floored approximately at 10^{-1}. Increasing the clipping ratio to one $\mu = 1$ leads to slight improvement of performance of the SFBC-OFDM system at the low E_b/N_o, however, the performance of both systems is floored ap-

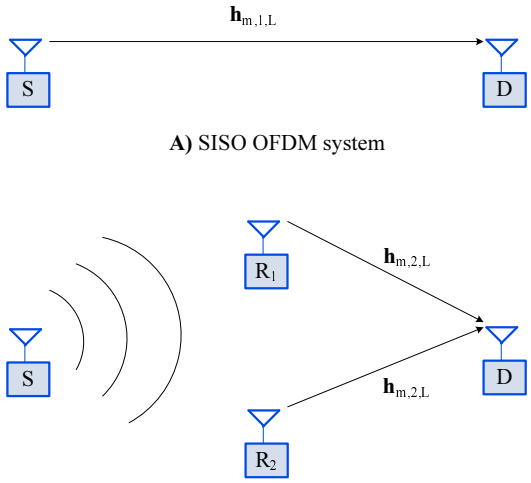

Figure 3.5. A) Block diagram of a SISO-OFDM system, B) Block diagram of a cooperative decode-and-forward SFBC-OFDM system.

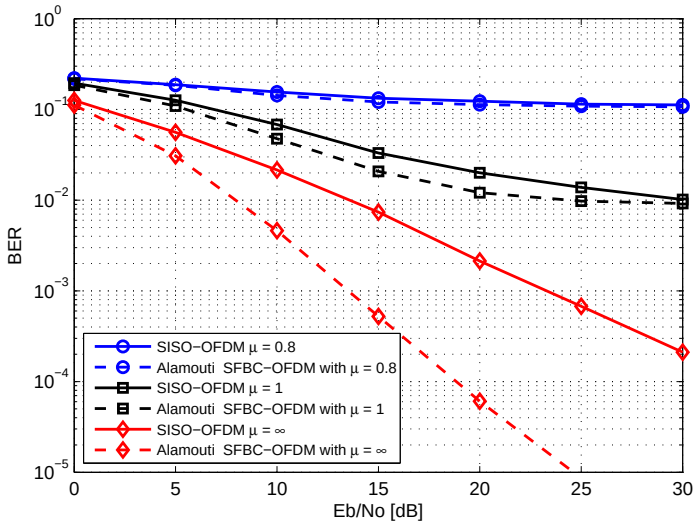

Figure 3.6. BER performance of clipped coded SISO-OFDM system depicted in Fig 3.5 part (A) and cooperative clipped decode-and-forward SFBC-OFDM system illustrated in Fig 3.5 part (B), in both systems the clipping process is implemented at the source node with various clipping ratios ($\mu = 0.8$, 1 and ∞ (nonclipped)) and frequency selective channels.

proximately at 10^{-2} at higher E_b/N_o. In general, this influence depends upon clipping level (μ).

3.5 Summary

A major disadvantage of OFDM is the high PAPR because an OFDM signal is a superposition of N sinusoids modulated by possibly coded data symbols. The peak power can theoretically be up to N times larger than the average power level. Moreover, the time domain OFDM signal can be approximated as a complex Gaussian distributed process with zero main and unity variance, when the number of subcarriers is large. The clipping process is the simplest approach to reduce PAPR, but it induces in-band distortion and out-of-band interferences. However, the PAPR of an OFDM signal can be reduced without any increase in the out-of-band interference by clipping the oversampled time domain signal followed by filtering using an FFT-based, frequency domain filter designed to reject out-of-band discrete frequency components. The filtering operation may cause slight peak regrowth. Therefore, repeated clipping and filtering operations can also be used to further reduce the overall peak regrowth after D/A conversion [60]. In addition, the oversampling process becomes less significant when the factor was greater than four. Then, to overcome the in-band distortion which was introduced by the clipping process, the IAR decoding scheme, which is proposed in [3] and [5], will be used in the cooperative network which contains a source node, four relay nodes and destination node. This will be explained in the next chapter.

Chapter 4

PAPR REDUCTION IN A DISTRIBUTED VIRTUAL MIMO-OFDM WIRELESS NETWORK

4.1 Introduction

By combining the OFDM modulation with a virtual multiple-input multiple-output (MIMO) system, distributed space frequency block codes (DSFBCs) are used to exploit the frequency diversity of the channel. However, the term distributed comes from the fact that the virtual multi-antenna transmitter is distributed between randomly located relay nodes [13]. The presence of multi-paths in broadband channels provides another means for achieving diversity across the frequency axis. Exploiting the frequency axis diversity can highly improve the system performance by achieving cooperative diversity orders. In other words, cooperative diversity is achieved through relay nodes that help the source node by forwarding information [44] and [61]. The strategy of distributed space frequency (DSFB) coding is to distribute the chan-

nel symbols over different space (transmit antennas of relay nodes) and frequency (OFDM tones) within one OFDM block [62].

Diversity techniques are effective means for combating the detrimental effects of broadband wireless channel fading. It is well known that MIMO systems can potentially significantly improve the reliability of communication over fading channels using space time block coding [63]. However, it is difficult to equip small mobile units with more than one antenna due to size and cost constraints. In this case, transmit diversity can generally only be achieved through cooperative multi-node transmission which is known as cooperative diversity [15], where one or more relay nodes are used to forward signals transmitted from the source node to the destination node. In a cooperative communication system, there are two main cooperative methods: decode-and-forward (DF) and amplify-and-forward (AF). Cooperative multi-node diversity schemes can be exploited by using a virtual MIMO-OFDM system. Therefore, this technique has received much attention in recent years [43] due to certain advantages such as high bandwidth efficiency and its robustness to multi-path fading channels. Closed loop extended orthogonal space frequency block coding (EO-SFBC) allows four relays to communicate cooperatively with a common destination as a virtual frequency selective MIMO-OFDM system.

The feedback is needed in the closed-loop system to achieve full spatial diversity and array gains. Although feedback methods can improve the closed-loop system performance, the major problems of such systems is bandwidth overhead. Therefore, two and one-bit feedback was therefore proposed in [1] and [2] to reduce the overhead, respectively. In a practical OFDM system, the angle feedback is required on

a per subcarrier basis. Hence, when using a two or one-bit feedback scheme for each subcarrier, $2N$ or N feedback bits are required per frame, respectively. However, in both schemes, the amount of feedback information is still too large for a practical OFDM system. To overcome this problem, the correlation among the feedback terms for the adjacent subcarriers is exploited. As a result, the amount of feedback can be reduced significantly.

An OFDM signal is a superposition of N usually statistically independent sinusoidal subchannels modulated by possibly coded data symbols. It can constructively sum up to high peaks which theoretically can be up to the number of OFDM subcarriers in magnitude. As a result of this drawback, the system may require more bits to cover a potentially broad dynamic range as well as a large linear range for the radio frequency (RF) power amplifier which is expensive. Moreover, commercial RF power amplifiers can lead to unwanted out-of-band interference and in-band distortion due to operating in the saturation region. Therefore, PAPR becomes even more important in MIMO-OFDM systems because there are multiple transmit antennas each of which would require its own DAC and RF power amplifier [31]. However, there are several solutions to the PAPR problem of OFDM [18]. The clipping method is the simplest solution which increases the BER and adds out-of-band interference. In general, amplitude clipping gives rise to in-band distortion as well as out-of-band interference. Oversampling and filtering is used to reduce out-of-band interference. Moreover, the iterative amplitude reconstruction (IAR) decoding technique proposed in [3] and [5] can be used to mitigate the harmful effects of clipping.

The particular focus in this chapter is a PAPR reduction technique for a general distributed DF and AF type virtual MIMO-OFDM system with four relays and two or one-bit group feedback, building upon the network structure proposed in [3]. The EO-SFBC encoding is implemented at the relay nodes. However, the oversampling, amplitude clipping and filtering are performed at the source and/or relay nodes respectively. The AF type mode is more likely to be a practical candidate when compared to the DF protocol which is proposed in [41] because the former protocol has lower complexity and no error propagation which often happens in the DF case. By exploiting group feedback in the form of phase rotation at two of the relay nodes of the closed loop EO-SFBC scheme it achieves essentially identical rate and cooperative diversity in addition to array gain as a two or one bit per tone scheme which requires increased bandwidth overhead.

4.1.1 The contributions of this work

In this chapter, the system model which has been proposed in [3], is extended by conventional open-loop space frequency block coding (SFBC) and closed-loop EO-SFBC at the relay nodes which allows two and four relays to communicate cooperatively as a virtual MIMO-OFDM system with a common destination over frequency selective fading channels. Moreover, an IAR decoding technique is used to recover the distortion which is introduced by the clipping process at the source node. In addition, the group feedback scheme is proposed to achieve essentially identical rate and cooperative spatial diversity gain in addition to array gain as two or one bit per tone schemes. Perfect knowledge of the channel state information is assumed to be available at the receiver.

4.1.2 The chapter organization

The chapter begins with a brief introduction of PAPR reduction by clipping the OFDM signal at the source node of a distributed cooperative virtual MIMO-OFDM wireless network. Then, the system model of DF distributed EO-SFBC at the relaying nodes includes broadcasting and relaying phases. Further analysis of an AF type distributed closed loop EO-SFBC system with PAPR reduction which includes implementation at the source node and at the relay nodes, together with the IAR decoding technique is presented. Additionally, feedback techniques which are needed to achieve full spatial diversity and array gains, such as two and one-bit feedback schemes and the proposed group feedback, are explained. Finally, simulations and conclusions are drawn.

4.2 System Model of DF Distributed EO-SFBC System with PAPR Reduction

Consider a wireless relay system with one single-antenna source node using clipping, one single-antenna destination node, and four half-duplex relay nodes, as depicted in Figure 4.1. Every relay node in the system has only one antenna which can be used for both transmission and reception. The relays are within the coverage of the source node and assist the source in conveying the information to the destination which is not included in the source coverage region due to path-loss or shadowing effects. Therefore, there is no direct link between the source and destination nodes. Assume the channel between any two terminals is quasi-static frequency selective Rayleigh fading.

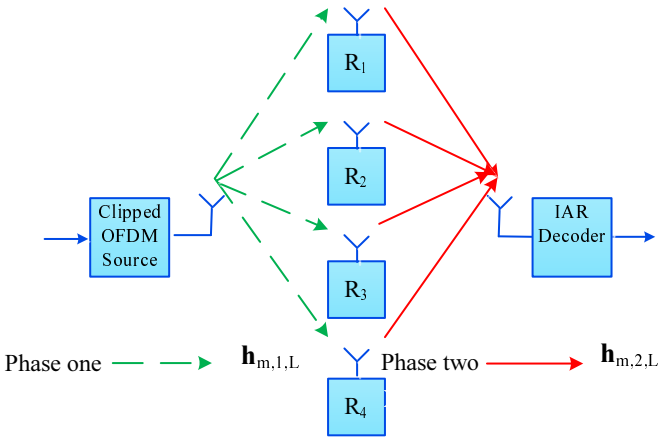

Figure 4.1. Open loop cooperative DF multi-node relaying network with clipped OFDM signal at the source node to reduce PAPR; EO-SFBC is formed at the four relay nodes and one destination with IAR decoding scheme to mitigate the harmful effects of the clipping process.

Next, a short description of the implementation of the clipping process at the source node, SFBC at the relay nodes and the IAR decoder at the destination node will be presented.

4.2.1 Broadcasting phase of clipping OFDM signal at the source node

To reduce the PAPR regrowth at the source (mobile equipment), the OFDM signal to be transmitted should be clipped before amplifying. Although the clipping process reduces the peaks of the OFDM signal, it also induces in-band distortion and out-of-band interference. To overcome the out-of-band interference problem, oversampling before clipping and filtering can reduce out-of-band energy, but may also produce some peak regrowth in the filtered signal. In practical applications, clipping and filtering are performed digitally before the *DAC*. The symbol

$X[k]$, $k = 0, 1, \cdots, N-1$, denotes the k^{th} sample of the OFDM symbol, where N is the number of OFDM subcarriers. The OFDM block is represented as $\mathbf{X} = \{[0],\ X[1],\ \ldots, X[N-1]\}$. To reduce the PAPR of time-domain signals $x[n]$, deliberate clipping might then be performed. Thus, the clipped OFDM sample denoted $\overline{x}[n]$ can be expressed as the aggregate of the original signal which is scaled by factor ξ and the clipping noise $d_{dis}[n]$ as $\overline{x}[n] = \xi x[n] + d_{dis}[n]$. To reduce this effect, before clipping an oversampling factor $J > 1$ can be used, and is achieved by extending $\mathbf{X}$ with $(J-1)N$ zeros. Next, the IFFT of the zero-padded data block $\mathbf{X}^J$ i.e. $\mathbf{x}^J = IFFT(\mathbf{X}^J)$, is clipped by an envelope limiter. Then, the clipped samples pass through a low-pass filter (LPF) which is obtained by using the FFT of $\overline{\mathbf{X}}^J = FFT(\overline{\mathbf{x}}^J)$, and then discarding $(J-1)N$ elements from the middle of the sequence $\overline{\mathbf{X}}^J$ which thereby suppresses out-of-band interference. This yields a vector of N modified frequency-domain samples which is then transformed back in the time domain through an N-point IFFT, and then each modulated block is appended with a cyclic prefix (CP). For convenience, this final time domain block is denoted $\overline{\mathbf{x}}$. In practice, the DAC would then convert the signal to analogue form and an RF radio frequency amplifier would be used before the source node broadcasts the data to the relay nodes.

4.2.2 Relaying phase at the relay nodes

During the relaying phase, the relay nodes receive the transmitted information symbols, the received signal vector $\mathbf{y}_{SR_m}$ of the m^{th} relay, is corrupted by both the multi-path fading coefficients between the source node and the m^{th} relay node $\mathbf{h}_{m,i,L}$ and the noise vector at the m^{th} relay $\mathbf{w}_{R_m}$ which is additive white Gaussian noise (AWGN). Therefore, the

received noisy signals at the relay nodes can be expressed as

$$\overline{\mathbf{y}}_{SR_m} = \sqrt{P_s}\mathbf{H}_{m,1,L}\overline{\mathbf{x}} + \mathbf{w}_{R_m}, \tag{4.2.1}$$

where $\mathbf{H}_{m,1,L}$ represent convolution matrices formed from the coefficients of the source-to-relay channels, the $\mathbf{w}_{R_m}$ vector and $\sqrt{P_s}$ represents the average input power of OFDM signal. The m^{th} relay node removes the cyclic prefix (CP) and then transforms the OFDM signals into the frequency domain by FFT and decodes them to form the vector $\overline{\mathbf{X}}$. However, it is assumed that an ideal DF scheme is used which is capable of fully recovering the original data sequence at the relay nodes. The EO-SFBC encoder generates the code matrix from the neighboring subcarriers, $k = 2v, 2v+1, v = 0, 1, ..., N/2-1$, as follows [64] and [65]:

$$\mathbf{C}[v] = \begin{bmatrix} \overline{X}[2v] & \overline{X}[2v] & -\overline{X}^*[2v+1] & -\overline{X}^*[2v+1] \\ \overline{X}[2v+1] & \overline{X}[2v+1] & \overline{X}^*[2v] & \overline{X}^*[2v] \end{bmatrix}. \tag{4.2.2}$$

Then, the relays generate four coded vectors $\overline{\mathbf{Y}}_{R_1}$, $\overline{\mathbf{Y}}_{R_2}$, $\overline{\mathbf{Y}}_{R_3}$, and $\overline{\mathbf{Y}}_{R_4}$ by extended orthogonal space frequency block encoding as shown below and as described in [64], [66] and [67],

$$\begin{aligned}
\overline{\mathbf{Y}}_{R_1} &= [\overline{X}[0] \quad \overline{X}[1] \quad \overline{X}[2] \quad \overline{X}[3] \quad . \quad . \quad . \quad \overline{X}[N-1]]^T, \\
\overline{\mathbf{Y}}_{R_2} &= [\overline{X}[0] \quad \overline{X}[1] \quad \overline{X}[2] \quad \overline{X}[3] \quad . \quad . \quad . \quad \overline{X}[N-1]]^T, \\
\overline{\mathbf{Y}}_{R_3} &= [-\overline{X}^*[1] \quad \overline{X}^*[0] \quad -\overline{X}^*[3] \quad \overline{X}^*[2] \quad . \quad . \quad . \quad -\overline{X}^*[N-2]]^T, \\
\overline{\mathbf{Y}}_{R_4} &= [-\overline{X}^*[1] \quad \overline{X}^*[0] \quad -\overline{X}^*[3] \quad \overline{X}^*[2] \quad . \quad . \quad . \quad -\overline{X}^*[N-2]]^T,
\end{aligned} \tag{4.2.3}$$

where $(\cdot)^*$ is the complex conjugate. Then, $\overline{\mathbf{Y}}_{R_1}$, $\overline{\mathbf{Y}}_{R_2}$, $\overline{\mathbf{Y}}_{R_3}$, and $\overline{\mathbf{Y}}_{R_4}$ are transmitted simultaneously from R_1, R_2, R_3 and R_4, respectively. The frequency domain representation of the source to relays and from relays to destination node are calculated as $\mathbf{\Lambda}_{m,i,L} = \mathbf{F}\mathbf{H}_{m,i,L}\mathbf{F}^H$ where $\mathbf{F}$ is a normalized DFT matrix. For convenience, as $\mathbf{\Lambda}_{m,i,L}$ is diagonal, a vector $\lambda_{m,i,L} = diag(\mathbf{\Lambda}_{m,i,L})$ is defined. The elements of $\lambda_{m,i,L}[k]$, k = 0, 1, . . ., N-1, denote the required channel gains [3]. The channel gains between adjacent subcarriers are approximately constant $\lambda_{m,i,L}[2v] \approx \lambda_{m,i,L}[2v+1]$, the equivalent channel matrices $\mathbf{C}_e[v]$ corresponding to the code in (4.2.2) used over four relay nodes are given by:

$$\mathbf{C}_e[v] = \begin{bmatrix} \lambda_{1,2,L}[2v] + \lambda_{2,2,L}[2v] & -\lambda_{3,2,L}[2v] - \lambda_{4,2,L}[2v] \\ \lambda^*_{3,2,L}[2v] + \lambda^*_{4,2,L}[2v] & \lambda^*_{1,2,L}[2v] + \lambda^*_{2,2,L}[2v] \end{bmatrix}. \tag{4.2.4}$$

Then, the signal at the receiver is given by

$$\begin{bmatrix} R[2v] \\ R^*[2v+1] \end{bmatrix} = \mathbf{C}_e[v] \begin{bmatrix} \overline{X}[2v] \\ \overline{X}^*[2v+1] \end{bmatrix} + \begin{bmatrix} Z[2v] \\ Z^*[2v+1] \end{bmatrix}. \tag{4.2.5}$$

Thus, the estimated signals $\widehat{\mathbf{X}}[2v]$ and $\widehat{\mathbf{X}}[2v+1]$ at the receiver node can be obtained as follows

$$\begin{bmatrix} \widehat{X}[2v] \\ \widehat{X}[2v+1] \end{bmatrix} = \Delta[v] \begin{bmatrix} \overline{X}[2v] \\ \overline{X}[2v+1] \end{bmatrix} + \mathbf{C}_e[v]^H \begin{bmatrix} Z[2v] \\ Z[2v+1] \end{bmatrix}, \tag{4.2.6}$$

where $\Delta[v] = \mathbf{C}_e[v]^H \mathbf{C}_e[v]$ all the off diagonal terms of which will be zero for an orthogonal block code, then the estimated signals can be given as

$$\begin{aligned} \widehat{X}[2v] &= [\Delta[v]]_{1,1} \overline{X}[2v] + Z'[2v] \\ \widehat{X}[2v+1] &= [\Delta[v]]_{2,2} \overline{X}[2v_1] + Z'[2v+1], \end{aligned} \tag{4.2.7}$$

where

$\overline{X}[2v] = \xi X[2v] + D[2v]$,

$[\Delta[v]]_{1,1} = \Delta[v]]_{2,2} = \alpha[v] + \beta[v]$,

$\alpha[v] = \sum_{m=1}^{4} |\lambda_{m,2,L}[2v]|^2$,

$\beta[v] = 2Re\{(\lambda^*_{2,2,L}[2v]\lambda_{1,2,L}[2v] + \lambda^*_{4,2,L}[2v]\lambda_{3,2,L}[2v])\}$, $Z'[2v] = \lambda^*_{1,2,L}[2v]Z[2v] + \lambda^*_{2,2,L}[2v]Z[2v] - \lambda_{3,2,L}[2v]Z^*[2v+1] - \lambda_{4,2,L}[2v]Z^*[2v+1]$ and

$Z'[2v+1] = \lambda^*_{3,2,L}[2v]Z[2v] + \lambda^*_{4,2,L}[2v]Z[2v] + \lambda_{1,2,L}[2v]Z^*[2v+1] + \lambda_{2,2,L}[2v]Z^*[2v+1]$.

It can be seen from (4.2.7) the estimated signals $\widehat{X}[2v]$ and $\widehat{X}[2v+1]$ can not be completely separated at the receiver because they are affected by clipping noises $D[2v]$ and $D[2v+1]$ from each relay transmission process. Therefore, the IAR scheme is exploited which is proposed in [5] and [68], to reconstruct the clipped EO-SFBC OFDM signals

by comparing the estimated of clipped and nonclipped OFDM samples. Amplify-and-forward distributed closed loop EO-SFBC system with the group feedback relay nodes network to mitigate the effect of the clipping process at the source node will be explained in the next section.

4.3 System Model of AF Type Distributed Closed Loop EO-SFBC System with PAPR Reduction

The cooperative multi-node OFDM communication system includes one clipped OFDM source node S, one destination node D and four half-duplex single antenna relay nodes R_m, $m = 1, 2, 3, 4$. It is also assumed that the received signals at the destination are only from the relays which means there is no direct path between the source and the destination as a consequence, for example, of shadowing loss. Moreover, the communication is based on the AF type technique which means the cooperative transmission is performed in two phases as in Fig. 4.2. In the first phase, the source node S broadcasts the clipped data to the four relay nodes and then stops sending during the second stage. In the second phase, the relay nodes implement a space frequency block coding of the received signals and transmit to the destination node. In addition, the channel impulse response (CIR) from the source node S to relay nodes R_m with channel length L, which are $\mathbf{h}_{m,1,L} = [h_{1,1,L},\ h_{2,1,L},\ h_{3,1,L},\ h_{4,1,L}]^T$ and from R_m to destination node D with the same channel length so the channel is $\mathbf{h}_{m,2,L} = [h_{1,2,L},\ h_{2,2,L},\ h_{3,2,L},\ h_{4,2,L}]^T$. These channel coefficients are assumed to be quasi-static frequency selective Rayleigh fading [61], [3], [69] and [70], as in a slowly varying mobile network.

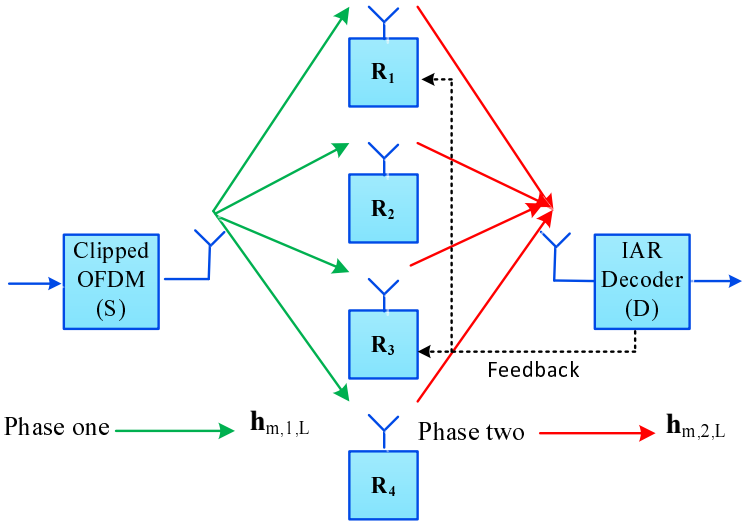

Figure 4.2. Block diagram of an amplify and forward distributed closed loop EO-SFBC OFDM cooperative system with two node feedback, clipped at the source and IAR decoder.

4.3.1 Implementation at the source node

In this phase, the source node broadcasts the clipped information symbols $\overline{X} = [\overline{X}[0], \overline{X}[1], \cdots, \overline{X}[N-1]]^T$ after converting the clipped frequency domain signal into the time domain with an IFFT, a cyclic prefix is added, passed through a DAC which converts the signal to analogue form and an RF power amplifier is used, to the relay nodes, where $(.)^T$ denotes vector transpose. During this phase, the relay nodes receive the transmitted information symbols, in fact, the received signal vector at the m^{th} relay, which is denoted as $\mathbf{y}_{SR_m}$, is corrupted by both the multi-path fading coefficients between the source node and the m^{th} relay node $\mathbf{h}_{m,i,L}$ and the noise vector at the m^{th} relay $\mathbf{w}_{R_m}$ which is an additive white Gaussian noise (AWGN). Therefore, the received noisy signals at the relay nodes can be expressed as

$$\overline{\mathbf{y}}_{SR_m} = \sqrt{P_s}\mathbf{H}_{m,1,L}\overline{\mathbf{x}} + \mathbf{w}_{R_m}, \tag{4.3.1}$$

where $\sqrt{P_s}$ represents the average input power of OFDM signal, $\mathbf{H}_{m,1,L}$ represent convolution matrices formed from the coefficients of the source-to-relay channels and $\mathbf{w}_{R_m}$ vector. Next, the source node stops sending during the second stage. In the second time slot, the four relay nodes generate space frequency block coding of the received signals and transmit to the destination node.

4.3.2 Implementation of EO-SFBC at the relay nodes

In the second phase, the four relay nodes convert their received clipped time domain signal into the frequency domain with the FFT and the relays generate four coded vectors $\overline{\mathbf{Y}}_{R_1}$, $\overline{\mathbf{Y}}_{R_2}$, $\overline{\mathbf{Y}}_{R_3}$, and $\overline{\mathbf{Y}}_{R_4}$ by space frequency block encoding, as in equation (4.3.2) which is described in [64] and [67].

$$\begin{aligned}
\overline{\mathbf{Y}}_{R_1} &= [\overline{Y}_1[0] \quad \overline{Y}_1[1] \quad \overline{Y}_1[2] \quad \overline{Y}_1[3] \quad . \quad . \quad . \quad \overline{Y}_1[N-1]]^T, \\
\overline{\mathbf{Y}}_{R_2} &= [\overline{Y}_2[0] \quad \overline{Y}_2[1] \quad \overline{Y}_2[2] \quad \overline{Y}_2[3] \quad . \quad . \quad . \quad \overline{Y}_2[N-1]]^T, \\
\overline{\mathbf{Y}}_{R_3} &= [-\overline{Y}_3^*[1] \quad \overline{Y}_3^*[0] \quad -\overline{Y}_3^*[3] \quad \overline{Y}_3^*[2] \quad . \quad . \quad . \quad -\overline{Y}_3^*[N-2]]^T, \\
\overline{\mathbf{Y}}_{R_4} &= [-\overline{Y}_4^*[1] \quad \overline{Y}_4^*[0] \quad -\overline{Y}_4^*[3] \quad \overline{Y}_4^*[2] \quad . \quad . \quad . \quad -\overline{Y}^*[N-2]]^T,
\end{aligned} \tag{4.3.2}$$

During the block, $\overline{\mathbf{Y}}_{R_1}$, $\overline{\mathbf{Y}}_{R_2}$, $\overline{\mathbf{Y}}_{R_3}$, and $\overline{\mathbf{Y}}_{R_4}$ are transmitted simultaneously from R_1, R_2, R_3 and R_4 respectively. It has been assumed that the total transmission power in the whole scheme is P_t, the power

of the source node is P_s and the power allocation which is used in this proposed scheme is:

$$P_s = M_R P_r = \frac{P_t}{2}, \tag{4.3.3}$$

where P_r denotes the average transmission power at every relay node and M_R is the number of relay nodes. The EO-SFBC encoder generates coding matrices for the neighboring subcarriers, $k = 2v, 2v+1, v = 0, 1, ..., \frac{N}{2} - 1$, across all four relays as follows [64]:

$$\mathbf{C}[v] = \rho \begin{bmatrix} \overline{Y}_1[2v] & \overline{Y}_2[2v] & -\overline{Y}_3^*[2v+1] & -\overline{Y}_4^*[2v+1] \\ \overline{Y}_1[2v+1] & \overline{Y}_2[2v+1] & \overline{Y}_3^*[2v] & \overline{Y}_4^*[2v] \end{bmatrix}, \tag{4.3.4}$$

where $\rho = \sqrt{\frac{P_r}{P_s+1}}$ and $Ps+1$ is the mean power of the relay signal due to the unit variance assumption of the elements of the additive noise vector $\mathbf{W}_{R_m}$. In this work only the spatial diversity is exploited in the channels. Practically, with higher number of subcarriers, the complex channel gains between adjacent subcarriers are approximately constant $\lambda_{m,i,L}[2v] \approx \lambda_{m,i,L}[2v+1]$, so the matrix $\mathbf{C}_e[v]$ is defined as:

$$\mathbf{C}_e[v] = \begin{bmatrix} \lambda_1[2v] + \lambda_2[2v] & -\lambda_3[2v] - \lambda_4[2v] \\ \lambda_3^*[2v] + \lambda_4^*[2v] & \lambda_1^*[2v] + \lambda_2^*[2v] \end{bmatrix}, \tag{4.3.5}$$

where

$$\begin{aligned}\lambda_1[2v] &= \lambda_{1,1,L}[2v]\lambda_{1,2,L}[2v],\\ \lambda_2[2v] &= \lambda_{2,1,L}[2v]\lambda_{2,2,L}[2v],\\ \lambda_3[2v] &= \lambda_{3,1,L}[2v]\lambda_{3,2,L}[2v],\\ \lambda_4[2v] &= \lambda_{4,1,L}[2v]\lambda_{4,2,L}[2v]\end{aligned} \tag{4.3.6}$$

and $\lambda_{m,1,L}[2v]$ and $\lambda_{m,2,L}[2v]$ are the channel frequency responses of the channel impulse response (CIR) of $\mathbf{h}_{m,1,L}$ and $\mathbf{h}_{m,2,L}$, $m = 1, 2, 3, 4$ which denote the four relay nodes in the system. The channel coefficients are modeled by independent zero-mean complex Gaussian random variables with 0.5 variance per dimension. Therefore, the signal vector at the receiver is given by

$$\begin{bmatrix} R[2v] \\ R^*[2v+1] \end{bmatrix} = \rho\mathbf{C}_e[v] \begin{bmatrix} \overline{X}[2v] \\ \overline{X}^*[2v+1] \end{bmatrix} + \begin{bmatrix} Z[2v] \\ Z^*[2v+1] \end{bmatrix}, \tag{4.3.7}$$

where

$$\begin{aligned}R[2v] = \rho(&\lambda_1[2v]\overline{X}[2v] + \lambda_2[2v]\overline{X}[2v] - \lambda_3[2v]\overline{X}[2v+1]\\ &-\lambda_4[2v]\overline{X}[2v+1]) + Z[2v]\end{aligned} \tag{4.3.8}$$

and

$$R[2v+1] = \rho(\lambda_3^*[2v]\overline{X}[2v] + \lambda_4^*[2v]\overline{X}[2v] + \lambda_1^*[2v]\overline{X}[2v+1] + \lambda_2^*[2v]\overline{X}[2v+1]) + Z[2v+1] \quad (4.3.9)$$

and $\mathbf{Z} = [Z[2v], Z[2v+1]]^T$ is the equivalent noise vector, $\overline{\mathbf{X}}$ is the transmitted clipped signal vector. Assuming the channel impulse responses are known or can be estimated accurately at the receiver, the space frequency decoder constructs the decision estimate vector $\widehat{\mathbf{X}}$ as:

$$\begin{bmatrix} \widehat{X}[2v] \\ \widehat{X}[2v+1] \end{bmatrix} = \Delta[v] \begin{bmatrix} \overline{X}[2v] \\ \overline{X}[2v+1] \end{bmatrix} + \mathbf{C}_e[v]^H \begin{bmatrix} Z[2v] \\ Z[2v+1] \end{bmatrix}, \quad (4.3.10)$$

where $\Delta[v] = \mathbf{C}_e[v]^H \mathbf{C}_e[v]$ all the off diagonal terms of will be zero for an orthogonal block code, then the estimated signals can be given as

$$\begin{aligned} \widehat{X}[2v] &= [\Delta[v]]_{1,1}\overline{X}[2v] + Z'[2v] \\ \widehat{X}[2v+1] &= [\Delta[v]]_{2,2}\overline{X}[2v_1] + Z'[2v+1], \end{aligned} \quad (4.3.11)$$

where

$\overline{X}[2v] = \xi X[2v] + D[2v]$,

$[\Delta[v]]_{1,1} = [\Delta[v]]_{2,2} = \alpha[v] + \beta[v]$,

$\alpha[v] = \sum_{m=1}^{4} |\lambda_m[2v]|^2$,

$\beta[v] = 2Re\{(\lambda_2^*[2v]\lambda_1[2v] + \lambda_4^*[2v]\lambda_3[2v])\}$,

$Z'[2v] = \lambda_1^*[2v]Z[2v] + \lambda_2^*[2v]Z[2v] - \lambda_3[2v]Z^*[2v+1] - \lambda_4[2v]Z^*[2v+1]$

and

$Z'[2v+1] = \lambda_3^*[2v]Z[2v] + \lambda_4^*[2v]Z[2v] + \lambda_1[2v]Z^*[2v+1] + \lambda_2[2v]Z^*[2v+1]$. It can also be seen from (4.3.11) the estimated signals $\widehat{X}[2v]$ and $\widehat{X}[2v+1]$ can not be completely separated at the receiver because they are affected by clipping noises $D[2v]$ from each relay transmission process. Therefore, the IAR scheme is exploited which is proposed in [5] and [68], to reconstruct the clipped EO-SFBC OFDM signals by comparing the estimated of clipped and nonclipped OFDM samples. The IAR implementation will be explained in the next subsection.

4.3.3 Destination node processing

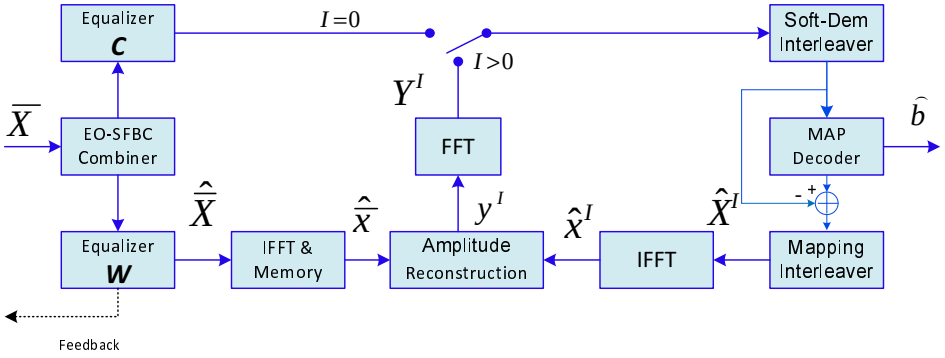

Figure 4.3. Block diagram of an iterative amplitude reconstruction decoder originally proposed in [3], where $\overline{\mathbf{x}}$ is the input to be decoded and $\widehat{\mathbf{b}}$ is the estimated symbol vector.

The IAR implementation is explained as follows:

1. **C** is the minimum mean square error (MMSE) equalizer tap coefficient vector. The main purpose of it is to obtain the initial estimate of the nonclipped samples at the k^{th} subcarrier, $C[k]$, is given by

$$C[k] = \frac{\xi P_{in}}{(\xi^2 P_{in} + \sigma_D^2)\Delta_{1,1}[k] + \sigma_{Z'}^2} \quad k = 0, 1, \cdots, N-1. \quad (4.3.12)$$

where $\sigma_{Z'}^2$ is the variance of the elements of $\mathbf{Z}'$. Then, the output of MMSE equalizer vector $\mathbf{C}$ is demapped, deinterleaved, and fed into a maximum a-posteriori (MAP) decoder. Thus, the non-clipped OFDM samples, $\widehat{X}^I[k]$, can be estimated from the extrinsic information of MAP decoder output, where I represents the iteration number and starts with an initial value of $I = 0$.

2. $\mathbf{W}$ is the minimum mean square error (MMSE) equalizer tap coefficient vector. The function of this equalizer is to estimate the clipped sample vector $\overline{\mathbf{x}}$, which is obtained and stored in memory by performing an IFFT on $\widehat{\overline{\mathbf{X}}}$ [5], [68] and [71]. The elements of $\mathbf{W}$ are given by

$$W[k] = \frac{\xi^2 P_{in} + \sigma_D^2}{(\xi^2 P_{in} + \sigma_D^2)\Delta_{1,1}[k] + \sigma_{Z'}^2} \quad k = 0, 1, \cdots, N-1. \quad (4.3.13)$$

3. **Soft decision** maps the input from the MMSE equalizer $\mathbf{C}$ into in-phase and quadrature components of the complex symbol. In general, a soft decision is simply performed on the received signals for BPSK and on separate in-phase and quadrature components for QPSK. However, it is quite complicated for 16-QAM modulation because each axis carries more than one bit in the soft-output demapper. $M = 2^4$ is the number of symbols of the square 16-

QAM constellation, so that bits are mapped into in-phase and quadrature components of the complex symbol. Let $Y^I[k] = Y_I^I[k]+jY_Q^I[k]$ denote the input signals and $\{D_{I,1}, D_{I,2}, D_{Q,1}, D_{Q,2}\}$ the output bit sequence of the soft demapper [72]. The in-phase terms $\{D_{I,1}, D_{I,2}\}$ can be evaluated as

$$D_{I,1} = \begin{cases} Y_I^I[k], & |Y_I^I[k]| \leq 2 \\ 2(Y_I^I[k]-1), & Y_I^I[k] > 2 \\ 2(Y_I^I[k]+1), & Y_I^I[k] < 2 \end{cases}, \tag{4.3.14}$$

$$D_{I,2} = -|Y_I^I[k]| + 2. \tag{4.3.15}$$

The soft decision for the two quadrature bits $\{D_{Q,1}, D_{Q,2}\}$ is the same as Equations (4.3.14) and (4.3.15) with $Y_I^I[k]$ replaced by $Y_Q^I[k]$. The output is demapped, deinterleaved, and fed into a maximum a-posteriori (MAP) decoder.

4. **Maximum a-posteriori (MAP) decoder** is used to estimate the nonclipped OFDM samples, $\widehat{X}^I[k]$ from the extrinsic information output, where I represents the iteration number and starts with an initial value of $I = 0$. However, MAP decoding exploits a-priori probabilities to minimize the bit error probability of all code words [36], [73] and [74]. Then, the estimates of the nonclipped time domain samples are formed by applying an IFFT, so $\widehat{\mathbf{x}}^I = IFFT(\widehat{\mathbf{X}}^I)$, is fed into the amplitude reconstruction stage.

5. **Amplitude reconstruction** compares the amplitude of the estimated clipped time domain samples $\hat{\mathbf{x}}^I$ with the estimated non-clipped time domain samples $\widehat{\bar{\mathbf{x}}}$ which generates a new sequence $\mathbf{y}^I$, the elements of which are found as

$$y^{(I)}[n] = \begin{cases} \widehat{\bar{x}}[n], & |\hat{x}^{(I)}[n]| \leq A \\ |\hat{x}^{(I)}[n]|e^{\arg\{\widehat{\bar{x}}[n]\}}, & |\hat{x}^{(I)}[n]| > A \end{cases}, \; n = 0, 1, \cdots, N-1. \tag{4.3.16}$$

6. The sequence $y^I[n]$ is converted to the frequency domain and then fed to the soft demapping, deinterleaving, and MAP decoding.

Also in this network scheme the feedback technique is required to reach full cooperative spatial diversity and array gains, which will generally cost bandwidth overhead. For this reason, feedback reduction techniques will be studied in the next section.

4.4 Feedback Reduction Techniques

For an orthogonal block code, all the off diagonal terms of $\Delta[v] = \mathbf{C}_e[v]^H\mathbf{C}_e[v]$ will be zero. It has been assumed that the complex channel gains between adjacent subcarriers are approximately constant $\lambda_1[2v] \approx \lambda_2[2v+1]$. It is thus reasonable to expect the EO-SFBC-OFDM transmit diversity system to achieve full diversity. However, the interference factor $\beta[v]$ as shown in equation (4.4.1) may reduce the performance of the scheme. In order to achieve maximum performance such as full diversity and array gain, the feedback scheme has been used to modify the transmitted signals from certain relay nodes by rotating with an

appropriate phase angle to ensure that the $\beta[v]$ term is positive and maximized during the transmission period [64]

$$\Delta[v] = \begin{bmatrix} \alpha[v] + \beta[v] & 0 \\ 0 & \alpha[v] + \beta[v] \end{bmatrix}, \tag{4.4.1}$$

where $\alpha[v] = \sum_{m=1}^{4} |\lambda_m[2v]|^2$ and the factor $\beta[v] = \beta_1[v] + \beta_2[v]$ where $\beta_1[v] = 2\Re\{\lambda_1[2v]\lambda_2^*[2v]\}$ and $\beta_2[v] = 2\Re\{\lambda_3[2v]\lambda_4^*[2v]\}$. These terms may reduce channel gain, and correspondingly the signal-to-noise ratio (SNR), which can be shown as

$$SNR = (\sum_{m=1}^{4} |\lambda_m[2v]|^2 + \beta_1[v] + \beta_2[v])\frac{\sigma_x^2}{\sigma_n^2}, \tag{4.4.2}$$

where the operator $|\cdot|^2$ denotes the modulus squared of a complex number, $\Re\{\cdot\}$ its real part, σ_x^2 is the total transmit power of the desired signal and σ_n^2 is the noise power at the receiver.

4.4.1 Two-bit feedback scheme proposed in [1]

In order to maximize the system gain, therefore, the phase of the two relay nodes is rotated by $e^{j\theta_1[v]}$ and $e^{j\theta_2[v]}$, which are denoted by $U_1[v]$ and $U_2[v]$ respectively. As in Fig. 4.2 the destination feedback is only to R_1 and R_3 which means before the signals are transmitted from the first and third relay nodes, they are multiplied by $U_1[v]$ and $U_2[v]$, respectively, which guarantees the factors $\beta_1[v]$ and $\beta_2[v]$ are non negative, so that the channel matrix of EO-SFBC is:

$$\mathbf{C}_e[v] = \begin{bmatrix} U_1[v]\lambda_1[2v] + \lambda_2[2v] & -U_2[v]\lambda_3[2v] - \lambda_4[2v] \\ U_2[v]\lambda_3^*[2v] + \lambda_4^*[2v] & U_1[v]\lambda_1^*[2v] + \lambda_2^*[2v] \end{bmatrix}. \quad (4.4.3)$$

So,

$$\begin{aligned} \beta_1[v] &= 2\Re\{U_1\lambda_1[2v]\lambda_2^*[2v]\} \\ \beta_2[v] &= 2\Re\{U_2\lambda_3[2v]\lambda_4^*[2v]\}, \end{aligned} \quad (4.4.4)$$

where $U_1[v] = e^{j\theta_1[v]}$ and $U_2[v] = e^{j\theta_2[v]}$ [64]. The exact phase angles $\theta_1[v]$ and $\theta_2[v]$ can be computed as

$$\begin{aligned} \theta_1[v] &= -angle(\lambda_1[2v]\lambda_2^*[2v]) \\ \theta_2[v] &= -angle(\lambda_3[2v]\lambda_4^*[2v]). \end{aligned} \quad (4.4.5)$$

The perfect rotation phase angle requires many feedback bits which in practice may not be possible due to the very limited feedback bandwidth. Therefore, the phase angles should be quantized, and then these levels are fed back to the relay nodes. As a good example, a two-bit feedback scheme which has been proposed in [1], [75] and [76], in this case, feeding back only four phase level angles, such that the phase angles are from the set of $\{\Theta_1[v], \Theta_2[v]\} \in \Omega = [0,\ \pi/2,\ \pi\ or\ 3\pi/2]$ then for the first relay node phase antenna adjustment, the discrete feedback information corresponding to the phases may be selected according to

$$\Theta_1[v] = \arg \max_{\theta_1[v] \in \Omega} \Re\{(\lambda_1[2v]\lambda_2^*[2v])e^{j\theta_1[v]}\}. \quad (4.4.6)$$

Similarly, for the third relay node antenna phase adjustment, the phases may be selected according to

$$\Theta_2[v] = \arg \max_{\theta_2[v]\in\Omega} \Re\{\lambda_3[2v]\lambda_4^*[2v])e^{j\theta_2[v]}\}. \tag{4.4.7}$$

Selecting the largest values of (4.4.6) and (4.4.7) may be preferable, as it would achieve full cooperative diversity advantage and provide the largest array gain. According to the analysis in [1] $U_1[v] = (-1)^{a[v]}$ and $U_2[v] = (-1)^{b[v]}$, where a[v], b[v] = 0, 1, which means using 0 or π as the rotation angle for the signals. The criterion to determine the two-bit feedback value of $U_1[v]$ and $U_2[v]$ is that each element of the feedback performance gain $\beta_1[v]$ and $\beta_2[v]$ in (4.4.10) should be nonnegative

$$(a[v], b[v]) = \begin{cases} (0,0), \text{if } \Re\{\lambda_1[2v]\lambda_2^*[2v]\} \geq 0 \text{ and } \Re\{\lambda_3[2v]\lambda_4^*[2v]\} \geq 0 \\ (0,1), \text{if } \Re\{\lambda_1[2v]\lambda_2^*[2v]\} \geq 0 \text{ and } \Re\{\lambda_3[2v]\lambda_4^*[2v]\} < 0 \\ (1,0), \text{if } \Re\{\lambda_1[2v]\lambda_2^*[2v]\} < 0 \text{ and } \Re\{\lambda_3[2v]\lambda_4^*[2v]\} \geq 0 \\ (1,1), \text{if } \Re\{\lambda_1[2v]\lambda_2^*[2v]\} < 0 \text{ and } \Re\{\lambda_3[2v]\lambda_4^*[2v]\} < 0 \end{cases} \tag{4.4.8}$$

In this scheme the number of feedback bits is still proportional to double the length of the OFDM block ($2N$). Therefore, in the next subsection another method to reduce the feedback overhead will be presented.

4.4.2 One-bit feedback scheme proposed in [2]

More feedback reduction can be exploited when $\theta_1[v] = \theta_2[v]$, which means just one common phaser $e^{j\theta[v]}$ can be used to rotate the transmitted symbols from the first and third relay nodes and the rotation angle is selected from a range between 0 and 2π. It is apparent that this does not change the transmitted power. Since the phase rotation on the transmitted symbols is effectively equivalent to rotating the phases of the corresponding channel coefficients, the new channel gain can be written as

$$SNR = (\sum_{m=1}^{4} |\lambda_m[2v]|^2 + \beta[v])\frac{\sigma_x^2}{\sigma_n^2}. \tag{4.4.9}$$

So,

$$\beta[v] = 2\Re\{\lambda_1[2v]\lambda_2^*[2v] + \lambda_3[2v]\lambda_4^*[2v]\}. \tag{4.4.10}$$

Then, the exact phase angles $\theta[v]$ can be computed as

$$\theta[v] = -angle(\lambda_1[2v]\lambda_2^*[2v] + \lambda_3[2v]\lambda_4^*[2v]). \tag{4.4.11}$$

Also, another good example for a one-bit feedback scheme has been proposed in [2]; in this case, feeding back only two phase level angles is employed, such that the phase angles are from the set of $\{\Theta[v]\} \in \Omega = [0,\ 2\pi]$; then for the first and third relay node phase antenna adjustment, the discrete feedback information corresponding to the phases

may be selected according to

$$\Theta[v] = \arg \max_{\theta[v] \in \Omega} \Re\{(\lambda_1[2v]\lambda_2^*[2v] + \lambda_3[2v]\lambda_4^*[2v])e^{j\theta[v]}\}. \quad (4.4.12)$$

Selecting the largest values of (4.4.12) may be preferable, as it would achieve full cooperative diversity advantage and provide the largest array gain. According to the analysis in [2] $U[v] = (-1)^{a[v]}$, where $a[v] = 0, 1$, which is the simplest feedback with minimal overhead could be one-bit feedback on $\theta[v]$ with two choices, either $\theta[v] = 0$ or π. The criterion to implement the one-bit feedback scheme as follows

$$a[v] = \begin{cases} 0, \text{if } \Re\{\lambda_1[2v]\lambda_2^*[2v] + \lambda_3[2v]\lambda_4^*[2v]\} \geq 0 \\ 1, \text{otherwise.} \end{cases} \quad (4.4.13)$$

In this scheme the number of feedback bits is still proportional to the length of OFDM block (N). Therefore, in the next subsection another efficient method to reduce the feedback overhead will be studied.

4.4.3 Feedback reduction via correlation among OFDM subcarriers

The group feedback strategy is to exploit the high correlation that exists among OFDM subcarriers. It is based on dividing the OFDM subcarriers into size N_g adjacent groups and hence feedback one quantized phase for each group instead for each subcarrier. The phase angles required are determined according to the majority of phase angles within each group. By this way, the feedback overhead can be reduced by a

factor from $\frac{N}{N_g}$ to $\frac{2N}{N_g}$, while the BER performance of the system will be shown to be almost the same as the one or two-bit per tone.

The effects of size of group feedback on the BER performance of the DF and AF distributed clipped closed loop EO-SFBC OFDM systems with one and two-bit feedbacks have been studied. For both schemes, a range of group sizes, N_g, e.g. 64, 32 and 16 have been considered and compared with full one or two-bits per OFDM tone. From the BER performance, exploiting 32 and 64 adjacent subcarriers leads to degradation in the BER, as shown in Figure 4.6; whereas, exploiting the correlation between 16 adjacent subcarriers achieves almost identical performance to the full one or two-bit per OFDM tone. This results in a saving of 93.75% in terms of total number of feedback bits required as compared with the one and two-bit per tone feedback.

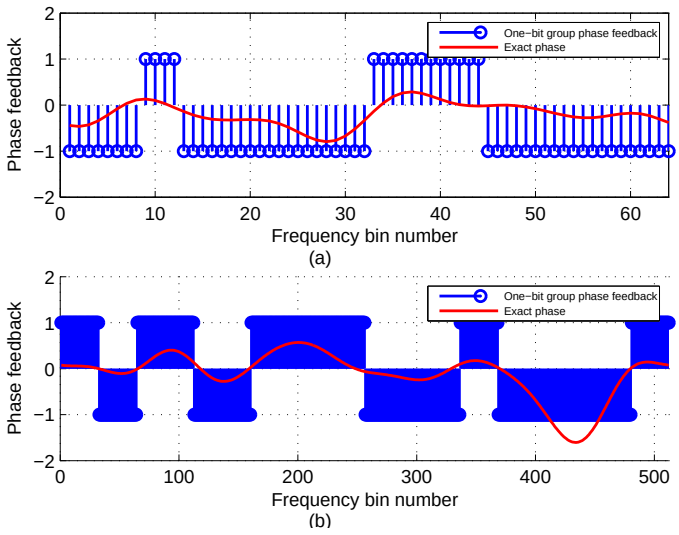

Figure 4.4. Instantaneous OFDM phase rotation and group feedback scheme with i.e. (a) OFDM block length $N = 128$ and group size $N_g = 4$ subcarriers using one-bit. (b) OFDM block length $N = 1024$ and group size $N_g = 16$ subcarriers using one-bit feedback.

Next, simulation results are presented.

4.5 Simulation Results

The simulation of the proposed DF and AF cooperative MIMO OFDM systems which consist of a source node (S), four relay nodes R_m and destination node (D) with IAR decoding scheme is presented. The main parameters of both systems are the clipping process at the source node, EO-SFBC at relay nodes, a coded OFDM signal with 1024 subcarriers, a 1/2-rate convolutional code with a constraint length of three, 16-QAM modulation constellation and the EO-SFBC encoding is applied in the relays. Additionally, all links are assumed to be quasi-static frequency selective channels.

4.5.1 Decode-and-forward cooperative network simulation

In the simulation, a comparison of the BER for the system with full per tone two-bit feedback and the proposed two-bit group feedback is performed. Moreover, decode and forward is assumed in distributed transmission.

The results are depicted Fig. 4.5 and it is confirmed that the performance of the DF distributed EO-SFBC cooperative system without feedback with three iterations of IAR scheme with the BER of 10^{-4} of the open loop EO-SFBC scheme requires approximately 17 dB. However, closed loop EO-SFBC with two-bit feedback scheme gives better performance by approximately 12.9 dB at 10^{-4} BER compared with open loop EO-SFBC. However, the former scheme has $2N$ bits overhead. To overcome this problem, the feedback correlation among subcarriers is exploited to reduce the feedback overhead significantly while

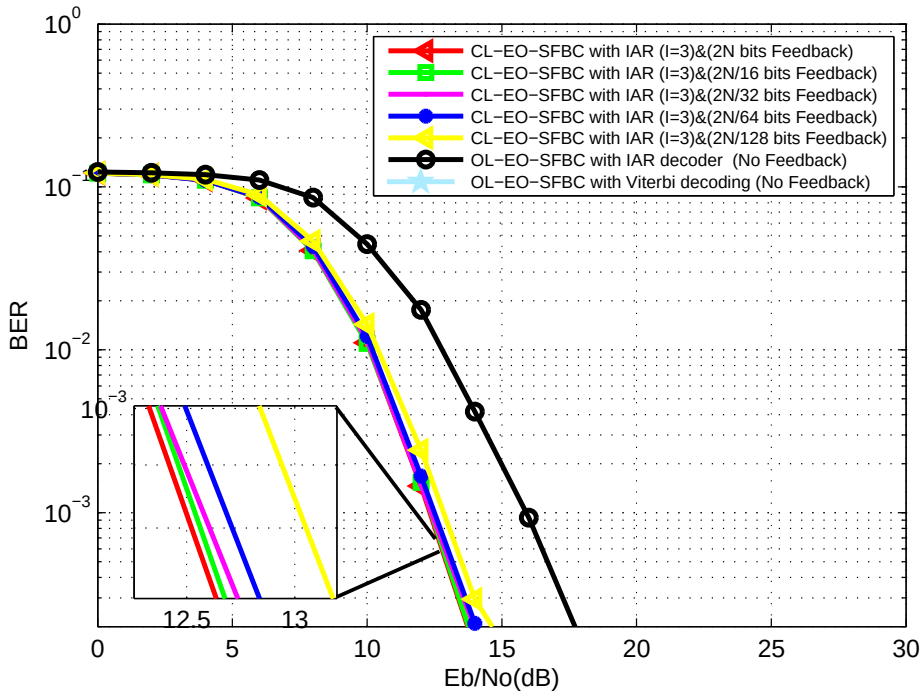

Figure 4.5. BER performance of the decode and forward distributed clipped closed loop EO-SFBC OFDM system, two-bit feedback ($2N$ = 2048 bits) and two-bit group feedback (128, 64, 32 and 16 bits per OFDM block) and decoded by the IAR scheme compared with clipped open loop EO-SFBC OFDM system decoded by Viterbi decoder. In both schemes the clipping ratio ($\mu = 1$).

maintaining satisfactory diversity performance. By exploiting the coherence of the channel in the frequency domain of 16 OFDM tones, as a group; very little degradation in BER performance is formed. For example, an OFDM block with 1024 subcarriers needs 2048 bits feedback, in contrast, by exploiting the correlation between 16 adjacent subcarriers as group feedback needs 128 bits to achieve almost identical performance, which means a saving of 93.75% as compared with two-bit feedback. In addition to that, exploiting 32 adjacent subcarriers leads to save 96.88% as compared with the previous scheme and it

degrades the BER by approximately 0.2 dB at 10^{-4}.

4.5.2 Amplify-and-forward cooperative network simulation

In this simulation, a comparison of the BER for the amplify-and forward system with full per tone one-bit feedback and the proposed one-bit group feedback is performed.

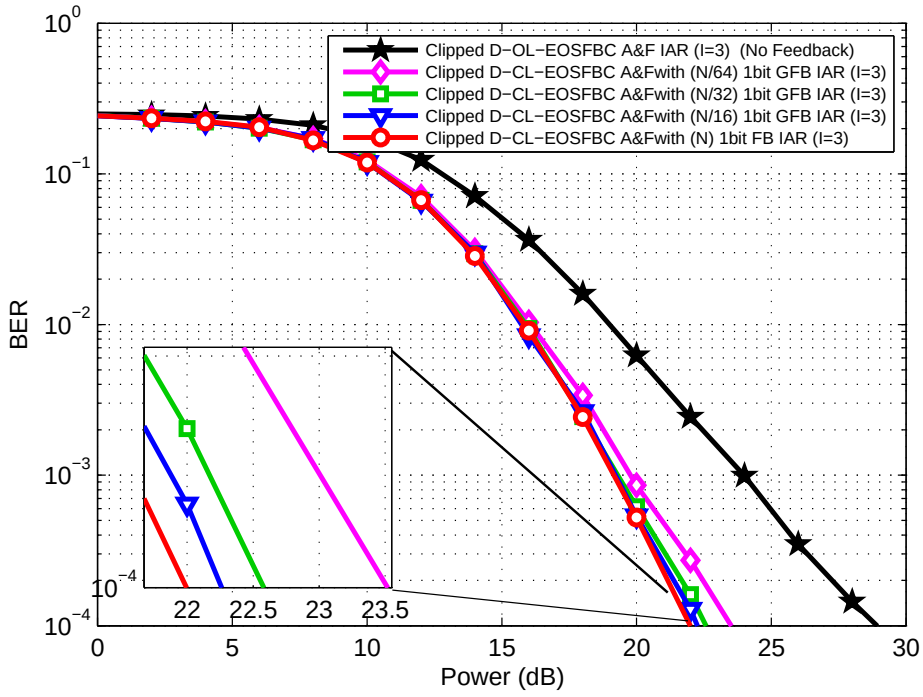

Figure 4.6. Comparison of BER performance of the amplify and forward distributed closed loop EO-SFBC OFDM system with one-bit group feedback (1024, 64, 32 and 16 bits per OFDM block) and decoded by the IAR scheme compared with clipped open loop EO-SFBC OFDM system decoded by Viterbi decoder. In both schemes the clipping ratio ($\mu = 1$).

The results are depicted Fig. 4.6 and the performance of the AF type distributed EO-SFBC cooperative system without feedback with three iterations of IAR scheme with the BER of 10-4 of the open loop

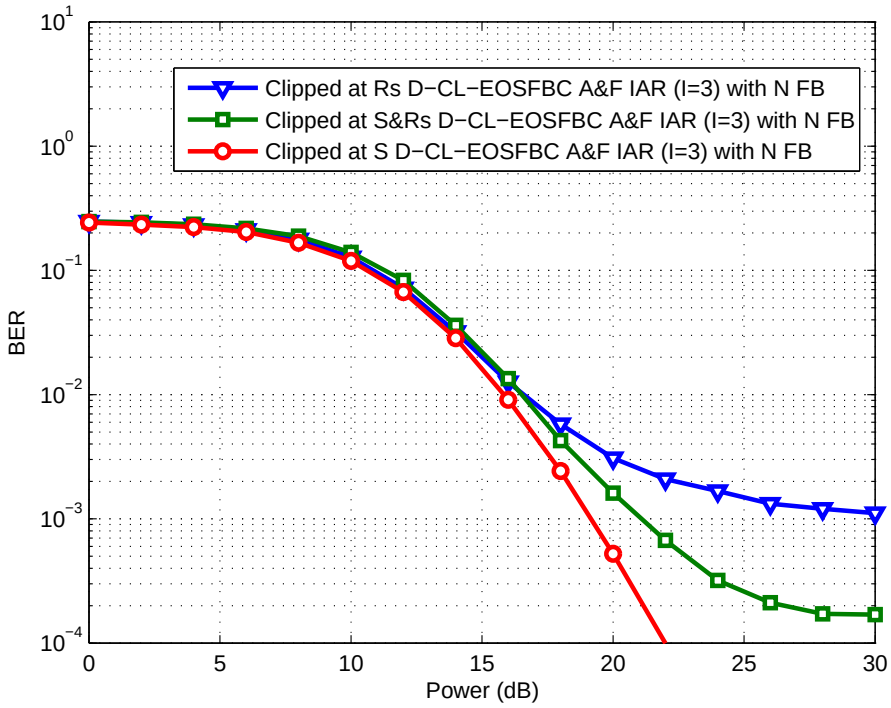

Figure 4.7. Comparison of BER performance when oversampling, clipping and filtering process at the source, relays and at both source and relays of amplify and forward distributed closed loop EO-SFBC OFDM system with one-bit feedback N feedback and decoded by IAR scheme.

EO-SFBC scheme requires approximately 29 dB. However, closed loop EO-SFBC with one-bit feedback gives significant improvement which is approximately 22 dB at 10^{-4} BER compared with open loop EO-SFBC. But, the former scheme has N bits overhead. To overcome this problem, the feedback correlation among subcarriers is exploited to reduce the feedback overhead significantly while maintaining satisfactory spatial diversity performance. For example, again by exploiting the correlation between 16 adjacent subcarriers as group feedback needs 64 bits to achieve almost identical performance, which means saving of 93.75%

as compared with one-bit feedback. In addition to that, exploiting 32 and 64 adjacent subcarriers leads to a saving of 96.87% and 98.4% as compared with the previous scheme and it degrades the BER by approximately 0.5 dB and 1.5 dB at 10^{-4}, respectively. Moreover, the simulation results illustrated in Fig. 4.7 confirm that using only oversampling, amplitude clipping and filtering at the relay nodes has the worst performance. This performance is considerably improved when the process is performed at the source and relay nodes together. On the other hand, oversampling, clipping and filtering only at the source node achieves the best performance. Improving performance with clipping at relays is a subject for future research.

4.6 Summary

This chapter addressed the PAPR reduction in a DF and AF distributed system for a synchronous cooperative virtual MIMO-OFDM network that utilizes EO-SFBC with clipped OFDM at the source. The EO-SFBC was performed at the relay nodes, and one destination node and limited feedback channels were used. The clipping process induced some problems; to overcome this, oversampling and filtering were used to reduce out-of-band interferences. Then, the IAR decoding scheme was used to overcome in-band distortion which was introduced by the clipping process. However, applying the oversampling, clipping and filtering operations in the source node and/or relay nodes in the AF distributed system confirmed that the best results are achieved when the clipping process is applied at the source node. In addition, full cooperative diversity and array gain were achieved by exploiting a two or one-bit feedback scheme for each subcarrier, which needs $2N$ or N

feedback bits per frame for both systems, respectively. For example, an OFDM block with 1024 subcarriers needs 2048 or 1024 bits feedback in both schemes respectively, in contrast, by exploiting the correlation between 16 adjacent subcarriers as two or one-bit group feedback need 128 or 64 bits to achieve almost identical performance for both schemes. However, these transmission overhead were reduced by 93.75% with negligible degradation in BER by exploiting the correlation among the feedback terms for the adjacent subcarriers of OFDM block in both systems. In the next chapter, relay selection techniques are considered to decrease the outage probability over multi-path fading channels.

Chapter 5

END-TO-END PERFORMANCE ANALYSIS OF COOPERATIVE SYSTEM OVER FREQUENCY SELECTIVE FADING CHANNELS

5.1 Introduction

Cooperative multi-node transmission is an important technique to exploit spatial and temporal diversity within a multi-path fading environment for future wireless services. Multi-path fading is a significant problem in wireless communication systems, and diversity techniques are significant methods to combat such fading [77]. This involves providing replicas of the transmitted signal over time or space. Both decode-and-forward (DF) and amplify-and-forward (AF) protocols can potentially achieve full spatial and temporal cooperative diversity. However, the

latter relaying protocol has lower complexity and no error propagation which happens in DF [43].

Today's wireless communication systems can be assessed by various quality of service measures. Outage probability is an important metric for the evaluation of the performance of a wireless communication system. It measures the probability of failing to achieve an output SNR threshold value required for a desired service. It is given by the cumulative distribution function (CDF) of the output SNR, i.e. $P_{out} = P[\gamma \leq \gamma_{th}]$ [13] and [78], where $P[\ .\ ]$ denotes probability.

5.1.1 The contributions of this chapter

Outage probability is a common measure of performance for cooperative communication systems and most previous works have focused on the context of Rayleigh flat fading and relay selection [24], [25], [79], [80], [81] and [82]. Particularly in [79] [81], the end-to-end outage probability analysis of AF for one relay selection with direct link between source and destination nodes was presented. In [24] and [25], outage probabilities for several DF cooperative diversity schemes with single relay selection were performed. Closed form expressions for Rayleigh frequency selective fading scenarios have generally not been studied with multiple relay selection. Recently, Park in [23] presented an OFDM-based relay network with one relay selection employing both DF and AF approaches and derived a lower bound on the outage probability and the diversity order achievable in frequency selective fading channels. In this chapter, the strengths of the L path time domain multi-path channels within a two-hop wireless multinode cooperative transmission are modeled as an Erlang distribution. The best single and the best two relay

pairs which maximize the end-to-end signal-to-noise ratio are selected for transmission. The closed form expression of the outage probability is then derived for the selection of the best single and the best two relay pair from M available relays, when $L = 2$ and 3, the same approach can be used for larger L but the complexity of the closed form expression increases substantially. The spatial and temporal cooperative diversity gain is then analysed. Moreover, general closed form expression for outage probability in terms of lower and upper bounds for an arbitrary channel length L and selecting the best single relay from an arbitrary number of relay nodes M are derived. In addition, exact form of outage probability for multi-path $L = 2$ and selecting the best single relay from an arbitrary number of relay nodes M is obtained. Finally, the analytical and simulation results are compared.

5.1.2 The chapter organization

The chapter begins with a brief introduction of cooperative wireless communication network and their assessment. Then, in the section two, the system model of a cooperative communication system over frequency selective channels is presented. Then, in the section three, outage probability analysis of selecting the best single and pair of relays from M available relays over limited number of multi-path channel length $L = 2$ and $L =3$ are studied. Also in this section, spatial and temporal cooperative diversity order of the network is considered. In the section four, exact outage probability analysis for specific number of channel length $L = 2$ is considered and deriving general formulas of single relay selection scheme of upper and lower bonds SNRs for an arbitrary channel length L and also an arbitrary number M of relay nodes

is obtained. Finally, simulation results and a summary are provided.

5.2 System Model of a Cooperative Communication System over Frequency Selective Channels

A cooperative multi-node communication system with one source node S, one destination node D and M relay nodes R_m, where $m = 1, 2, \cdots, M$ is considered. No direct link is assumed to exist between the source node and the destination node, i.e., the destination node can only receive signals from the relay nodes, as a consequence of shadowing or distance, and every node operates in half-duplex mode that can not transmit and receive simultaneously. Moreover, the communication is based on the AF protocol which means the cooperative transmission is performed in two phases as in Fig 5.1. In the first transmission phase, the source node S broadcasts the data to the M relay nodes and then stops sending during the second phase, during which, the relay nodes retransmit the data to the destination node. In addition, the channel impulse response (CIR) from the source node S to the relay nodes R_m with channel length L, is $\mathbf{h}_{m,1,L} = [h_{m,1,1}, h_{m,1,2}, \cdots, h_{m,1,L}]^T$ and from R_m to the destination node D with the same channel length is $\mathbf{h}_{m,2,L} = [h_{m,2,1}, h_{m,2,2}, \cdots, h_{m,2,L}]^T$. Relay selection is also represented in Fig 5.1, the solid lines represent the selected relay paths whereas the broken lines are not selected. These channel coefficients are assumed to represent quasi-static multi-path channels of the form $\mathbf{h}_{m,i,L}(t) = \sum_{l=1}^{L} h_{m,i,l}\delta(t - \tau_{m,i,l})$ where L is the multi-path channel length and $h_{m,i,l}$ and $\tau_{m,i,l}$ are the complex fading amplitude and time delay of the L^{th} path, respectively [23].

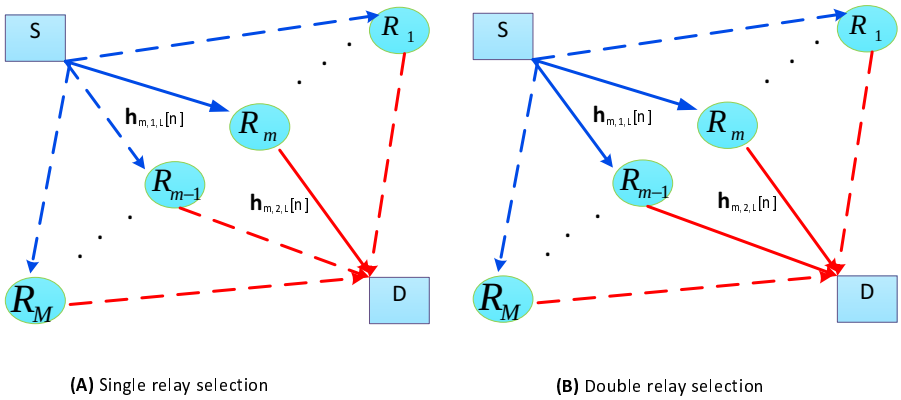

Figure 5.1. System model of multi-path and two-hop wireless transmission selecting the best single (A) and the best two relay pair (B) from M available relays.

It is assumed that all channel coefficients within $\mathbf{h}_{m,1,L}$ and $\mathbf{h}_{m,2,L}$ are uncorrelated with each other, with distribution $CN(0, N_0)$. Equations (5.2.1) and (5.2.2) represent the transmitted signal vector models over the first and second hops, respectively

$$\mathbf{y}_{SR_m} = \sqrt{P_s}\mathbf{H}_{m,1,L}\mathbf{x} + \mathbf{w}_{R_m}, \qquad m = 1, \ldots, M \tag{5.2.1}$$

and

$$\mathbf{y}_{R_m D} = \sqrt{P_m}\mathbf{H}_{m,2,L}\mathbf{y}_{SRm} + \mathbf{w}_D, \qquad m = 1, \ldots, M, \tag{5.2.2}$$

where $\mathbf{H}_{m,1,L}$ and $\mathbf{H}_{m,2,L}$ represent convolution matrices formed from the coefficients of the source to relays channels and relays to destination channels, respectively. The elements of $\mathbf{w}_{R_m} \sim CN(0, \sigma_1^2)$ and $\mathbf{w}_D \sim$

$CN(0, \sigma_2^2)$ are additive white Gaussian noise (AWGN) at the m^{th} relay and the destination, respectively. The relay gain denoted by $\sqrt{P_m}$ is calculated from $P_m = P_s/(P_s\|\mathbf{h}_{m,1,L}\|^2 + N_0)$ where P_s is the average energy per symbol, $\|\mathbf{h}_{m,1,L}\|^2$ is the channel gain between source and m^{th} relay node and N_0 is the noise variance [15]. Then, the exact instantaneous end-to-end SNR for the m^{th} relay is given by

$$\gamma_{ExD_m} = \frac{\gamma_{m,1,L}\gamma_{m,2,L}}{1 + \gamma_{m,1,L} + \gamma_{m,2,L}}, \qquad m = 1, \ldots, M, \tag{5.2.3}$$

where $\gamma_{m,1,L} = \|\mathbf{h}_{m,1,L}\|^2 P_s/N_0$ and $\gamma_{m,2,L} = \|\mathbf{h}_{m,2,L}\|^2 P_s/N_0$ are the instantaneous SNRs of the $S \longrightarrow R_m$ and $R_m \longrightarrow D$ links, respectively. The full outage probability analysis of selecting the best single and the best two relay pair together with the spatial and temporal cooperative diversity order of the network over frequency selective fading channels will be explained in the next section.

5.3 Outage Probability Analysis of Frequency Selective Fading Channels

The average error probability of a slowly fading channel has limited value for system evaluation [36]. In contrast, practically, there is more interest in the probability that the system will not be able to guarantee a target rate. This probability is called the outage probability P_{out}. In other words, the outage probability is defined as when the average end-to-end SNR falls below a certain predefined threshold value, i.e. $\gamma = 2^{2R} - 1$, where R is the target rate [13] [78]. The outage probability can be expressed as

$$P_{out} = \int_0^{\gamma} f_{\gamma}(\gamma) d\gamma = F_{\gamma}(\gamma), \tag{5.3.1}$$

where $f_{\gamma}(\gamma)$ is the probability density function (PDF) and $F_{\gamma}(\gamma)$ is the cumulative distribution function (CDF) of the SNR.

For frequency selective Rayleigh fading channels, the PDF and CDF of the sum of L independent paths of each channel can be modeled as an Erlang distribution, with $u \in (SR_m, R_m D)$ links, which is given by

$$f_{\gamma_u}(\gamma) = \frac{\gamma^{L-1} e^{-\frac{\gamma}{\overline{\gamma}}}}{\Gamma(L)\overline{\gamma}^{L}}, \tag{5.3.2}$$

where $\Gamma(L) = \int_0^{\infty} s^{L-1} e^{-s} ds = (L-1)!$ which is termed the complete Gamma function, where L is called the shape parameter which represents the number of paths in each channel, $\overline{\gamma}$ is called the scale parameter and is denoted as the average SNR. Equation (5.3.2) has the same distribution as the sum of L independent exponential distribution random variables with circular complex normal distribution $CN(\mu, \sigma^2)$ where $\mu = L\overline{\gamma}$ and $\sigma^2 = L\overline{\gamma}^2$ are the mean and the variance of the Erlang distribution, respectively, as in Fig. 5.2. This illustrates that the PDF of the sum squared coefficients of the frequency selective channel is an Erlang distribution with different numbers of paths L so when $L = 1$ the PDF is exponentially distributed which is equivalent to the flat fading channel [83]. Thus, the CDF can be obtained by taking the integral of the PDF in (5.3.2) with respect to γ, yielding (5.3.3)

$$F_{\gamma_u}(\gamma) = 1 - e^{-\frac{\gamma}{\overline{\gamma}}} \sum_{k=0}^{L-1} \frac{\gamma^k}{k!\ \overline{\gamma}^k}, \tag{5.3.3}$$

where $\overline{\gamma}$ denotes the mean SNR for all links.

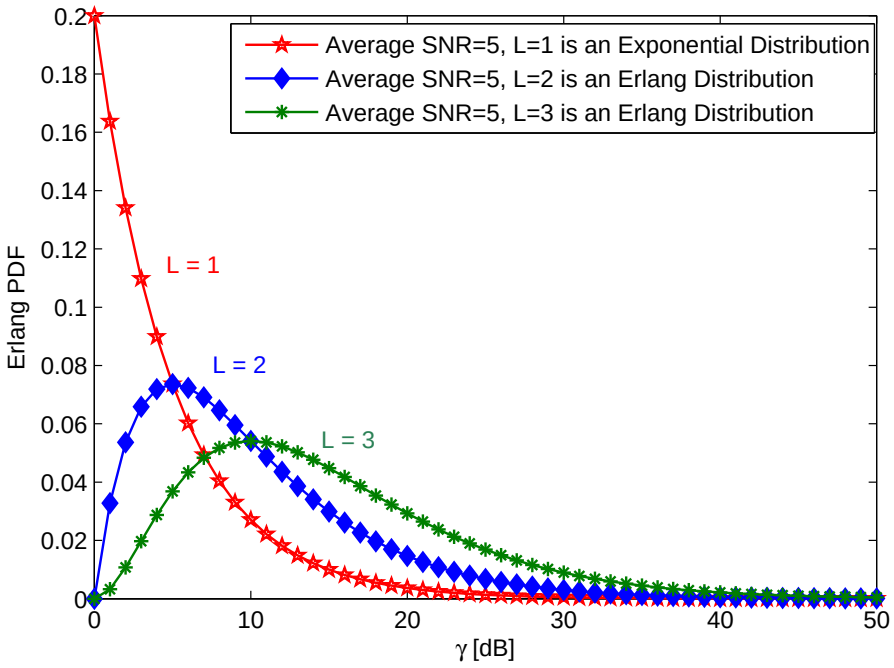

Figure 5.2. Different probability density functions used to model the sum squared coefficients of a frequency selective fading channel where L is the number of paths and the average SNR ($\overline{\gamma}$) is five in (5.3.2).

In order to calculate the outage probability, similarly to [81], the following upper bound on the SNR is used

$$\gamma_m = \min(\gamma_{m,1,L}, \gamma_{m,2,L}) > \gamma_{ExD_m}, \tag{5.3.4}$$

and therefore, to find the CDF of $\gamma_m = \min(\gamma_{m,1,L}, \gamma_{m,2,L})$ which can be expressed as (5.3.5)

$$\begin{aligned} F_{\gamma_m}(\gamma) &= 1 - P_r(\gamma_{m,1,L} > \gamma) P_r(\gamma_{m,2,L} > \gamma) \\ &= 1 - [1 - P_r(\gamma_{m,1,L} \leq \gamma)][1 - P_r(\gamma_{m,2,L} \leq \gamma)]. \end{aligned} \tag{5.3.5}$$

By substituting (5.3.3) into (5.3.5), an end-to-end CDF will be obtained

$$F^L_{\gamma_m}(\gamma) = 1 - e^{-\frac{2\gamma}{\overline{\gamma}}} \left[\sum_{k=0}^{L-1} \frac{\gamma^k}{k!\ \overline{\gamma}^k} \right] \left[\sum_{\acute{k}=0}^{L-1} \frac{\gamma^{\acute{k}}}{\acute{k}!\ \overline{\gamma}^{\acute{k}}} \right], \tag{5.3.6}$$

where a superscript L is used on the left hand side to denote the channel length of a link. For algebraic convenience, special cases of (5.3.6) by limiting the channel length to $L = 2$ and $L = 3$ are considered, yielding

$$F^2_{\gamma_m}(\gamma) = 1 - e^{-\frac{2\gamma}{\overline{\gamma}}} - \frac{2e^{-\frac{2\gamma}{\overline{\gamma}}}\gamma}{\overline{\gamma}} - \frac{e^{-\frac{2\gamma}{\overline{\gamma}}}\gamma^2}{\overline{\gamma}^2} \tag{5.3.7}$$

and

$$F^3_{\gamma_m}(\gamma) = 1 - e^{-\frac{2\gamma}{\overline{\gamma}}} - \frac{2e^{-\frac{2\gamma}{\overline{\gamma}}}\gamma}{\overline{\gamma}} - \frac{2e^{-\frac{2\gamma}{\overline{\gamma}}}\gamma^2}{\overline{\gamma}^2} - \frac{e^{-\frac{2\gamma}{\overline{\gamma}}}\gamma^3}{\overline{\gamma}^3} - \frac{e^{-\frac{2\gamma}{\overline{\gamma}}}\gamma^4}{4\overline{\gamma}^4}. \tag{5.3.8}$$

The full outage probability analysis of selecting the best single relay from M relays will be considered in the next subsection.

5.3.1 Outage probability analysis of selecting the best single relay from M available relays

In this approach selecting the best relay node from M available relays can be achieved, namely, select the maximum γ_{opt} from the M relays instantaneous SNR. Lower and upper bounds for the equivalent SNR can be given as

$$\gamma_{low} \leq \gamma_{ExD_m} < \gamma_{up}, \tag{5.3.9}$$

where $\gamma_{low} = \frac{1}{2}\sum_{m=1}^{M}\gamma_m$ and $\gamma_{up} = \sum_{m=1}^{M}\gamma_m$. To find γ_{opt} by adopting the following relay selection criterion

$$\gamma_{opt} = \max_{m}\{\min(\gamma_{m,1,L}, \gamma_{m,2,L})\} \quad m = 1, 2, \cdots, M. \tag{5.3.10}$$

Building upon (5.3.6), the CDF and PDF of γ_{opt} can be expressed as

$$F^L_{\gamma_{opt}}(\gamma) = [F^L_{\gamma_m}(\gamma)]^M \qquad \text{and} \qquad f^L_{\gamma_{opt}}(\gamma) = M f^L_{\gamma_m}(\gamma)[F^L_{\gamma_m}(\gamma)]^{M-1} \tag{5.3.11}$$

where M is the number of available relay nodes in the system.

Then the CDF of γ_{opt} cab be obtained for $L = 2$ and 3, respectively, by substituting (5.3.7) and (5.3.8) into the left side of (5.4.8), yielding

$$F^2_{\gamma_{opt}}(\gamma) = \frac{e^{-\frac{2M\gamma}{\overline{\gamma}}}\left(-\overline{\gamma}^2 e^{\frac{2\gamma}{\overline{\gamma}}} + (\overline{\gamma}+\gamma)^2\right)^M}{\overline{\gamma}^{2M}} \tag{5.3.12}$$

and

$$F^3_{\gamma_{opt}}(\gamma) = \frac{e^{-\frac{2M\gamma}{\overline{\gamma}}}\left(-4\overline{\gamma}^4 e^{\frac{2\gamma}{\overline{\gamma}}} + (2\overline{\gamma}^2 + 2\overline{\gamma}\gamma + \gamma^2)^2\right)^M}{2^{2M}\overline{\gamma}^{4M}}. \tag{5.3.13}$$

Next, the full outage probability analysis of selecting the best two relay pair from M available relays will be considered.

5.3.2 Outage probability analysis for the best two relay pair selection from M available relays

In this approach the best two relay nodes from M available relays in the same cluster can be selected, namely, select γ_{opt} and γ_{opt-1} which are the maximum and second largest, from the M relays instantaneous SNR. To find these values the following relay selection criteria are adopted

$$\begin{aligned} \gamma_{opt} &= \max_{m}\{\min(\gamma_{m,1,L}, \gamma_{m,2,L})\} \\ \gamma_{opt-1} &= \max_{m-1}\{\min(\gamma_{m,1,L}, \gamma_{m,2,L})\} \\ & m = 1, 2, .., M. \end{aligned} \tag{5.3.14}$$

Clearly, choosing the second largest is dependent on the first maximum, therefore, according to [84], the joint distribution of the two most maximum values can be found. Using the CDF expression in (5.3.6) and its derivative to provide the PDF, the joint CDF of γ_{opt} and γ_{opt-1}

can be expressed as

$$f_{X,Y}^{L}(x,y) = M(M-1) f_X^L(x) f_Y^L(y) [F_Y^L(y)]^{M-2}, \tag{5.3.15}$$

where M is the number of relay nodes in the system, $\gamma_{opt} = X$ and $\gamma_{opt-1} = Y$ which are the first and second largest maximum values, respectively. Equation (5.3.15) represents the general PDF form of the multi-path environment transmission with L paths per link and M relays. To simplify (5.3.15), the channel length in this work will be limited to be either $L = 2$ or 3, then (5.3.15) can be rewritten as either:

$$\begin{aligned} f_{X,Y}^{2}(x,y) = M(M-1) &\left[\frac{2e^{-\frac{2x}{\overline{\gamma}}}x}{\overline{\gamma}^2} + \frac{2e^{-\frac{2x}{\overline{\gamma}}}x^2}{\overline{\gamma}^3}\right] \\ &\left[\frac{2e^{-\frac{2y}{\overline{\gamma}}}y}{\overline{\gamma}^2} + \frac{2e^{-\frac{2y}{\overline{\gamma}}}y^2}{\overline{\gamma}^3}\right] \\ &\left[1 - e^{-\frac{2y}{\overline{\gamma}}} - \frac{2e^{-\frac{2y}{\overline{\gamma}}}y}{\overline{\gamma}} - \frac{e^{-\frac{2y}{\overline{\gamma}}}y^2}{\overline{\gamma}^2}\right]^{M-2} \end{aligned} \tag{5.3.16}$$

or

$$\begin{aligned} f_{X,Y}^{3}(x,y) = M(M-1) &\left[\frac{e^{-\frac{2x}{\overline{\gamma}}}x^2}{\overline{\gamma}^3} + \frac{e^{-\frac{2x}{\overline{\gamma}}}x^3}{\overline{\gamma}^4} + \frac{e^{-\frac{2x}{\overline{\gamma}}}x^4}{2\overline{\gamma}^5}\right] \\ &\left[\frac{e^{-\frac{2y}{\overline{\gamma}}}y^2}{\overline{\gamma}^3} + \frac{e^{-\frac{2y}{\overline{\gamma}}}y^3}{\overline{\gamma}^4} + \frac{e^{-\frac{2y}{\overline{\gamma}}}y^4}{2\overline{\gamma}^5}\right] \\ &\left[1 - e^{-\frac{2y}{\overline{\gamma}}} - \frac{2e^{-\frac{2y}{\overline{\gamma}}}y}{\overline{\gamma}} - \frac{2e^{-\frac{2y}{\overline{\gamma}}}y^2}{\overline{\gamma}^2} - \frac{e^{-\frac{2y}{\overline{\gamma}}}y^3}{\overline{\gamma}^3} - \frac{e^{-\frac{2y}{\overline{\gamma}}}y^4}{4\overline{\gamma}^4}\right]^{M-2}, \end{aligned} \tag{5.3.17}$$

where again the superscripts in the left-hand side correspond to L. Then, the integration of (5.3.15) will find the outage probability, yield-

ing

$$F^{L}_{\gamma_{opt}}(\gamma) = \int_{0}^{\gamma/2}\int_{y}^{\gamma-y} f^{L}_{X,Y}(x,y)dxdy. \tag{5.3.18}$$

Without loss of generality, the CDF of channel length two can be calculated by substituting (5.3.16) in (5.3.18) as

$$F^{2}_{\gamma_{opt}}(\gamma) = M(M-1)\sum_{k=0}^{M-2}\binom{M-2}{k}(-1)^{k}\sum_{i=0}^{k}\binom{k}{i}\sum_{j=0}^{i}\binom{i}{j}\int_{0}^{\gamma/2}\int_{y}^{\gamma-y} \left[\frac{2e^{-\frac{2x}{\overline{\gamma}}}x}{\overline{\gamma}^{2}} + \frac{2e^{-\frac{2x}{\overline{\gamma}}}x^{2}}{\overline{\gamma}^{3}}\right]\left[\frac{2e^{-\frac{2y}{\overline{\gamma}}}y}{\overline{\gamma}^{2}} + \frac{2e^{-\frac{2y}{\overline{\gamma}}}y^{2}}{\overline{\gamma}^{3}}\right]\frac{e^{\frac{-2yk}{\overline{\gamma}}}2^{i-j}y^{i+j}}{\overline{\gamma}^{i+j}}dxdy \tag{5.3.19}$$

and likewise for channel length ($L = 3$)

$$F^{3}_{\gamma_{opt}}(\gamma) = M(M-1)\sum_{k=0}^{M-2}\binom{M-2}{k}(-1)^{k}\sum_{i=0}^{k}\binom{k}{i}\sum_{j=0}^{i}\binom{i}{j}\sum_{t=0}^{j}\binom{j}{t}\sum_{f=0}^{t}\binom{t}{f} \int_{0}^{\gamma/2}\int_{y}^{\gamma-y}\left[\frac{e^{-\frac{2x}{\overline{\gamma}}}x^{2}}{\overline{\gamma}^{3}} + \frac{e^{-\frac{2x}{\overline{\gamma}}}x^{3}}{\overline{\gamma}^{4}} + \frac{e^{-\frac{2x}{\overline{\gamma}}}x^{4}}{2\overline{\gamma}^{5}}\right]\left[\frac{e^{-\frac{2y}{\overline{\gamma}}}y^{2}}{\overline{\gamma}^{3}} + \frac{e^{-\frac{2y}{\overline{\gamma}}}y^{3}}{\overline{\gamma}^{4}} + \frac{e^{-\frac{2y}{\overline{\gamma}}}y^{4}}{2\overline{\gamma}^{5}}\right] \frac{e^{\frac{-2yk}{\overline{\gamma}}}2^{i-t}y^{i+j+t+f}}{4f\overline{\gamma}^{i+j+t+f}}dxdy \tag{5.3.20}$$

and to evaluate (5.3.19), firstly, calculating the part of the expression in the outer most summation for when k = 0

$$F^{2,k=0}_{\gamma_{opt}}(\gamma) = \frac{1}{2} - \frac{\left(2\gamma^{5} + 15\gamma^{4}\overline{\gamma} + 40\gamma^{3}\overline{\gamma}^{2} + 60\gamma^{2}\overline{\gamma}^{3} + 60\gamma\overline{\gamma}^{4} + 30\overline{\gamma}^{5}\right)e^{-\frac{2\gamma}{\overline{\gamma}}}}{60\overline{\gamma}^{5}} \tag{5.3.21}$$

and then the full closed form expression for the CDF when $L = 2$ becomes

$$
\begin{aligned}
F^2_{\gamma_{opt}}(\gamma) \;=\; & M(M-1)\,[F^{2,K=0}_{\gamma_{opt}}(\gamma) + \sum_{k=1}^{M-2}\binom{M-2}{k}(-1)^k \sum_{i=0}^{k}\binom{k}{i} \\
& \sum_{j=0}^{i}\binom{i}{j} 2^{-2(2+j)}\gamma^{i+j}\overline{\gamma}^{-2-i-j}e^{-\frac{2\gamma}{\overline{\gamma}}} \\
& (-\frac{8\gamma^2(\frac{\gamma k}{\overline{\gamma}})^{-i-j}(\Gamma(2+i+j)-\Gamma(2+i+j,\frac{\gamma k}{\overline{\gamma}}))}{k^2} \\
& - \frac{16\gamma\overline{\gamma}(\frac{\gamma k}{\overline{\gamma}})^{-i-j}(\Gamma(2+i+j)-\Gamma(2+i+j,\frac{\gamma k}{\overline{\gamma}}))}{k^2} \\
& - \frac{8\overline{\gamma}^2(\frac{\gamma k}{\overline{\gamma}})^{-i-j}(\Gamma(2+i+j)-\Gamma(2+i+j,\frac{\gamma k}{\overline{\gamma}}))}{k^2} \\
& + \frac{8\overline{\gamma}^2 e^{\frac{2\gamma}{\overline{\gamma}}}\left(\frac{\gamma(2+k)}{\overline{\gamma}}\right)^{-i-j}(\Gamma(2+i+j)-\Gamma(2+i+j,\frac{\gamma(2+k)}{\overline{\gamma}}))}{(2+k)^2} \\
& - \frac{4\gamma^2(\frac{\gamma k}{\overline{\gamma}})^{-i-j}(\Gamma(3+i+j)-\Gamma(3+i+j,\frac{\gamma k}{\overline{\gamma}}))}{k^3} \\
& + \frac{4\overline{\gamma}^2(\frac{\gamma k}{\overline{\gamma}})^{-i-j}(\Gamma(3+i+j)-\Gamma(3+i+j,\frac{\gamma k}{\overline{\gamma}}))}{k^3} \\
& + \frac{12\overline{\gamma}^2 e^{\frac{2\gamma}{\overline{\gamma}}}(\frac{\gamma(2+k)}{\overline{\gamma}})^{-i-j}(\Gamma(3+i+j)-\Gamma(3+i+j,\frac{\gamma(2+k)}{\overline{\gamma}}))}{(2+k)^3} \\
& + \frac{4\gamma\overline{\gamma}(\frac{\gamma k}{\overline{\gamma}})^{-i-j}(\Gamma(4+i+j)-\Gamma(4+i+j,\frac{\gamma k}{\overline{\gamma}}))}{k^4} \\
& + \frac{2\overline{\gamma}^2(\frac{\gamma k}{\overline{\gamma}})^{-i-j}(\Gamma(4+i+j)-\Gamma(4+i+j,\frac{\gamma k}{\overline{\gamma}}))}{k^4} \\
& + \frac{6\overline{\gamma}^2 e^{\frac{2\gamma}{\overline{\gamma}}}(\frac{\gamma(2+k)}{\overline{\gamma}})^{-i-j}(\Gamma(4+i+j)-\Gamma(4+i+j,\frac{\gamma(2+k)}{\overline{\gamma}}))}{(2+k)^4} \\
& - \frac{\overline{\gamma}^2(\frac{\gamma k}{\overline{\gamma}})^{-i-j}(\Gamma(5+i+j)-\Gamma(5+i+j,\frac{\gamma k}{\overline{\gamma}}))}{k^5} \\
& + \frac{\overline{\gamma}^2 e^{\frac{2\gamma}{\overline{\gamma}}}(\frac{\gamma(2+k)}{\overline{\gamma}})^{-i-j}(\Gamma(5+i+j)-\Gamma(5+i+j,\frac{\gamma(2+k)}{\overline{\gamma}}))}{(2+k)^5})]
\end{aligned}
\tag{5.3.22}
$$

and to evaluate (5.3.20), firstly calculating the part of the expression in the outer most summation for when k = 0

$$F_{\gamma_{opt}}^{3,k=0}(\gamma) = \frac{1}{8} - \frac{1}{80640\overline{\gamma}^9}(2\gamma^9 + 27\gamma^8\overline{\gamma} + 192\gamma^7\overline{\gamma}^2 + 840\gamma^6\overline{\gamma}^3 + 2688\gamma^5\overline{\gamma}^4 + 6720\gamma^4\overline{\gamma}^5 + 13440\gamma^3\overline{\gamma}^6 + 20160\gamma^2\overline{\gamma}^7 + 20160\gamma\overline{\gamma}^8 + 10080\overline{\gamma}^9)e^{-\frac{2\gamma}{\overline{\gamma}}} \tag{5.3.23}$$

and then the full closed form expression for the CDF when $L = 3$ is given in **Appendix A** due to its complexity. Next, the spatial and temporal cooperative diversity order of the network of the best single relay and best two relay pair selection from M will be presented for different channel lengths.

5.3.3 Spatial and temporal cooperative diversity order of the network

The available spatial and temporal cooperative diversity order of this network can be derived as in [23]. Firstly, the left side of (5.3.6) can be rewritten as

$$F_{\gamma_{opt}}(\gamma) = \prod_{m=1}^{M} F_{\gamma_m}(\gamma), \tag{5.3.24}$$

where M is the number of available relay nodes in the system and it is assumed, $\overline{\gamma}$, the mean SNR is the same for all paths, and droping the superscript L for generality. Then, after simple manipulation of equation (5.3.5) can be obtained

$$F_{\gamma_m}(\gamma) = F_{\gamma_{m,1,L}}(\gamma) + F_{\gamma_{m,2,L}}(\gamma) - F_{\gamma_{m,1,L}}(\gamma) \times F_{\gamma_{m,2,L}}(\gamma). \tag{5.3.25}$$

By using the definition of the moment generating function (MGF) given by

$$M_{\gamma_{m,i,L}}(s) = \int_0^\infty e^{-s\gamma} f_{\gamma_{opt}}(\gamma) d\gamma \qquad i = 1, 2, \tag{5.3.26}$$

where s is the complex variable in the Laplace transform, the MGF of $\gamma_{m,i,L}$ is given by

$$M_{\gamma_{m,i,L}}(s) = \prod_{l=1}^{L_{m,i}} \frac{1}{(1 - s\overline{\gamma})}. \tag{5.3.27}$$

It is assumed that the channel has a uniform multi-path intensity profile (MIP) for all L, the CDF can be simplified to

$$F_{\gamma_{m,i,L}}(\gamma) = \frac{\Gamma(L_{m,i}, L_{m,i}\gamma/\overline{\gamma})}{\Gamma(L_{m,i})}, \tag{5.3.28}$$

where $\Gamma(L, x) = \int_0^x s^{L-1} e^{-s} ds$ and $\Gamma(L) = \int_0^\infty s^{L-1} e^{-s} ds = (L-1)!$ which are incomplete and complete Gamma function, respectively.

By substituting (5.3.28) and (5.3.25) into (5.3.24), to derive the spatial and temporal cooperative diversity order achievable in the network

$$\begin{aligned} F_{\gamma_{opt}}(\gamma) = \prod_{m=1}^{M} [& \frac{\Gamma(L_{m,1}, L_{m,1}\gamma/\overline{\gamma})}{\Gamma(L_{m,1})} + \frac{\Gamma(L_{m,2}, L_{m,2}\gamma/\overline{\gamma})}{\Gamma(L_{m,2})} \\ & - \frac{\Gamma(L_{m,1}, L_{m,1}\gamma/\overline{\gamma})}{\Gamma(L_{m,1})} \times \frac{\Gamma(L_{m,2}, L_{m,2}\gamma/\overline{\gamma})}{\Gamma(L_{m,2})}], \end{aligned} \tag{5.3.29}$$

where $\Gamma(L, x)$ can be written as a series expansion as in [85]

$$\Gamma(L,x)=\sum_{n=0}^{\infty}\frac{(-1)^n x^{L+n}}{n!(n+L)}. \tag{5.3.30}$$

Approximating (5.4.13) by using only first term in (5.3.30) so that

$$\begin{aligned}F_{\gamma_{opt}}(\gamma)\approx\prod_{m=1}^{M}[&\frac{(L_{m,1}\gamma/\overline{\gamma})^{L_{m,1}}}{L_{m,1}\Gamma(L_{m,1})}+\frac{(L_{m,2}\gamma/\overline{\gamma})^{L_{m,2}}}{L_{m,2}\Gamma(L_{m,2})}\\&-\frac{(L_{m,1}\gamma/\overline{\gamma})^{L_{m,1}}}{L_{m,1}\Gamma(L_{m,1})}\times\frac{(L_{m,2}\gamma/\overline{\gamma})^{L_{m,2}}}{L_{m,2}\Gamma(L_{m,2})}]\end{aligned} \tag{5.3.31}$$

and defining $x=\frac{1}{\overline{\gamma}}, c_{m,i}=\frac{(L_{m,i}\gamma)^{L_{m,i}}}{L_{m,i}\Gamma(L_{m,i})}, \quad i=1,2$, then

$$F_{\gamma_{opt}}(\gamma)\approx\prod_{m=1}^{M}\left[c_{m,1}x^{L_{m,1}}+c_{m,2}x^{L_{m,2}}-c_{m,1}x^{L_{m,1}}\times c_{m,2}x^{L_{m,2}}\right] \tag{5.3.32}$$

and with the assumption that $\overline{\gamma}$ is large, then

$$c_{m,1}x^{L_{m,1}}+c_{m,2}x^{L_{m,2}}-c_{m,1}x^{L_{m,1}}\times c_{m,2}x^{L_{m,2}}>\min(c_{m,1}x^{L_{m,1}},c_{m,2}x^{L_{m,2}}). \tag{5.3.33}$$

Therefore, the lower-bound of (5.3.32) can be expressed as

$$\lim_{\gamma\to\infty}F_{\gamma_{opt}}(\gamma)\approx\prod_{m=1}^{M}\min\left(\frac{c_{m,1}}{\overline{\gamma}^{L_{m,1}}}\ ,\ \frac{c_{m,2}}{\overline{\gamma}^{L_{m,2}}}\right), \tag{5.3.34}$$

by taking the term with the lowest degree in the series representation of $\Gamma(L,x)$, where $c_{m,1}$ and $c_{m,2}$ are some constants. Thus, the total spatial and temporal cooperative diversity order of the network is given by

$$\begin{aligned} D_g &= -\lim_{\gamma\to\infty} \frac{\log F_{\gamma_{opt}}(\gamma)}{\log \gamma} \\ &= \sum_{m=1}^{M} \min(L_{m,1}, L_{m,2}), \end{aligned} \tag{5.3.35}$$

where $F_{\gamma_{opt}}(\gamma)$ is the outage probability.

5.4 General Closed Form Outage Probability Analysis for Selecting the Best Single Relay from an Arbitrary Number of Relay Nodes M Based on Upper, Lower Bounds and Exact SNR

In the previous section, outage probability analysis based on upper bound end-to-end SNR for an arbitrary number of relay nodes and limited multipath channel lengths of $L = 2$ and 3 with best single and best two relay pair selection from M available relays is calculated. Therefore, in this section further analysis for general closed form outage probability analysis for selecting the best single relay from an arbitrary number of relay nodes M based on upper, lower bounds and exact SNR is presented.

5.4.1 CDF upper bound SNR analysis for an arbitrary multi-path channel length L

In order to calculate the CDF for upper bound end-to-end SNR, it is necessary to find the CDF of $\gamma_{UB_m} = \min(\gamma_{m,1,L}, \gamma_{m,2,L})$ which can be

expressed as (5.4.1)

$$\begin{aligned} F_{\gamma_{UB_m}}(\gamma) &= 1 - P_r(\gamma_{m,1,L} > \gamma)P_r(\gamma_{m,2,L} > \gamma) \\ &= 1 - [1 - P_r(\gamma_{m,1,L} \leq \gamma)][1 - P_r(\gamma_{m,2,L} \leq \gamma)] \\ &= 1 - [1 - F_{\gamma_{m,1,L}}(\gamma)][1 - F_{\gamma_{m,2,L}}(\gamma)]. \end{aligned} \tag{5.4.1}$$

By simple manipulation of (5.4.1), the upper bound end-to-end CDF can be found as

$$F_{\gamma_{UB_m}}(\gamma) = F_{\gamma_{m,1,L}}(\gamma) + F_{\gamma_{m,2,L}}(\gamma) - F_{\gamma_{m,1,L}}(\gamma)F_{\gamma_{m,2,L}}(\gamma). \tag{5.4.2}$$

The CDF of (5.3.2) can be obtained by taking the integral with respect to γ, yielding equation (5.4.3)

$$F_{\gamma_{m,i,L}}(\gamma) = 1 - \frac{\Gamma(L_{m,i}, \gamma/\overline{\gamma})}{\Gamma(L_{m,i})}, \quad i = 1, 2, \tag{5.4.3}$$

where $F_{\gamma_{m,i,L}}(\gamma)$ is the CDF of the channel where L is the number of paths and $i = 1, 2$ is the number of hops.

5.4.2 CDF lower bound SNR analysis for an arbitrary multi-path channel length L

In order to calculate the CDF for lower bound end-to-end SNR, it is also necessary to find the CDF of $\gamma_{LB_m} = \frac{1}{2}\min(\gamma_{m,1,L}, \gamma_{m,2,L})$ which can be expressed as (5.4.4)

$$\begin{aligned} F_{\gamma_{LB_m}}(\gamma) &= 1 - P_r(\gamma_{m,1,L} > 2\gamma)P_r(\gamma_{m,2,L} > 2\gamma) \\ &= 1 - [1 - P_r(\gamma_{m,1,L} \leq 2\gamma)][1 - P_r(\gamma_{m,2,L} \leq 2\gamma)] \\ &= 1 - [1 - F_{\gamma_{m,1,L}}(2\gamma)][1 - F_{\gamma_{m,2,L}}(2\gamma)]. \end{aligned} \tag{5.4.4}$$

After simple manipulation of (5.4.4), the lower bound end-to-end CDF can be expressed as

$$F_{\gamma_{LB_m}}(\gamma) = F_{\gamma_{m,1,L}}(2\gamma) + F_{\gamma_{m,2,L}}(2\gamma) - F_{\gamma_{m,1,L}}(2\gamma)F_{\gamma_{m,2,L}}(2\gamma). \tag{5.4.5}$$

5.4.3 CDF exact SNR analysis for limited number of multi-path channel length L

Based on (5.2.3), $\gamma_{m,i,L}$ is a Gamma random variable with $f_{\gamma_{m,i,L}}(\gamma) = \frac{\gamma^{L_{m,i}-1}e^{-\frac{\gamma}{\overline{\gamma}}}}{\Gamma(L_{m,i})\overline{\gamma}^{L_{m,i}}}$ and $F_{\gamma_{m,i,L}}(\gamma) = 1 - \frac{\Gamma(L_{m,i},\gamma/\overline{\gamma})}{\Gamma(L_{m,i})}$ where $f(\cdot)$ and $F(\cdot)$ denote, respectively, the PDF and the CDF of i^{th} hop and $i = 1, 2$. It is assumed that $X = \gamma_{m,1,L}$ and $Y = \gamma_{m,2,L}$, then, $f_X(x) = f_{\gamma_{m,1,L}}(\gamma)$ and $f_Y(y) = f_{\gamma_{m,2,L}}(\gamma)$, where $x > 0$ and $y > 0$, and exploiting independence, obtain

$$f_{XY}(x, y) = f_X(x)f_Y(y). \tag{5.4.6}$$

Then, the CDF of $z = \frac{xy}{x+y+1}$, where $z = \gamma_{Ex}$ as in equation (5.2.3), becomes

$$\begin{aligned} F_Z(z) &= P(\frac{xy}{x+y+1} \leq z) = P(x \leq \frac{yz+z}{y-z}) \\ &= \int_0^z \int_0^\infty f_{X,Y}(x,y)dxdy \int_z^\infty \int_0^{\frac{yz+z}{y-z}} f_{X,Y}(x,y)dxdy, \end{aligned} \tag{5.4.7}$$

where $P(\cdot)$ denotes probability value. Therefore,

$$\begin{aligned} F_{\gamma_{Ex_D}}(\gamma) &= \int_0^\gamma \int_0^\infty f_{X,Y}(x,y)dxdy \int_\gamma^\infty \int_0^{\frac{y\gamma+\gamma}{y-\gamma}} f_{X,Y}(x,y)dxdy \\ &\int_0^\gamma \int_0^\infty \frac{x^{L-1}e^{\frac{x}{\overline{\gamma}}}}{\Gamma(L)\overline{\gamma}^L} \frac{y^{L-1}e^{\frac{y}{\overline{\gamma}}}}{\Gamma(L)\overline{\gamma}^L} dxdy \int_\gamma^\infty \int_0^{\frac{y\gamma+\gamma}{y-\gamma}} \frac{x^{L-1}e^{\frac{x}{\overline{\gamma}}}}{\Gamma(L)\overline{\gamma}^L} \frac{y^{L-1}e^{\frac{y}{\overline{\gamma}}}}{\Gamma(L)\overline{\gamma}^L} dxdy, \end{aligned} \tag{5.4.8}$$

where L is the channel length.

5.4.4 Outage probability analysis of selecting the best single relay from an arbitrary M relays based on upper, lower and exact SNR analysis

In this approach the selection of the best relay node from M available relays, namely, select the maximum γ_{opt} from the M relays instantaneous SNR. According to [86], the selection of the best relay is performed in two steps. Firstly, the weaker link between the first and second hop of each relay node is obtained. Secondly, these weak links are ordered and the one with the highest SNR is selected as the candidate to relay the data to the destination [87]

$$\gamma_{LB} \leq \gamma_{Ex_{Dm}} < \gamma_{UB}, \tag{5.4.9}$$

where $\gamma_{LB} = \frac{1}{2}\sum_{m=1}^{M}\gamma_m$, $\gamma_{UB} = \sum_{m=1}^{M}\gamma_m$ and $\gamma_{EX_{Dm}}$ is the exact formula as in equation (5.2.3). Then, the outage probability is defined as when the average end-to-end SNR falls below a certain predefined threshold value, $\gamma = 2^{2R} - 1$, where R is the target rate. By using the relay selection criterion in equation (5.3.10) the $\gamma_{UB_{opt}}$, $\gamma_{LB_{opt}}$ and $\gamma_{EX_{opt}}$ can be found, then, the outage probability can be expressed as

$$P_{out}^{UB} = \int_0^{\gamma} f_{\gamma}(\gamma)d\gamma = F_{\gamma_{UB_{opt}}}(\gamma) = \prod_{m=1}^{M} F_{\gamma_{UB_m}}(\gamma), \tag{5.4.10}$$

$$P_{out}^{LU} = \int_0^{\gamma} f_{\gamma}(\gamma)d\gamma = F_{\gamma_{LB_{opt}}}(\gamma) = \prod_{m=1}^{M} F_{\gamma_{LB_m}}(\gamma), \tag{5.4.11}$$

$$P_{out}^{EX} = \int_0^{\gamma} f_{\gamma}(\gamma)d\gamma = F_{\gamma_{EX_{opt}}}(\gamma) = \prod_{m=1}^{M} F_{\gamma_{Ex_m}}(\gamma), \tag{5.4.12}$$

where M is the number of relay nodes in the system.

By substituting (5.3.28) into (5.4.2) and (5.4.5), then, into (5.4.10) and (5.4.11), the closed form of outage probability of lower and upper bounds for arbitrary channel lengths L and M relay nodes can be obtained as (5.4.13) and (5.4.14). Exact form of outage probability can be obtained by integrating special cases of (5.4.8) by limiting the channel length e.g. to $L = 2$ and substituting in (5.4.12) yields (5.4.15)

$$F_{\gamma_{UB_{opt}}}(\gamma) = \prod_{m=1}^{M}[\frac{\Gamma(L_{m,1}, L_{m,1}\gamma/\overline{\gamma})}{\Gamma(L_{m,1})} + \frac{\Gamma(L_{m,2}, L_{m,2}\gamma/\overline{\gamma})}{\Gamma(L_{m,2})} - \frac{\Gamma(L_{m,1}, L_{m,1}\gamma/\overline{\gamma})}{\Gamma(L_{m,1})} \times \frac{\Gamma(L_{m,2}, L_{m,2}\gamma/\overline{\gamma})}{\Gamma(L_{m,2})}], \tag{5.4.13}$$

$$F_{\gamma_{LB_{opt}}}(\gamma) = \prod_{m=1}^{M}[\frac{\Gamma(L_{m,1}, L_{m,1}2\gamma/\overline{\gamma})}{\Gamma(L_{m,1})} + \frac{\Gamma(L_{m,2}, L_{m,2}2\gamma/\overline{\gamma})}{\Gamma(L_{m,2})} - \frac{\Gamma(L_{m,1}, L_{m,1}2\gamma/\overline{\gamma})}{\Gamma(L_{m,1})} \times \frac{\Gamma(L_{m,2}, L_{m,2}2\gamma/\overline{\gamma})}{\Gamma(L_{m,2})}], \tag{5.4.14}$$

$$\begin{aligned} F_{\gamma_{EX_{opt}}}(\gamma) = \prod_{m=1}^{M}[&-\left(-\overline{\gamma} + \mathrm{e}^{-\frac{\gamma}{\overline{\gamma}}}\overline{\gamma} + \mathrm{e}^{-\frac{r}{\overline{\gamma}}}\gamma\right)\overline{\gamma}^{-1} - 2\,\gamma^{5/2}\mathrm{e}^{-2\,\frac{\gamma}{\overline{\gamma}}}\sqrt{\gamma+1} \\ &\mathrm{K}\left(1,\, 2\,\frac{\sqrt{\gamma+1}\sqrt{\gamma}}{\overline{\gamma}}\right)\overline{\gamma}^{-3} - 2\,\gamma^{3}\mathrm{e}^{-2\,\frac{\gamma}{\overline{\gamma}}} \\ \mathrm{K}\left(0,\, 2\,\frac{\sqrt{\gamma+1}\sqrt{\gamma}}{\overline{\gamma}}\right)\overline{\gamma}^{-3} &- 2\,\gamma^{3/2}\mathrm{e}^{-2\,\frac{\gamma}{\overline{\gamma}}}\sqrt{\gamma+1}\mathrm{K}\left(1,\, 2\,\frac{\sqrt{\gamma+1}\sqrt{\gamma}}{\overline{\gamma}}\right)\overline{\gamma}^{-3} \\ &-2\,\gamma^{2}\mathrm{e}^{-2\,\frac{\gamma}{\overline{\gamma}}}\mathrm{K}\left(0,\, 2\,\frac{\sqrt{\gamma+1}\sqrt{\gamma}}{\overline{\gamma}}\right)\overline{\gamma}^{-3} + (\gamma+1)\,\gamma\,(-\overline{\gamma}-\gamma)\,\mathrm{e}^{-2\,\frac{\gamma}{\overline{\gamma}}} \\ \left(2\,\mathrm{K}\left(0,\, 2\,\frac{\sqrt{\gamma+1}\sqrt{\gamma}}{\overline{\gamma}}\right) + 2\,\overline{\gamma}\mathrm{K}\right.&\left.\left(1,\, 2\,\frac{\sqrt{\gamma+1}\sqrt{\gamma}}{\overline{\gamma}}\right)\frac{1}{\sqrt{\gamma+1}}\frac{1}{\sqrt{\gamma}}\right)\overline{\gamma}^{-3} + \\ 2\,(-\overline{\gamma}-\gamma)\,\mathrm{e}^{-2\,\frac{\gamma}{\overline{\gamma}}}\gamma^{3/2}\sqrt{\gamma+1}\mathrm{K}&\left(1,\, 2\,\frac{\sqrt{\gamma+1}\sqrt{\gamma}}{\overline{\gamma}}\right)\overline{\gamma}^{-3} + \mathrm{e}^{-\frac{\gamma}{\overline{\gamma}}} + \mathrm{e}^{-\frac{\gamma}{\overline{\gamma}}}\gamma\overline{\gamma}^{-1}]. \end{aligned} \tag{5.4.15}$$

where $\mathrm{K}(0,\cdot)$ and $\mathrm{K}(1,\cdot)$ are the modified Bessel function of the first and second order, respectively. The Maple software package is used to get these results. In the next section, the simulation results of the outage probability analysis, cooperative diversity order of the network and analysis of the end-to-end bit error rate (BER) as a function of SNR are presented.

5.5 Simulation Results

5.5.1 Simulation results of outage probability analysis

In order to verify the results obtained from (5.3.12), (5.3.13), (5.3.22) and (5.3.23), it is assumed that all the relay node links have the same average SNR, there is no direct link between the transmitter and the receiver due to shadowing, or distance, and all nodes are equipped with a single antenna. In this sub-section and in sub-section **5.5.2**, the multi-path channel gains, $\|\mathbf{h}_{m,i,L}\|$, are equal to L, in order to preserve the full temporal diversity. The outage probability performance of different numbers of path and best single relay and best two relay pair selection from M available relays, when $L = 2$ and $L = 3$ for different number of relays, and SNR = 5 dB is shown. Therefore, both cooperative spatial and temporal diversity gain are considered.

Fig. 5.3 shows the comparison of the outage probability of the best single relay selection and the best two relay pair selection schemes from M available relays of two-hop wireless transmission when the channel length is two $L = 2$, using the formulae given in (5.3.12) and (5.3.22). The simulated values, as in Figs. 5.3, 5.4, 5.6 and 5.7 are found by generating random channels and applying the $\max\{\min(.,.)\}$ operation. Generally, increasing the number of relays M, decreases the outage probability, and hence when the number of relays is large, the outage event becomes less likely. Selecting the best single relay scheme, for example, with the total number of available relays increasing from 4 to 12, the outage probability is decreased, i.e. 90% to 70% when the threshold value γ is 12 dB and the transmission rate R =1.85 bps/Hz. However,

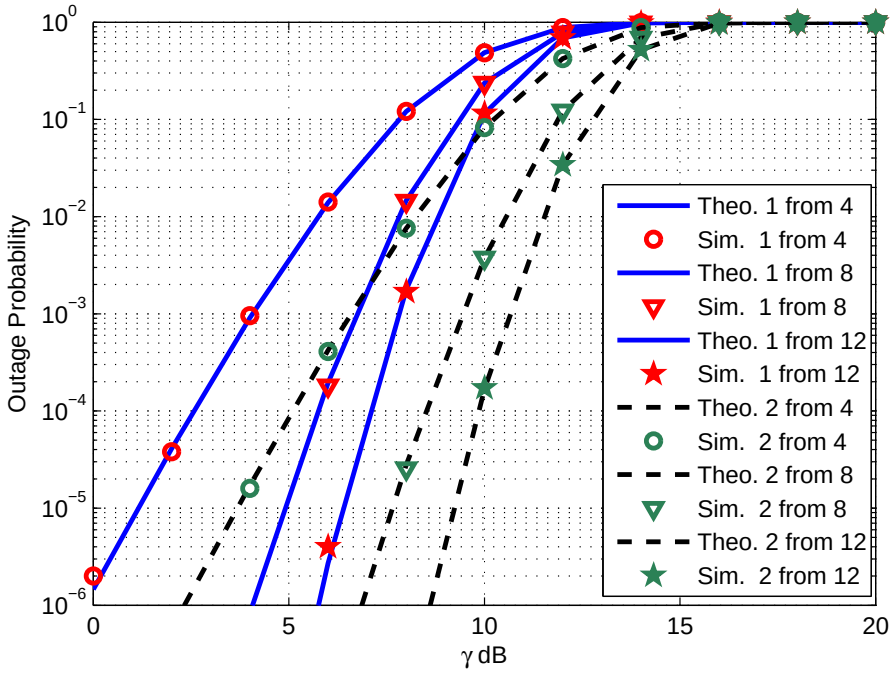

Figure 5.3. Comparison of the outage probability of the best single relay selection and the best two relay pair selection schemes from M relays of two-hop wireless transmission with two paths L = 2, with $\overline{\gamma} = 5$ dB. The theoretical results are shown in line style and the simulation results as points.

selecting the best two relay pair scheme, with the same threshold value, channel length and number of available relays, the outage probability is significantly decreased from 40% to 3.5%.

Fig. 5.4 shows the comparison of the outage probability of the best single relay selection and the best two relay pair selection schemes from M relays of two-hop wireless transmission when the channel length is three $L = 3$ using the formulae given in (5.3.13) and (5.3.23). When the total number of available relays increases from 4 to 12, the outage probability of a single relay selection is decreased from approximately 40% to 15%, at the same time, the outage probability of the best two re-

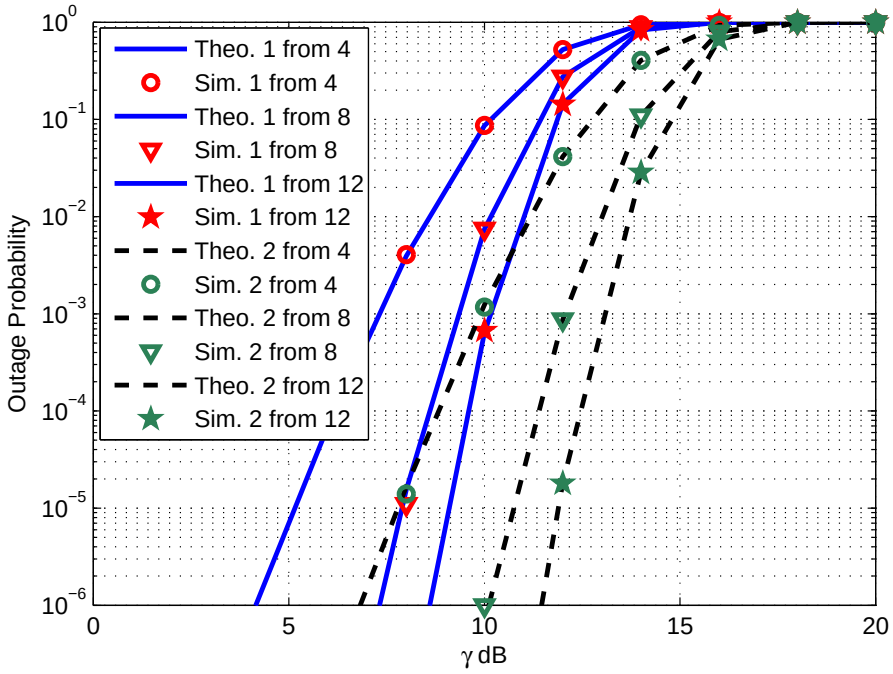

Figure 5.4. Comparison of the outage probability of the best single relay selection and the best two relay pair selection schemes from M relays of two-hop wireless transmission with three paths L = 3, with $\overline{\gamma} = 5$ dB. The theoretical results are shown in line style and the simulation results as points.

lay pair selection is significantly decreased from almost 4% to 0.002%, when the threshold value γ is 12 dB and the transmission rate $R =$ 1.95 bps/Hz. This result confirms that the best two relay pair selection provides more robust transmission than single relay selection.

In Fig. 5.3 selecting the best two relay pair scheme improves the outage probability performance by approximately 5 dB at 10^{-6} compared with the best single relay selection scheme. According to Fig. 5.4, the best two relay pair selection improves the outage probability performance by approximately 3 dB at 10^{-6} when the channel length $L = 3$.

These results confirm that increasing the channel length potentially provides more robust transmission. For example, when the number of available relays is 12, the threshold value γ is 12 dB, and the channel length increases from 2 to 3 the outage probability sharply decreases, from 15% to 0.002%. However, in practical transmission, more sophisticated coding and decoding schemes will be required to benefit from this temporal diversity [19].

5.5.2 Comparison of outage probability analysis upper, lower and exact SNR

The comparison of upper bound, lower bound and exact outage probability analysis through the cumulative density function (CDF) of the end-to-end SNR for an arbitrary multi-path channel length L and an arbitrary number of relay nodes M with best single relay selection. In this result, the multipath channel length $L = 2$, number of relays $M = 4$, and the average channel SNR $\overline{\gamma} = 5\ dB$.

In Fig. 5.5 comparison of the theoretical and simulation results of upper, lower and exact outage probability of the best single relay selection schemes from M available relays of two-hop wireless transmission when the channel length is two $L = 2$ is provided. The upper bound and lower bound can be confirmed, because the real simulation results are in between the lower and upper bound. In addition, upper bound SNR leads to lower bound outage bound and vise versa for lower bound SNR. It is noted, however, that at lower γ these bounds are not very tight, but these are easier to work with for general L. Equation (5.4.15) repre-

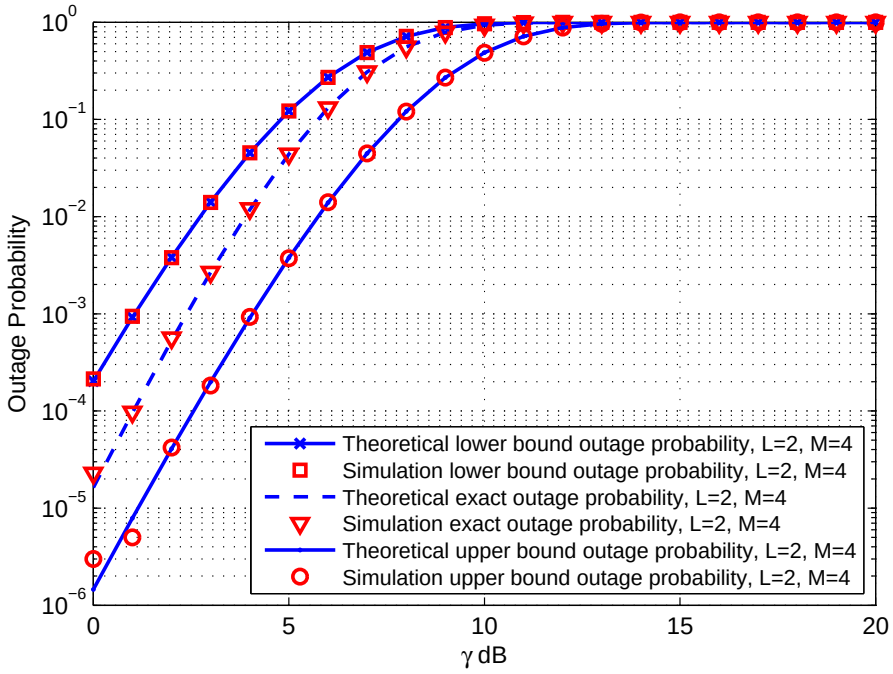

Figure 5.5. Analysis and simulation of upper bound and lower bound compared with the exact outage probability analysis, when $L = 2$, $M = 4$, and $\overline{\gamma} = 5$ dB. The theoretical results are shown in line style and the simulation results as points.

sents the calculation of exact outage probability when $L = 2$, however, the complexity of exact analysis increases exponentially with the number of multipath L. Whereas the simple equations (5.4.13) and (5.4.14) represent the calculation analysis of the closed form of outage probability of lower and upper bounds for an arbitrary number of channel lengths L and also an arbitrary number of relay nodes M.

5.5.3 Simulation analysis of cooperative diversity order of the network over multi-path channels

In this subsection, the outage probability vs SNR of a cooperative communication system over multi-path channels with best single and best two relay pair selection using the AF relaying network is evaluated. By employing the identical channel models in the network as in Subsection **5.5.1**. The overall cooperative diversity order has a spatial and temporal component.

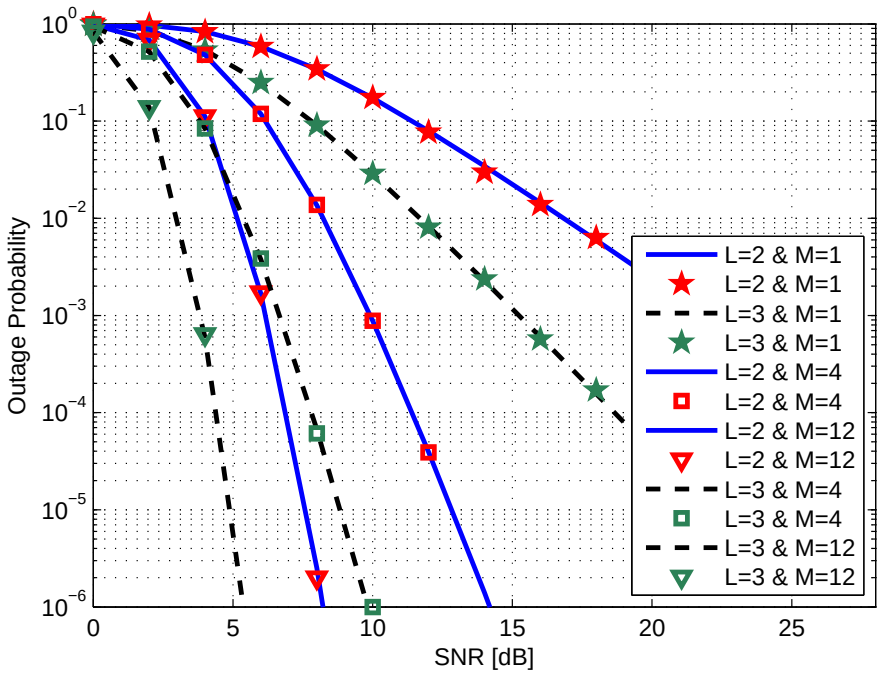

Figure 5.6. Comparison of the outage probability vs SNR of the best single relay selection scheme from M relays of two-hop wireless transmission when channel length two $L = 2$ and three $L = 3$, for a threshold value $\gamma = 5$ dB. The theoretical results are shown in line style and the simulation results as points.

In Fig. 5.6 the outage probability is plotted versus the SNR, without

relay selection when i.e. $M = 1$ and with the best single relay selection from M available relays with channel length two $L = 2$ and three $L = 3$. It is clearly seen that the system without relay selection, and increasing channel length from 2 to 3 improves the temporal diversity gain, for example, the diversity gains were found to be approximately 1.92 and 2.92, respectively. Whereas the theoretical values for $L = 2$ and 3 are 2 and 3, respectively, these measured and theoretical values will only match for infinitely large SNR as in definition (5.3.35). And likewise when selecting the best relay from 4 relays and the channel lengths are 2 and 3, the overall cooperative diversity gains are found to be approximately 7.14 and 10.0, and the theoretical values are 8 and 12, respectively. These confirm the overall cooperative diversity gain is significantly improved when the number of relays is increased.

In Fig. 5.7 the outage probability is also plotted versus the SNR, without relay selection when i.e. $M = 2$ and with the best two relay pair selection from M available relays with channel length two $L = 2$ and three $L = 3$. It can be seen that the system without relay selection, and increasing channel length from 2 to 3 improves the temporal cooperative diversity gain, for example, Fig. 5.7 confirms that the spatial and temporal cooperative diversity gain are approximately 3.94 and 5.73, respectively, whereas the theoretical values for $L = 2$ and 3 are 4 and 6, respectively. In this scheme, when selecting the best two relay pair from 4 relays and channel length are 2 and 3, the spatial and temporal cooperative diversity gains are approximately 7.41 and 10.53, and the theoretical values are 8 and 12, respectively. Again the measured and theoretical values will only match as the SNR tends to infinity. Clearly, the overall cooperative diversity gain can significantly

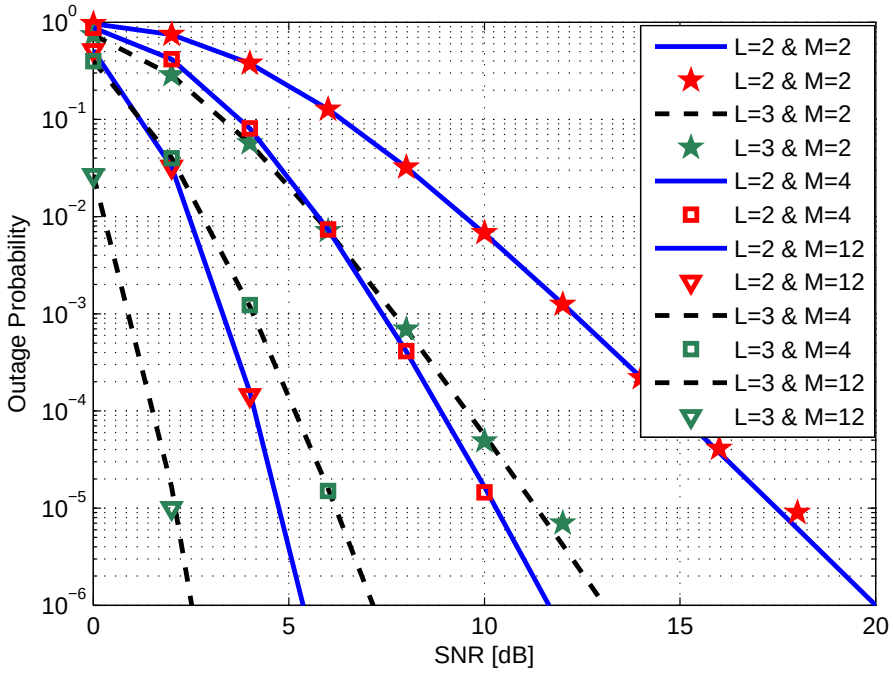

Figure 5.7. Comparison of the outage probability vs SNR of the best two relay pair selection scheme from M relays of two-hop wireless transmission when channel length is two $L = 2$ and three $L = 3$, for a threshold value $\gamma = 5$ dB. The theoretical results are shown in line style and the simulation results as points.

reduce the outage probability.

5.5.4 Analysis of the BER vs SNR

In this section, a comparison of the BER for a two-hop amplify-and-forward relaying cooperative communication system selecting the best one and best two relay pair from M available relays is performed. The main parameters of this simulation are 12 relays, uncoded transmission, quadrature phase-shift keying (QPSK) symbols, distributed space time block coding (DSTBC) and frequency selective channels, with $L = 3$ and $\|\mathbf{h}_{m,i,L}\| = 1$.

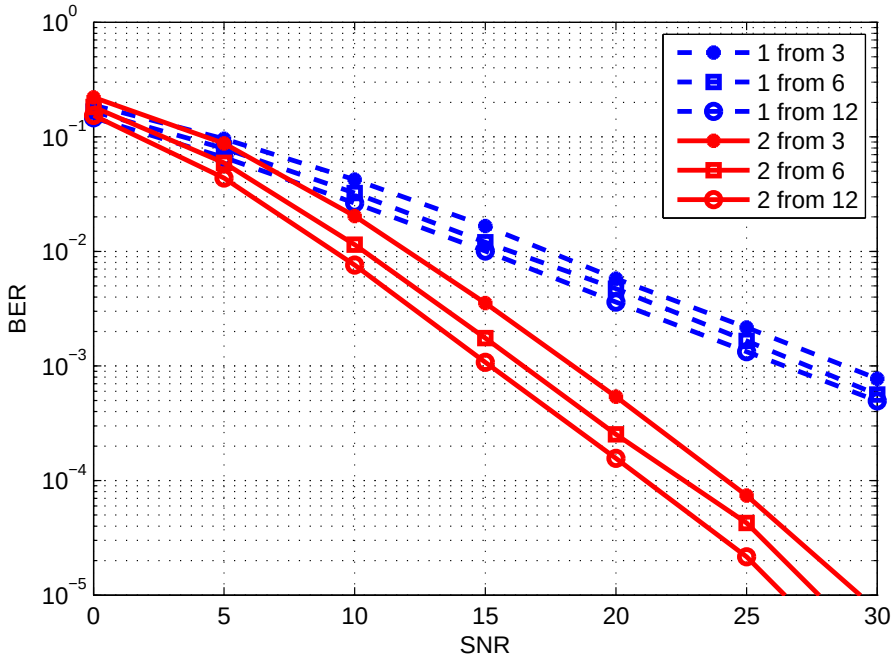

Figure 5.8. Comparison of best single and best two relay pair selection from M available relays of a two-hop wireless transmission with frequency selective channel when M is 3, 6 and 12.

Fig. 5.8 illustrates clearly the increased robustness of the best two relay pair selection scheme over the single relay selection scheme when the number of available relays in the system is increased. For example, at a BER of 10^{-3}, selecting the best single relay from three available relays requires approximately 27 dB SNR. However, selecting the best two relay pair gives equal performance with reduction in SNR by 10 dB with the same number of available relays. On the other hand, when the number of available relays M is increased from 3 to 12 the improvement of the single relay scheme is approximately 2.5 dB, where the improvement of the best two relay pair scheme scheme is approximately 3.5 dB, respectively. In Fig. 5.8 can be highlighted that, there

is not such a dramatic increase in performance with number of relays as in the earlier figures due to the channel normalization to unity gain and the block transmission. In addition, this figure presents only the spatial cooperative diversity gain while Fig. 5.6 and Fig. 5.7 illustrate both temporal and spatial cooperative diversity gains. In other words, the performance improvement is a consequence of increased cooperative spatial diversity gain; exploitation of the additional cooperative temporal diversity gain would require more sophisticated coding schemes as in [19] which are not the focus of this thesis.

5.6 Summary

In this chapter, outage probabilities for a cooperative two-hop amplify-and-forward system using transmission over multi-path channels with single and two relay pair selection were derived. A straightforward approach based on a Gamma distribution with positive integer scale parameter which has the same distribution as the sum of L independent exponential distribution random variables was used. The results indicate that the theoretical calculation and simulations are very close at different channel lengths $L = 2$ and 3. In addition, the robustness of the best two relay pair selection scheme over the single relay selection scheme was confirmed. Moreover, increasing the channel length and/or the number of relays improved the outage probability. In addition, the slopes of the outage probability vs SNR become steeper as the number L of multi-paths increases. Generalization of outage probability equation for L paths and M relays is dependent upon the channel normalization; without normalization outage probability will reduce with increasing L beyond 3, however the complexity of the closed form ex-

pression as in (5.3.23) meant it was presented in the Appendix A. The complexity of the exact analysis increases potentially with the number of multipaths L. Whereas the derived formulas of single relay selection scheme of upper and lower bonds SNRs are simple, applicable to an arbitrary number of channel length L and also to an arbitrary number M of relay nodes, they are not particulary tight. Therefore, in the next chapter, outage probability analysis of a cooperative communication system with the best single and pair of relays selection and clipped OFDM transmission will be presented.

Chapter 6

OUTAGE PROBABILITY ANALYSIS OF AN AF COOPERATIVE MULTI-RELAY NETWORK WITH BEST RELAY SELECTION AND CLIPPED OFDM TRANSMISSION

6.1 Introduction

Cooperative multi-node communication with selection relaying has received increasing attention recently due to improved bandwidth utilization and spatial diversity. Cooperative diversity (spatial and temporal) is one of the most effective techniques to mitigate fading in the multipath wireless environment [86] and [88]. Spatial cooperative diversity can be naturally exploited in a multi-relay environment as a virtual

multi-input multi-output orthogonal frequency division multiplexing (MIMO-OFDM) system. Moreover, an OFDM technique is able to transform a frequency selective fading channel to parallel flat fading channels. An OFDM signal is a superposition of N subcarrier channels usually carrying coded data symbols. It can constructively sum up to high peaks in the time domain which theoretically can be up to the number of OFDM subcarriers in magnitude. As a result of this drawback, the system may require more bits to cover a potentially broad dynamic range as well as a large linear range for the radio frequency (RF) power amplifier, which is expensive. Moreover, commercial RF power amplifiers can lead to unwanted out-of-band (OOB) interference and in-band distortion due to operating in the saturation region. PAPR becomes even more important in MIMO-OFDM systems because there are multiple transmit antennas each of which would require its own digital-to-analog converter (DAC) and RF power amplifier. According to [89], the efficiency and gain of the RF power amplifier stage are a tradeoff. Therefore, clipping an OFDM signal at the source not only allows the use of an efficient RF power amplifier, but also, acts as input back-off (IBO) to avoid the nonlinear effect of the RF power amplifier by decreasing the average power of the input signal. This implies the OFDM signal to be transmitted is in the linear region of the RF power amplifier [90]. In [18] there are several solutions to the PAPR problem of OFDM. The clipping method is generally the simplest solution computationally, which is the focus of this thesis, but it increases the BER and adds out-of-band interference.

6.1.1 The contributions of this chapter

Outage probability is a common measure of performance for cooperative communication systems but most previous works have not considered the evaluation of networks with PAPR reduction [79], [80] and [81]. However, in [91], the end-to-end outage probability analysis of AF network with one relay and direct link between source and destination node, and RF power amplifier nonlinear distortions at the relay nodes was presented. In this chapter, a theoretical analysis of outage probability when a clipped OFDM signal is transmitted over a multi-path fading channel of length L with an arbitrary number of relay nodes M together with best single and best two relay selection is performed. The clipping process is modeled as an aggregate of an attenuated signal component and clipping noise. The signal before clipping can be assumed to be Gaussian distributed provided N_{FFT} is large enough. Thus, the magnitude squared of the signal scaled by the clipping factor can be modeled by an exponential distribution. The clipping noise can be assumed to play the same role as channel noise. However, the PDF of the multi-path two-hop wireless transmission is modeled in the time domain as an Erlang distribution function which is used in selecting the best single relay. In both cases, the analytical expression for the CDF of the end-to-end signal-to-noise ratio (SNR) is obtained. Moreover, the analysis shows how the clipping process affects the outage probability for different clipping ratio levels. Finally, for both cases, the theoretical results are compared with simulated results to confirm the validity of the analysis.

6.1.2 The chapter organization

The chapter begins with a brief introduction of cooperative multi-node communication considering PAPR reduction by clipping the OFDM signal at the source node. In the section two, the system model of a cooperative system with clipping at the source over multi-path channels is presented. In the section three outage probability analysis based on CDF of the upper bound SNR is studied. Then, in the section four and five the outage probability analysis of selecting one relay and selecting the best two relay pairs from M Relays are explained, respectively. Finally, simulations are represented and conclusions are drawn.

6.2 System Model of a Cooperative System with Clipping at the Source

The cooperative multi-node communication system includes one clipped OFDM source node S, one destination node D and M relay nodes R_m, where $m = 1, 2, \cdots, M$. The main assumptions are, firstly, the terminals operate in a half-duplex mode, secondly, the received signals at the destination are only from the relays which means there is no direct path between the source and the destination as a consequence, for example, of shadowing loss. Moreover, the cooperative transmission technique is implemented with three wireless links as described and represented in (A) part (II) of Fig. 6.1. The effect of the clipping process at the transmitter is modeled as one transmission link. The other two links are presented by two AF type communication phases as in part (I) of Fig 6.1.

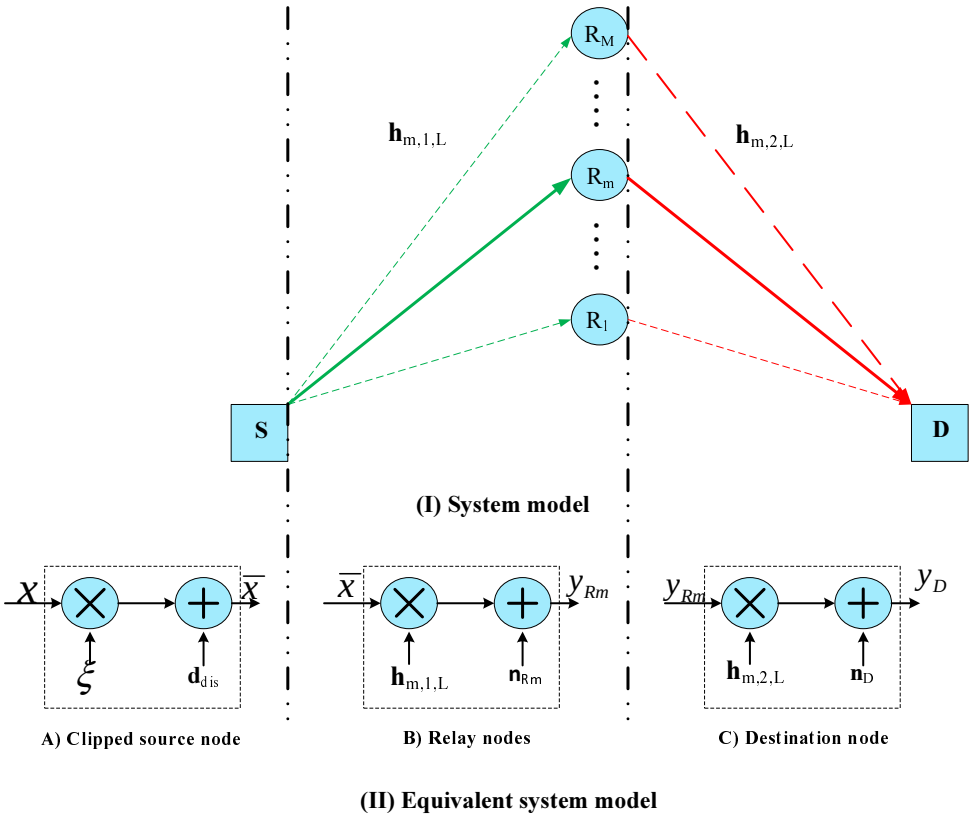

Figure 6.1. (I) System model and (II) Equivalent system model of clipped source multi-path and two-hop wireless transmission with the best single relay selection where solid lines represents the selected relay and dashed line represents the non-selected relay nodes.

In the first transmission phase, the source node S broadcasts the clipped signals to the M relay nodes. Then, during the second phase, the relay nodes retransmit the data to the destination node. In addition, the channel impulse response (CIR) from the source node S to the relay nodes R_m with channel length L, is $\mathbf{h}_{m,1,L} = [h_{m,1,1}, h_{m,1,2}, \cdots, h_{m,1,L}]^T$ and from R_m to the destination node D with the same channel length is $\mathbf{h}_{m,2,L} = [h_{m,2,1}, h_{m,2,2}, \cdots, h_{m,2,L}]^T$ as also represented in equation (6.2.1). These channel coefficients are assumed to represent quasi-static frequency selective Rayleigh fading models as

$$\mathbf{h}_{m,i,L}(t) = \sum_{l=1}^{L} h_{m,i,l}\delta(t - \tau_{m,i,l}), \tag{6.2.1}$$

where L is the number of multi-paths and $h_{m,i,l}$ and $\tau_{m,i,l}$ are the complex fading amplitude and time delay of the L^{th} path, respectively. The continuous time t is sampled so that it has a discrete time channel model [23] and [92].

It is assumed that all channel coefficients within $\mathbf{h}_{m,1,L}$ and $\mathbf{h}_{m,2,L}$ are uncorrelated with each others. Equation (6.2.2) represents the PDF of the strength of the constructive sum of L independent paths of each channel, which has an Erlang distribution, which is given by

$$f_{\gamma_{m,i,L}}(\gamma) = \frac{\gamma^{L_{m,i}-1}e^{-\frac{\gamma}{\overline{\gamma}}}}{\Gamma(L_{m,i})\overline{\gamma}^{L_{m,i}}}, \quad i = 1, 2, \tag{6.2.2}$$

where $\Gamma(L) = \int_0^\infty s^{L-1}e^{-s}ds = (L-1)!$ which is termed the complete Gamma function, where L is called the shape parameter which represents the number of paths in each channel, $\overline{\gamma}$ is called the scale parameter and is denoted as the average SNR [57]. The CDF of (6.2.2) can be obtained by taking the integral with respect to γ, yielding equation (6.2.3)

$$F_{\gamma_{m,i,L}}(\gamma) = 1 - \frac{\Gamma(L_{m,i}, \gamma/\overline{\gamma})}{\Gamma(L_{m,i})}, \quad i = 1, 2, \tag{6.2.3}$$

where $\Gamma(L, x) = \int_0^x s^{L-1}e^{-s}ds$ is the incomplete Gamma function.

6.2.1 Implementation at the clipped source node

Clipping is generally the simplest approach computationally to reduce the PAPR in an OFDM waveform. In practice, the clipping process is performed by using an envelope limiter, which mathematically can be implemented by equation (6.2.4) [59] and [58]. However, this process induces in-band distortion and out-of-band interference [18] and [93]. After clipping the time domain samples $\mathbf{x}$ which generates a new clipped sequence $\overline{\mathbf{x}}$, the elements of which are given by

$$\begin{aligned}\overline{x}[n] &= \mathcal{C}_A(x[n]) \\ &= \begin{cases} x[n] & |x[n]| \leq A \\ Ae^{\arg\{x[n]\}} & |x[n]| > A \end{cases} \qquad n = 0, 1, \cdot\cdot, N-1.\end{aligned} \tag{6.2.4}$$

According to the Bussgang theorem [55] [56] [57], the output memoryless nonlinear can be modeled as in equation (6.2.5) which is an aggregate of the original signal which is scaled by factor ξ and clipping noise $\mathbf{d}_{dis}$ as

$$\overline{\mathbf{x}} = \xi\mathbf{x} + \mathbf{d}_{dis}. \tag{6.2.5}$$

The scale factor ξ can be calculated as equation (6.2.6) as in [53] and [54]

$$\begin{aligned}\xi &= \frac{R_{x\overline{x}}(0)}{R_{xx}(0)} = \frac{E\{x\overline{x}\}}{E\{xx\}} \\ &= \frac{\int_0^A x^2 f_X(x)dx + \int_A^\infty Ax f_X(x)dx}{P_x} \\ &= 1 - e^{-\mu^2} + \frac{\sqrt{\pi}\mu}{2} erfc(\mu),\end{aligned} \tag{6.2.6}$$

where P_x is the average input power of the nonclipped OFDM signal, μ is a clipping ratio and defined as $\mu = A/\sqrt{P_x}$ and A is a clipped amplitude. According to the central limit theorem, the time domain OFDM signal can be approximated as a complex Gaussian distributed process with zero main and variance σ_x^2, when the number of subcarriers is large. Therefore, the OFDM envelope converges to a Rayleigh envelope distribution [53], [54], it has probability density function (PDF), i.e. $f_X(x) = \frac{2x}{P_x} e^{-x^2/P_x}$. However, equation (6.2.5) contains both output signal power $P_{cs} = \xi^2 P_x$ and a power of distortion noise P_{dis}. Therefore, the total output power $P_{out} = P_{\overline{x}} = P_{cs} + P_{dis}$, then, the output-to-input average power ratio η can be obtained as (with the assumption P_x is close to unity) [94]

$$\begin{aligned} \eta \cong \frac{P_{\overline{x}}}{P_x} &= \frac{\int_0^\infty |\overline{x}[n]|^2 f_X(x) dx}{P_x} \\ &= \frac{\int_0^A x^2 \frac{2x}{P_x} e^{-x/P_x} dx + \int_A^\infty A^2 \frac{2x}{P_x} e^{-x^2/P_x} dx}{P_x} \\ &= 1 - e^{-\mu^2}. \end{aligned} \tag{6.2.7}$$

Next, the source node broadcasts the clipped signal to the relay nodes, in the first stage and then the relay nodes resend the data to the destination, during the second stage.

6.2.2 Received clipped signal at the relay nodes and destination node

The received signal vectors of the relay nodes can be written as

$$\begin{aligned}\mathbf{y}_{SR_m} &= \sqrt{P_s}\mathbf{H}_{m,1,L}\overline{\mathbf{x}}_m + \mathbf{w}_{R_m} \\ &= G_1\xi\sqrt{P_s}\mathbf{H}_{m,1,L}\mathbf{x} + G_1\mathbf{H}_{m,1,L}\mathbf{d}_{dis} + \mathbf{w}_{R_m}.\end{aligned} \tag{6.2.8}$$

Then, the signal received by the destination during the second transmission stage is given by:

$$\begin{aligned}\mathbf{y}_{R_mD} &= \mathbf{H}_{m,2,L}\mathbf{y}_{SR_m} + \mathbf{w}_D \\ &= \xi G_1 G_2\sqrt{P_s}\mathbf{H}_{m,2,L}\mathbf{H}_{m,1,L}\mathbf{x} \\ &+ G_1 G_2\mathbf{H}_{m,2,L}\mathbf{H}_{m,1,L}\mathbf{d}_{dis} \\ &+ G_2\mathbf{H}_{m,2,L}\mathbf{w}_{R_m} + \mathbf{w}_D,\end{aligned} \tag{6.2.9}$$

where $\mathbf{H}_{m,1,L}$ and $\mathbf{H}_{m,2,L}$ represent convolution matrices formed from the coefficients of the source to relays channel and relays to destination channel, respectively. The elements of $\mathbf{w}_{R_m} \sim CN(0, \sigma_n^2)$ and $\mathbf{w}_D \sim CN(0, \sigma_n^2)$ are additive white Gaussian noise (AWGN) at the mth relay and the destination D, respectively, and also the elements of the clipping noise $\mathbf{d}_{dis}$ has a variance $\sigma_{dis}^2 = P_s(1 - e^{-\mu^2} - \xi^2)$.

6.2.3 End-to-end SNR of clipped source cooperative AF network

From equation (6.2.9), the exact end-to-end SNR at the receiving end can then be written as equation (6.2.10), where $P_s = P_x$ is the average energy per symbol, $\|\mathbf{h}_{m,1,L}\|^2$ and $\|\mathbf{h}_{m,2,L}\|^2$ are the channel gains, which denote Euclidean squared norm, between source and m^{th} relay nodes and destination node. The parameters σ_n^2 and σ_{dis}^2 are the noise variance of the nonclipped and clipped signal, respectively. G_1 is the clipped

source normalization gain and G_2 is the amplification gain at the m^{th} relay node which is used to normalize the received signal $\mathbf{y}_{R_m D}$, given as in [91]

$$\gamma_{ExD_m} = \frac{P_s G_1^2 G_2^2 \|\mathbf{h}_{m,2,L}\|^2 \|\mathbf{h}_{m,1,L}\|^2}{G_1^2 G_2^2 \|\mathbf{h}_{m,2,L}\|^2 \|\mathbf{h}_{m,1,L}\|^2 \sigma_{dis}^2 + G_2^2 \|\mathbf{h}_{m,2,L}\|^2 \sigma_n^2 + \sigma_n^2}, \quad (6.2.10)$$

$$G_1 = \frac{\sqrt{P_s}}{\sqrt{\xi^2 P_s + \sigma_{dis}^2}}, \quad (6.2.11)$$

$$G_2 = \frac{\sqrt{P_r}}{\sqrt{\xi^2 G_1^2 P_s \|\mathbf{h}_{m,1,L}\|^2 + G_1^2 \|\mathbf{h}_{m,1,L}\|^2 \sigma_{dis}^2 + \sigma_n^2}}, \quad (6.2.12)$$

where P_s is the average energy per symbol. By substituting (6.2.11) and (6.2.12) into (6.2.10), and $\gamma_{m,1,L} = \|\mathbf{h}_{m,1,L}\|^2 P_s/\sigma_n^2$, $\gamma_{m,2,L} = \|\mathbf{h}_{m,2,L}\|^2 P_r/\sigma_n^2$ and $\gamma_{clip} = \xi^2 P_s/\sigma_{dis}^2$. Then, the instantaneous exact end-to-end signal-to-noise ratio (γ_{ExD_m}) is obtained as equation (6.2.13)

$$\gamma_{ExD_m} = \frac{\gamma_{clip}\gamma_{m,1,L}\gamma_{m,2,L}}{\gamma_{m,1,L}\gamma_{m,2,L} + \gamma_{clip}\gamma_{m,2,L} + \gamma_{clip}\gamma_{m,1,L} + \gamma_{m,2,L} + \gamma_{m,1,L} + \gamma_{clip} + 1}, \quad (6.2.13)$$

where $\gamma_{m,1,L}$ and $\gamma_{m,2,L}$ are the instantaneous SNR of the $S \longrightarrow R_m$ and $R_m \longrightarrow D$ links, respectively, and γ_{clip} represents the effect of the clipping process, which is modeled as an exponential wireless link. The outage probability analysis will be explained in the next section.

6.3 Outage Probability Analysis

The outage probability is defined as when the average end-to-end SNR falls below a certain predefined threshold value, i.e. $\gamma = 2^{2R} - 1$, where R is the target rate [13]. The outage probability can be expressed as in [82], [95]

$$P_{out} = \int_0^{\gamma} f_{\gamma}(\gamma) d\gamma = F_{\gamma}(\gamma), \tag{6.3.1}$$

where $f_{\gamma}(\gamma)$ is the probability density function (PDF) and $F_{\gamma}(\gamma)$ is the cumulative distribution function (CDF) of the SNR. Next, the upper bound analysis is considered.

6.3.1 CDF analysis of upper bound

Lower and upper bounds for the equivalent SNR can be given as

$$\gamma_{LB} \leq \gamma_{ExD_m} \leq \gamma_{UB}, \tag{6.3.2}$$

where $\gamma_{LB} = \frac{1}{2}\sum_{m=1}^{M} \gamma_m$ and $\gamma_{UB} = \sum_{m=1}^{M} \gamma_m$. To find γ_{UB}, the following relay selection criterion is adopted as in [91]

$$\gamma_{UB} = \min(\gamma_{m,1,L}, \gamma_{m,2,L}, \gamma_{clip}) \geq \gamma_{ExD_m}. \tag{6.3.3}$$

In order to calculate the theoretical analysis of upper bound outage probability through the CDF of the end-to-end signal-to-noise ratio (SNR) for an arbitrary multi-path channel length L, then, the CDF of $\gamma_{UB_m} = \min\{\gamma_{m,1,L}, \gamma_{m,2,L}, \gamma_{Clip}\}$ is considered which can be expressed

as (6.3.4)

$$\begin{aligned} F_{\gamma_{UB_m}}(\gamma) &= 1 - P_r(\gamma_{m,1,L} > \gamma)P_r(\gamma_{m,2,L} > \gamma)P_r(\gamma_{Clip} > \gamma) \\ &= 1 - [1 - P_r(\gamma_{m,1,L} \leq \gamma)][1 - P_r(\gamma_{m,2,L} \leq \gamma)] \\ &\quad [1 - P_r(\gamma_{Clip} \leq \gamma)] \\ &= 1 - [1 - F_{\gamma_{m,1,L}}(\gamma)][1 - F_{\gamma_{m,2,L}}(\gamma)][1 - F_{\gamma_{clip}}(\gamma)], \end{aligned} \tag{6.3.4}$$

where $F_{\gamma_{m,1,L}}(\gamma) = [1 - \frac{\Gamma(L_{m,1},\gamma/\overline{\gamma})}{\Gamma(L_{m,1})}]$, $F_{\gamma_{m,2,L}}(\gamma) = [1 - \frac{\Gamma(L_{m,2},\gamma/\overline{\gamma})}{\Gamma(L_{m,2})}]$ and $F_{\gamma_{clip}}(\gamma) = [1 - e^{-\gamma/\overline{\gamma}_{clip}}]$, $\overline{\gamma}_{clip} = \mu^2$ represents the average SNR of the clipped signal at source, $F_{\gamma_{m,1,L}}(\gamma)$ and $F_{\gamma_{m,2,L}}(\gamma)$, are the CDF of the multi-path channels with length L, which represent the first and second hops, whereas, $F_{\gamma_{clip}}(\gamma)$ is the CDF of the clipping operation at the source, which is modeled as an exponential distribution. By simple manipulation of (6.3.4), upper bound end-to-end CDF can be obtained

$$F_{\gamma_{UB_m}}(\gamma) = 1 - \frac{\Gamma(L_{m,1},\gamma/\overline{\gamma})}{\Gamma(L_{m,1})} \times \frac{\Gamma(L_{m,1},\gamma/\overline{\gamma})}{\Gamma(L_{m,1})} \times e^{-\gamma/\overline{\gamma}_{clip}}. \tag{6.3.5}$$

The full outage probability analysis of selecting one relay from M relays will be considered in the next section.

6.4 Outage Probability of Selecting One Relay from M Relays

In this approach the best relay node from M available relays can be selected, namely, select the maximum $\gamma_{UB_{opt}}$ from the M relays instantaneous SNR. The selection of the best relay is performed in two steps [86]. The first step is to obtain the weaker link between the first and second hop of each relay node as in equation (6.3.3) which represents the simulation part, whereas (6.3.5) represent theoretical analysis of upper bound. Secondly, these weak links are ordered and the one

with the highest SNR is selected as the candidate to relay the data to the destination, which is expressed in equation (6.4.1)

$$\gamma_{UB_{opt}} = \max_{m}\{\min(\gamma_{m,1,L}, \gamma_{m,2,L}, \gamma_{clip})\} \quad m = 1, 2, ..., M. \tag{6.4.1}$$

Building upon (6.3.5), the CDF of $\gamma_{UB_{opt}}$ can be expressed as in [23]

$$F_{\gamma_{UB_{opt}}}(\gamma) = \prod_{m=1}^{M} F_{\gamma_{UB_m}}(\gamma), \tag{6.4.2}$$

where M is the number of relay nodes in the system.

By substituting (6.3.5) into (6.4.2), the outage probability for an arbitrary number of relay nodes M and arbitrary multi-path channel lengths L with best single relay selection from M available relays is obtained

$$F_{\gamma_{UB_{opt}}}(\gamma) = \prod_{m=1}^{M}[1 - \frac{\Gamma(L_{m,1}, \gamma/\overline{\gamma})}{\Gamma(L_{m,1})} \times \frac{\Gamma(L_{m,1}, \gamma/\overline{\gamma})}{\Gamma(L_{m,1})} \times e^{-\gamma/\overline{\gamma}_{clip}}]. \tag{6.4.3}$$

Next, simulation results of outage probability are presented, without and with relay selection.

6.5 Outage Probability of Selecting the Best Two Relay Pairs from M Relays

The selection of the best two relay nodes from M available relays in the same cluster is achieved, by selecting $\gamma_{UB_{opt}}$ and $\gamma_{UB_{opt-1}}$ which are the maximum and second largest, from the M relays instantaneous SNR. The selection of the best couple of relays is performed in two steps [86]. The first step is to obtain the weaker link between the first and second

hop of each relay node as in equation (6.3.3). Secondly, these weak links are ordered and the two links with the first and second maximum SNR are selected as the candidates to relay the data to the destination, which are expressed

$$\begin{aligned} \gamma_{UB_{opt}} &= \max_{m}\{\min(\gamma_{m,1}, \gamma_{m,2}, \gamma_{clip})\} \\ \gamma_{UB_{opt-1}} &= \max_{m-1}\{\min(\gamma_{m,1}, \gamma_{m,2}, \gamma_{clip})\} \\ & \qquad m = 1, 2, .., M. \end{aligned} \tag{6.5.1}$$

Clearly, choosing the second largest is dependent on the first maximum, therefore, according to [84], it can be found as the joint distribution of the two most maximum values. Using the CDF expression in (6.3.5) and its derivative to provide the PDF, the joint CDF of $\gamma_{UB_{opt}}$ and $\gamma_{UB_{opt-1}}$ can be expressed as

$$f^L_{X,Y}(x, y) = M(M-1) f^L_X(x) f^L_Y(y) [F^L_Y(y)]^{M-2}, \tag{6.5.2}$$

where M is the number of relay nodes in the system, $\gamma_{UB_{opt}} = X$ and $\gamma_{UB_{opt-1}} = Y$ which are the first and second largest maximum values, respectively. Based upon the fact that the OFDM technique has the ability to transform a frequency selective fading channel, which is multipath in the time domain, to parallel flat fading channels, which can be represented as one path in the time domain ($L = 1$), therefore, equation (6.3.4) can be written as

$$\begin{aligned} F_{\gamma_{UB_m}}(\gamma) &= 1 - \frac{1}{\overline{\gamma}_{m,1}} e^{-\frac{\gamma}{\overline{\gamma}_{m,1}}} \times \frac{1}{\overline{\gamma}_{m,2}} e^{-\frac{\gamma}{\overline{\gamma}_{m,2}}} \times e^{-\gamma/\overline{\gamma}_{clip}} \\ &= 1 - \frac{1}{\overline{\gamma}_{m,i,clip}} e^{-\frac{\gamma}{\overline{\gamma}_{m,i,clip}}}, \end{aligned} \tag{6.5.3}$$

where $\overline{\gamma}_{m,1} = \overline{\gamma}_{m,2} = \overline{\gamma}_{m,i}$ and $\overline{\gamma}_{m,i,clip} = \frac{\overline{\gamma}_{m,i}}{2+\frac{\overline{\gamma}_{m,i}}{\overline{\gamma}_{clip}}}$. By substituting (6.5.3) into (6.5.2), so, the PDF form can be expressed as

$$f^1_{X,Y}(x,y) = M(M-1)\left[\frac{1}{\overline{\gamma}_{m,i,clip}}e^{-\frac{x}{\overline{\gamma}_{m,i,clip}}}\right] \left[\frac{1}{\overline{\gamma}_{m,i,clip}}e^{-\frac{y}{\overline{\gamma}_{m,i,clip}}}\right] \left[1-\frac{1}{\overline{\gamma}_{m,i,clip}}e^{-\frac{y}{\overline{\gamma}_{m,i,clip}}}\right]^{M-2}. \tag{6.5.4}$$

Then, by integrating (6.5.2), the outage probability can be expressed as

$$F^L_{\gamma_{opt}}(\gamma) = \int_0^{\gamma/2}\int_y^{\gamma-y} f^L_{X,Y}(x,y)dxdy. \tag{6.5.5}$$

The CDF equation can be found by substituting (6.5.4) in (6.5.5)

$$F^1_{\gamma_{opt}}(\gamma) = N(N-1)\sum_{k=0}^{N-2}\binom{N-2}{k}(-1)^k \int_0^{\gamma/2}\int_y^{\gamma-y} \left[\frac{1}{\overline{\gamma}_{m,i,clip}}e^{-\frac{x}{\overline{\gamma}_{m,i,clip}}}\right] \left[\frac{1}{\overline{\gamma}_{m,i,clip}}e^{-\frac{y}{\overline{\gamma}_{m,i,clip}}}\right] \left[\frac{1}{\overline{\gamma}_{m,i,clip}}e^{-\frac{yk}{\overline{\gamma}_{m,i,clip}}}\right] dxdy. \tag{6.5.6}$$

To evaluate (6.5.6), firstly, calculating the part of the expression in the outer most summation when k = 0

$$F^{1,k=0}_{\gamma_{opt}}(\gamma) = \frac{1}{2}\frac{(\overline{\gamma}_{m,i,clip}e^{\frac{\gamma}{\overline{\gamma}_{m,i,clip}}} - \overline{\gamma}_{m,i,clip} - \gamma)e^{\frac{-\gamma}{\overline{\gamma}_{m,i,clip}}}}{\overline{\gamma}_{m,i,clip}}. \tag{6.5.7}$$

Finally, the full CDF closed form expression as

$$F^{1}_{\gamma_{opt}}(\gamma) = N(N-1)\ \Big[F^{1,K=0}_{\gamma_{opt}}(\gamma) + \sum_{k=1}^{N-2}\binom{N-2}{k}(-1)^{k} \frac{(e^{\frac{\gamma}{\overline{\gamma}_{m,i,clip}}}k - 2 - k + 2e^{-\frac{\gamma k}{2\overline{\gamma}_{m,i,clip}}})e^{\frac{-\gamma}{\overline{\gamma}_{m,i,clip}}}}{(2+k)k}\Big]. \tag{6.5.8}$$

Next, results of outage probability simulation and analysis of the best single and two relay pair selection scheme are presented.

6.6 Simulation Results

6.6.1 Outage probability analysis of clipped OFDM transmission for the best single relay selection scheme

To verify the results which are obtained from (6.4.3), it is assumed that the links between source to relay nodes and from relays to destination nodes have the same average SNR; no direct link is assumed between the transmitter and the receiver due to shadowing, or distance, and all nodes are equipped with a single antenna. In this section, the outage probability performance of different numbers of path L, different number of relays and different clipping ratio (μ) are derived. The multi-path channel gains, $\|\mathbf{h}_{m,i,L}\|$, are equal to L, and the average SNR, $\overline{\gamma} = 5$ dB. The simulated values, as in Figs. 6.2, 6.3, 6.4 and 6.5 are found by generating random channels and applying the $\max\{\min(.,.,.)\}$ operation. Moreover, it is assumed that the destination knows perfectly all the channels and that the relay knows perfectly the source-relay channel.

Figs. 6.2 and 6.3 illustrate the comparison of the outage probability without relay selection $M = 1$ and with best single relay selection from M available relays and when the channel lengths are one $L = 1$ and three $L = 3$, respectively. Both cases have been investigated when the

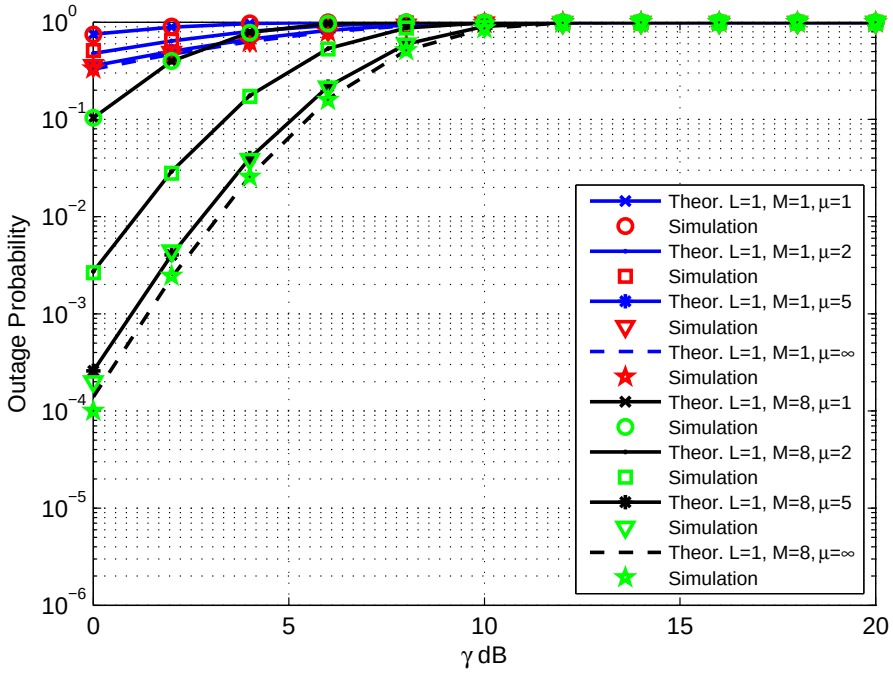

Figure 6.2. Comparison of outage probability, theoretical analysis and simulation of clipped OFDM at the source of a two-hop wireless transmission with one path L = 1, without relay selection $M = 1$, with best single relay selection $M = 8$ and with various clipping ratios (μ = 1, 2, 5 and ∞ (nonclipped) represented by dash line). Theoretical results are shown in line style and the simulation results as points.

clipping process is implemented at the source node and with various clipping ratio levels μ. Generally, the best single relay selection scheme implies best performance compared with the system without relay selection as in Fig. 6.2 and Fig. 6.3. However, when $\mu = 1$ both systems have the worst performance and the outage probability is approximately identical for the same number of relays and different channel lengths L , e.g. $L = 1$ and 3. On the other hand, according to Figs. 6.2 and 6.3, increasing clipping ratio μ from 1 to 2, the outage probability is decreased, that is, 90 to 30% when $L = 1$, $M = 8$, and from 70 to 1%

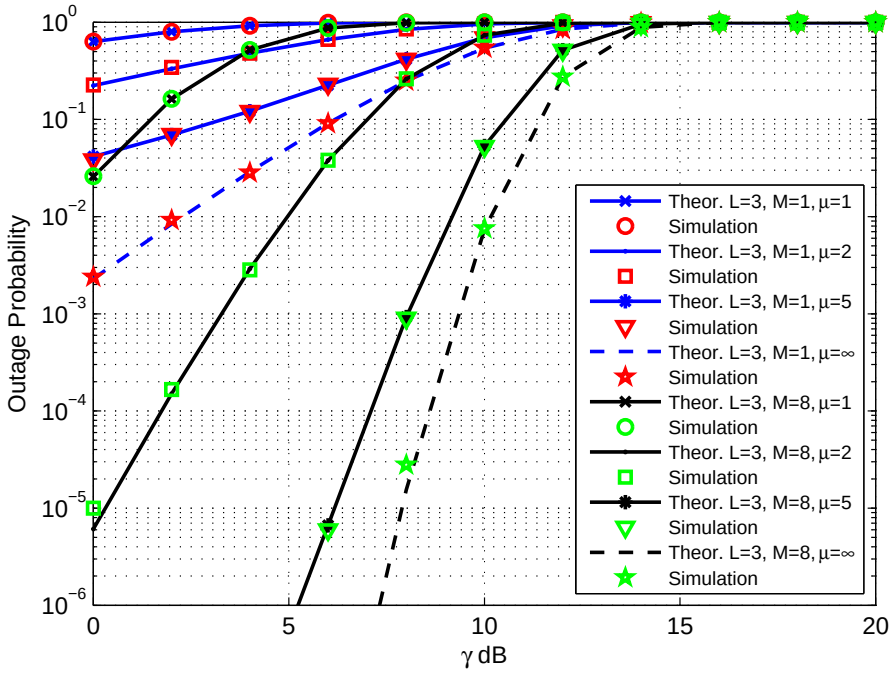

Figure 6.3. Comparison of outage probability, theoretical analysis and simulation of clipped OFDM at the source of a two-hop wireless transmission with three path $L = 3$, without relay selection $M = 1$, with best single relay selection $M = 8$ and with various clipping ratios ($\mu = 1$, 2, 5 and ∞ (nonclipped) represented by dash line). Theoretical results are shown in line style and the simulation results as points.

when $L = 3$, $M = 8$, respectively, for the same threshold value γ is 5 dB which is equal to $R = 1.29$ bps/Hz of transmission rate.

These results confirm that deep clipping ratio increases the outage probability and selecting the best single relay from a large number of relay nodes potentially provides more robust transmission, and hence the outage event becomes less likely. Moreover, the analytical and simulation results are very close to each other for all curves.

6.6.2 Outage probability vs SNR of clipped OFDM transmission for the best single relay selection scheme

The theoretical outage probability results are obtained by using equation (6.4.3) where the threshold value is fixed at $\gamma = 2^{2R} - 1 = 5\ dB$ and the average SNR values $\overline{\gamma}$ is varied. The simulation results are generated by using random channels and applying the $\max\{\min(.,.,.)\}$ operation as in equation (6.4.1). Figs. 6.4 and 6.5 illustrate the system without relay selection when i.e. $M = 1$ and with the best single relay selection from $M = 8$ available relays with channel lengths $L = 1$ and $L = 3$, respectively.

From both figures, it is seen that both schemes without and with relay selection have the worst performance when the clipping ratio $\mu = 1$, which is 0 dB. However, increasing μ to 2, yields very slight improvement in the system without relay selection, where the performance floored at approximately 0.7 dB, whereas slight improvement is achieved by the system when selecting the best one from 8 relay nodes, where the performance is floored at approximately 0.07 dB. Moreover, the performance of the system with relay selection when clipped by $\mu = 5$ is close to nonclipped performance of the same system. In addition, due to increasing the channel length L, the performance is floored at different SNR values but at the same outage probability for the same clipping ratio μ.

Also these results confirm that the deep clipping ratio destroys the performance of both schemes e.g. floored at 0 dB. In contrast, slightly increasing the clipping ratio leads to potential improvement on the system with the best single relay from M available relay nodes compared with the system without relay selection.

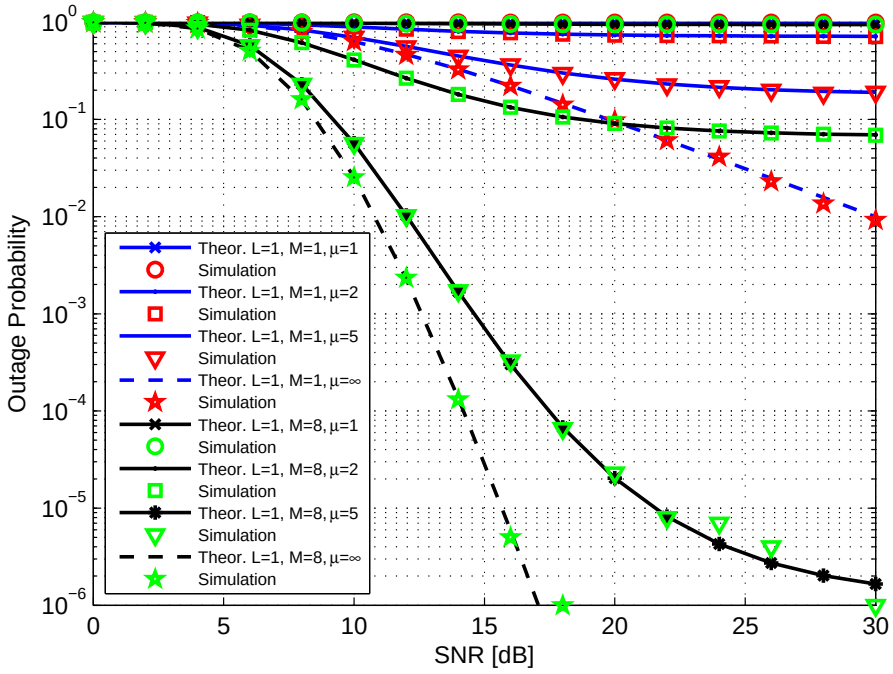

Figure 6.4. Comparison of outage probability, theoretical analysis and simulation of clipped OFDM at the source of a two-hop wireless transmission with one path $L = 1$, without relay selection $M = 1$, with best single relay selection $M = 8$ and with various clipping ratios (μ = 1, 2, 5 and ∞ (nonclipped) represented by dash line). Theoretical results are shown in line style and the simulation results as points.

The performance of the OFDM system can be represented by $L = 1$, based upon the fact that the OFDM technique is able to transform a frequency selective fading channel to parallel flat fading channels. Moreover, in order to preserve the full temporal diversity, the multi-path channel gains, $\|\mathbf{h}_{m,i,L}\|$ are equal to L, is exploited.

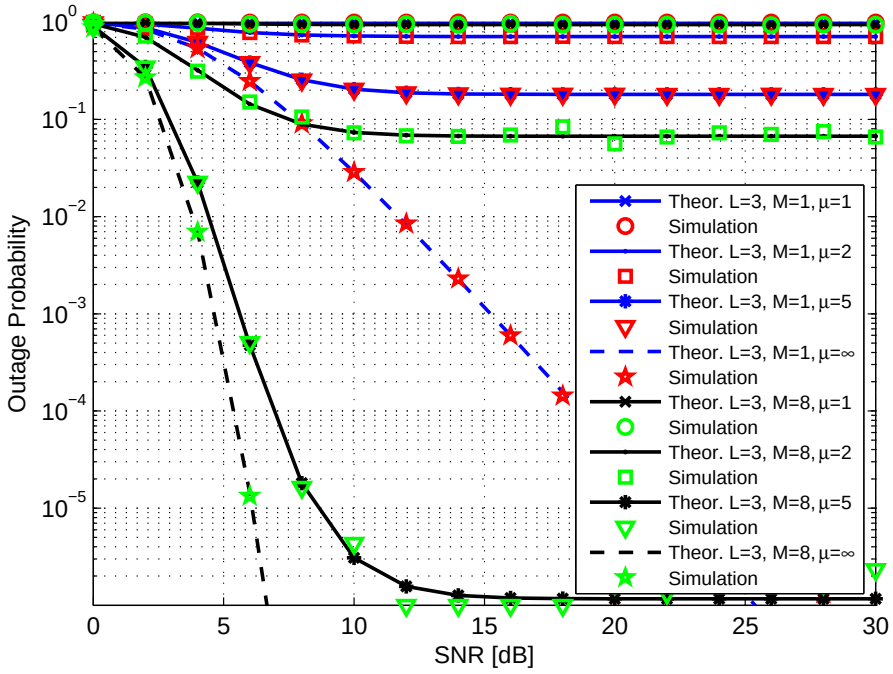

Figure 6.5. Comparison of outage probability, theoretical analysis and simulation of clipped OFDM at the source of a two-hop wireless transmission with three path $L = 3$, without relay selecting $M = 1$, with best single relay selection $M = 8$ and with various clipping ratios ($\mu = 1$, 2, 5 and ∞ (nonclipped) represented by dash line). Theoretical results are shown in line style and the simulation results as points.

6.6.3 Outage probability analysis of clipped OFDM transmission for the best two relay pair selection scheme

To verify the results which are obtained from (6.5.8), it is assumed that the links between source to relay nodes and from relays to destination nodes have the same average SNR. It is assumed that no direct link exists between the transmitter and the receiver due to shadowing, or distance, and all nodes are equipped with a single antenna. In this section, it is shown that outage probability performance of different number of relays and different levels of clipping ratio (μ) and it is assumed

that the SNR $\overline{\gamma} = 5\ dB$. The simulated values, as in Fig. 6.6 are found by generating random channels and applying the $\max\{\min(.,.,.)\}$ operation. Moreover, it is assumed that the destination knows perfectly all the channels and that the relay knows perfectly the source-relay channel.

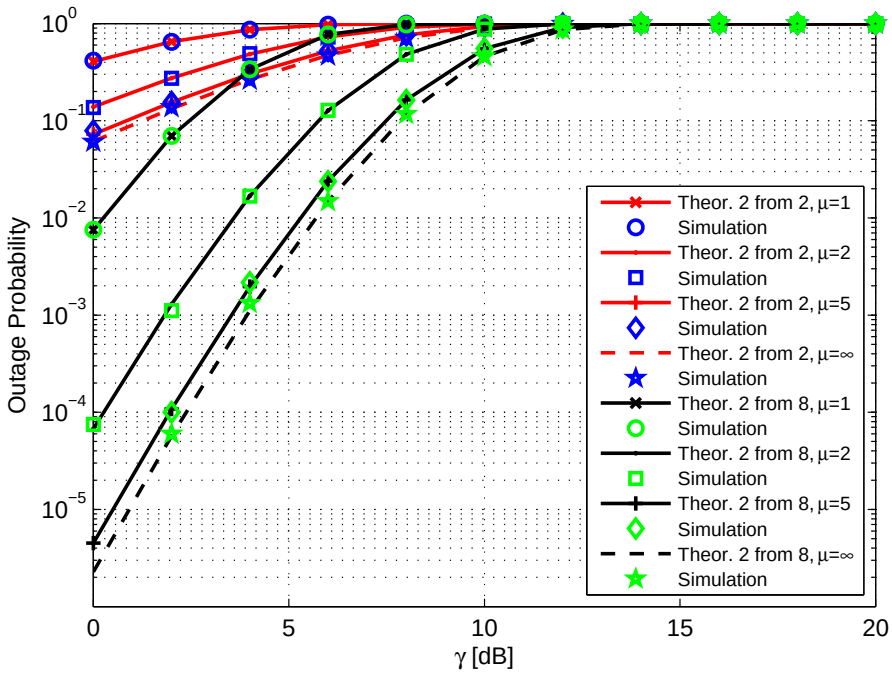

Figure 6.6. Comparison of outage probability of clipped OFDM at the source without relay selecting $M = 2$ and with best two relay selection $M = 8$ and with various clipping ratios ($\mu = 1$, 2, 5 and ∞ (nonclipped) represented by dash line). Theoretical results are shown in line style and the simulation results as points.

Fig. 6.6 illustrates the comparison of the outage probability without relay selection $M = 2$ and with best pair relay selection from eight available relay nodes. Both cases have been investigated when the clipping process is implemented at the source node and with various clipping ratio levels μ. Generally, selecting the best two relay pairs

from eight available relay nodes implies best performance compared with the system without relay selection. For example, when $\mu = 1$ and the threshold value is $\gamma = 5$ dB which is equal to $R = 1.16$ bps/Hz of transmission rate, the outage performance of the system which has just two relay nodes is approximately 90%, whereas, the outage performance of the system when selecting the best two relays from eight available relay nodes is approximately 30% which approximately equals the non-clipped performance of the former system. In addition, the selection system provides significant improvement of outage when clipping level μ is increased to 2, which is 0.02% at the threshold value is $\gamma = 5$ dB. Finally, the performance of the system with relay selection clipped by 5 is close to the nonclipped performance, which is represented by the dashed line in Fig. 6.6.

6.6.4 Outage probability vs SNR of clipped OFDM transmission for the best two relay pair selection scheme

Equation (6.5.8) is used to plot the theoretical outage probability versus the SNR by fixing the threshold value $\gamma = 2^{2R} - 1 = 5$ dB and varying the average SNR values $\overline{\gamma}$ in dB. On the other hand, simulation results generated by using random channels and applying the $\max\{\min(\gamma_{m,1,L}, \gamma_{m,2,L}, \gamma_{clip})\}$ operation as in equation (6.5.1) are included.

From Fig. 6.7, it is clearly seen that the scheme without relay selection has the worst performance when the clipping ratio $\mu = 1$, the outage is 100%. However, slight improvement is achieved with the selection system. Additionally, when the clipping ratio is greater than one, the performance of the selection scheme is significantly improved

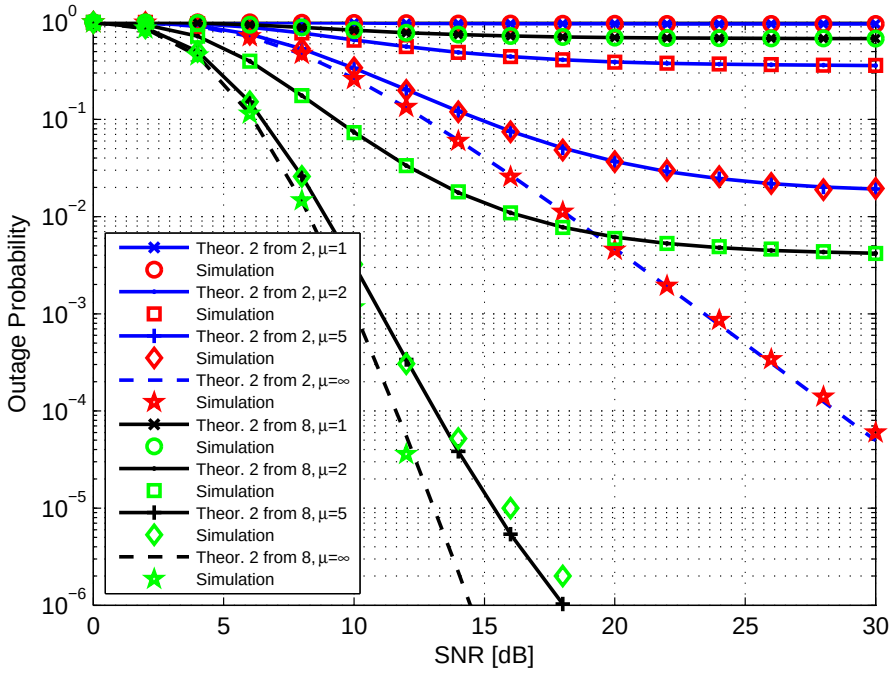

Figure 6.7. Comparison of outage probability vs SNR of clipped OFDM at the source without relay selection $M = 2$ and with best two relay selection $M = 8$ with various clipping ratios ($\mu = 1$, 2, 5 and ∞ (nonclipped) which represented by dash line). Theoretical results are shown in line style and the simulation results as points.

compared with the nonselection system. For example, at SNR = 15 dB, the outage probability of the system having just 2 relay nodes is approximately 100%, 50%, 10% and 4%, for $\mu = 1$, 2, 5 and ∞ (nonclipped), respectively. Whereas, the outage probability of the system which selecting the best two relays from 8 available relay nodes is approximately 70%, 1%, 0.001% and 0.0001%, for $\mu = 1$, 2, 5 and ∞ (nonclipped), respectively.

These results confirm that the selection of the best two relay pairs from a large number of available relay nodes provides more robust transmission compared with the system having just two relay nodes. More-

over, the analytical and simulation results are very close to each other for all curves.

6.7 Summary

In this chapter, the outage probabilities of clipped OFDM source for a cooperative amplify-and-forward system with the best single and best two relay pairs selection from M available relay nodes were derived. The derived formulas are simple, and applicable to an arbitrary number of relay nodes M. However, the two-hop wireless transmission was modeled in the time domain as an Erlang distribution function which is used in selecting the best single relay and as flat fading for selecting the best two relay pairs for simplicity. The nonlinear distortions introduced by the clipping process were modeled as an aggregate of attenuation factor and clipping noise, and the magnitude squared of the signal scaled by the clipping factor was modeled as an exponential distribution. The clipping noise has therefore been assumed to play the same role as channel noise. The clipping process caused a degradation of the system performance and the degradation depends upon the clipping ratio. However, to some extent, selecting the best two relay pairs from a large number of relay nodes overcomes this degradation. The results indicate that the theoretical calculation and simulation were close for different numbers of available relay nodes. In the next chapter, the summary and conclusion to the thesis and suggestions for future work will be provided.

Chapter 7

CONCLUSIONS AND FUTURE WORK

In this chapter, the results that were presented in this thesis are summarized. Then, conclusions are drawn from the contribution chapters. Finally, suggestions for future work are provided.

7.1 Conclusions

This thesis focuses on PAPR reduction with the clipping method applied at the source node in a cooperative MIMO-OFDM network. The SFBC scheme is exploited at the relay nodes and the IAR decoding scheme is employed at the destination node. Full cooperative diversity and array gain can be achieved with a limited bandwidth feedback channel. Therefore, a group feedback scheme was proposed to make the proposed system more practical and feasible. To further enhance the system performance, particular relay selection approaches were proposed. Finally, the effect of the clipping process at the source node on the network performance over frequency selective fading channels with relay selection was evaluated through outage probability analysis.

In Chapter 1, a general introduction to wireless communication sys-

tems including the basic concepts of MIMO and OFDM systems were provided. Furthermore, a short description of the PAPR problem in a virtual MIMO-OFDM system was given. In addition, a relay selection technique was also presented. Finally, the outline of the thesis was briefly discussed.

In Chapter 2, an overview of a MIMO-OFDM system was provided. Then details of SISO-OFDM based transmission including transmitter and receiver stages such as a convolutional encoder, interleaving, an appropriate modulation technique and a Viterbi decoding scheme were studied. Then, descriptions of conventional MIMO and cooperative MIMO systems were presented. In addition, SFBC was used to exploit the benefit of the combination of SISO-OFDM with a MIMO system virtually. Finally, on the basis of the analysis in the chapter, combining MIMO and OFDM is to improve the quality of a wireless link in terms of transmission rate, transmission range and the transmission reliability. Moreover, exploiting a cooperative relay network (virtual MIMO-OFDM system) mitigates some of the conventional system drawbacks.

In Chapter 3, an introduction and a brief overview of PAPR mitigation methods, including definition and statistical properties of PAPR techniques, were presented. Then, a simple approach to limit the amplitude peaks in an OFDM waveform was described. In addition to this, oversampling and filtering after clipping were studied to reduce the harmful effects induced by the clipping process. Finally, according to the chapter results, the clipping process is identified as the simplest approach to reduce PAPR, but it induces in-band distortion and out-of-band interferences. The out-of-band interference induced by the

clipping process can be reduced the oversampling the time domain signal followed by filtering using an FFT-based, frequency domain filter designed to reject out-of-band discrete frequency components. In addition, the oversampling process was found to be less significant when the factor was greater than four.

In Chapter 4, a brief introduction of PAPR reduction by clipping the OFDM signal at the source node of a distributed cooperative virtual MIMO-OFDM wireless network was described. Then, the system model of distributed open loop EO-SFBC at the relaying nodes including broadcasting and relaying phases, together with the IAR decoding technique was presented. In addition, feedback techniques which are needed to achieve full spatial diversity and array gains, are explained. The IAR decoding scheme was used to overcome the in-band distortion which was introduced by the clipping process. Feedback channels were required to achieve full cooperative diversity and array gain. Therefore, bandwidth limited feedback schemes such as two or one-bit quantized feedback scheme for each subcarrier, which needs $2N$ or N feedback bits per frame for both systems, were presented. For example, an OFDM block with 1024 subcarriers needs 2048 or 1024 feedback bits in both schemes respectively. In contrast, by exploiting the correlation between 16 adjacent subcarriers as two or one-bit group feedback only 128 or 64 bits are required to achieve almost identical performance for both schemes. In summary, a 93.75% reduction in transmission with negligible degradation in BER was achieved by exploiting the correlation among the feedback terms for the adjacent subcarriers of OFDM block in both systems.

In Chapter 5, end-to-end performance analysis of a cooperative am-

plify and forward network over frequency selective fading channels with a multi-relay selection scheme was provided. Multi-path fading channels were modeled with a Gamma distribution with positive integer scale parameter which has the same distribution as the sum of L independent exponential distribution random variables. Simulation results verified the analytical results for different channel lengths ($L = 2$ and 3). In addition, the robustness of the best two relay pair selection scheme over the single relay selection scheme was confirmed. Moreover, increasing the channel length and/or the number of relays improved the outage probability. In addition, the slopes of the outage probability vs SNR become steeper as the number L of multi-paths increases. For example, when selecting the best relay from 4 relays and the channel lengths are 2 and 3, the overall cooperative diversity gains are found to be approximately 7.14 and 10.0, and the theoretical values are 8 and 12, respectively. The complexity of the exact analysis increases with the number of multi-paths L. On the other hand the derived formulas of the upper and lower bound SNRs were simple for single relay selection, and applicable to an arbitrary channel length L and also to an arbitrary number M of relay nodes, although they are not particulary tight.

In Chapter 6, PAPR reduction by clipping the OFDM signal at the source node of a cooperative amplify and forward network over frequency selective fading channels with a multi-relay selection scheme was provided. The two-hop wireless transmission was modeled in the time domain as an Erlang distribution function which is used in selecting the best single relay. Then, the nonlinear distortions introduced by the clipping process were modeled as an aggregate of attenuation factor

and clipping noise, and the magnitude squared of the signal scaled by the clipping factor was modeled as an exponential distribution. The clipping noise was assumed to play the same role as channel noise. In summary, the results indicate that the clipping process caused a degradation of the system performance and the degradation depends upon the clipping ratio. However, to some extent, selecting the best relay scheme from a large number of relay nodes overcomes this degradation. Also the results indicate that the theoretical calculation and simulation were close for different numbers of available relay nodes.

In summary, this thesis firstly considered PAPR reduction by clipping at the source node and IAR decoding for in band noise reduction. Improvment in system performance and cooperative diversity gain was demonstrated. Secondly, the outage probability of a multi-relay selection scheme in a cooperative AF network over frequency selective fading channels was investigated. Finally, the effect of the clipping process at the OFDM source node was modeled and the network performance over frequency selective fading channels with relay selection was evaluated with outage probability analysis which confirmed the advantage of multiple diversity.

7.1.1 Future work

There are several directions in which the research presented in this thesis can be extended. A few of which are highlighted below:

- The solution presented here for PAPR reduction is amplitude clipping at the source node. Applying the reduction schemes both at the source node and relay nodes may achieve more reduction in PAPR; however, it may cost complexity in the system.

- The proposed schemes exploit half-duplex transmission, it would be interesting to examine more sophisticated duplexing operations.

- The work in this thesis assumes that perfect channel state information (CSI) was available at the destination node. In reality, CSI can only be estimated which obviously will introduce errors. An interesting study would be examining the proposed schemes in this thesis with imperfections in the CSI, and designing robust algorithms to overcome this issue.

- The proposed schemes in this thesis so far consider only the case of a single source node wishing to communicate with a single destination node via cooperative relay nodes. The issue can be extended and generalized to multiuser environments which is a major potential research direction in practical wireless systems.

- In Chapter 5, the channel is assumed frequency selective fading and modeled as an Erlang distribution but there are other classes of fading channel conditions, namely, Nakagami-m distribution [96]. This fading distribution has gained much attention lately, since the Nakagami-m distribution often gives the best fit to land-mobile and indoor mobile multi-path propagation as well as scintillating ionospheric radio links [97], therefore, it could be used in future work.

- Also in Chapter 5 and 6, the outage probability analysis of the best single relay selection scheme over frequency selective fading channels is only confirmed by theoretical and simulation results. In future work, a practical measurement should be consid-

ered. Furthermore, generalization of outage probability analysis for best relay pair selection could be considered.

- Finally, most of the existing wireless networks and devices follow fixed spectrum access policies, which mean that radio spectral bands are licensed to dedicated users and services. Cognitive radio is an emerging paradigm to increase spectrum efficiency wireless communication allowing an opportunistic user, namely the secondary user, to access the spectrum of the licensed user, known as the primary user; this assumes that the secondary transmission does not harmfully affect the primary user [98], [99] and [100]. Therefore, an interesting extension of the work in this thesis is to extend it to a cognitive environment.

Appendix A

The CDF expression when $L = 3$ for one-way system

The full closed form expression for the CDF when $L = 3$ for one-way system.

$$
\begin{aligned}
F^{3}_{\gamma_{opt}}(\gamma) \;=\; & M(M-1)\,[F^{3,k=0}_{\gamma_{opt}}(\gamma) \;+\; \sum_{k=1}^{N-2}\binom{N-2}{k}(-1)^{k}\sum_{i=0}^{k}\binom{k}{i}\sum_{j=0}^{i}\binom{i}{j} \\
& \sum_{t=0}^{j}\binom{j}{t}\sum_{f=0}^{t}\binom{t}{f}2^{-5+i-t}\overline{\gamma}^{-10-f-i-j-t}e^{-\frac{2\gamma}{\overline{\gamma}}} \\
& \left(\frac{1}{(2+k)^{3}}2^{-f-i-j-t}\gamma^{f+i+j+t}\overline{\gamma}^{10}e^{\frac{2\gamma}{\overline{\gamma}}}\left(\frac{\gamma(2+k)}{\overline{\gamma}}\right)^{-f-i-j-t}\right. \\
& \left.\left(\Gamma(3+f+i+j+t)-\Gamma\left(3+f+i+j+t,\frac{\gamma(2+k)}{\overline{\gamma}}\right)\right)-\right. \\
& \frac{1}{\left(-\frac{4}{\overline{\gamma}}+\frac{2(2+k)}{\overline{\gamma}}\right)^{3}}2\gamma^{4+f+i+j+t}\overline{\gamma}^{3}\left(\gamma\left(-\frac{4}{\overline{\gamma}}+\frac{2(2+k)}{\overline{\gamma}}\right)\right)^{-f-i-j-t} \\
& \left.\left(\Gamma(3+f+i+j+t)-\Gamma\left(3+f+i+j+t,\frac{1}{2}\gamma\left(-\frac{4}{\overline{\gamma}}+\frac{2(2+k)}{\overline{\gamma}}\right)\right)\right)-\right. \\
& \frac{1}{\left(-\frac{4}{\overline{\gamma}}+\frac{2(2+k)}{\overline{\gamma}}\right)^{3}}8\gamma^{3+f+i+j+t}\overline{\gamma}^{4}\left(\gamma\left(-\frac{4}{\overline{\gamma}}+\frac{2(2+k)}{\overline{\gamma}}\right)\right)^{-f-i-j-t} \\
& \left.\left(\Gamma(3+f+i+j+t)-\Gamma\left(3+f+i+j+t,\frac{1}{2}\gamma\left(-\frac{4}{\overline{\gamma}}+\frac{2(2+k)}{\overline{\gamma}}\right)\right)\right)\right) \\
& \frac{1}{\left(-\frac{4}{\overline{\gamma}}+\frac{2(2+k)}{\overline{\gamma}}\right)^{3}}16\gamma^{2+f+i+j+t}\overline{\gamma}^{5}\left(\gamma\left(-\frac{4}{\overline{\gamma}}+\frac{2(2+k)}{\overline{\gamma}}\right)\right)^{-f-i-j-t} \\
& \left.\left(\Gamma(3+f+i+j+t)-\Gamma\left(3+f+i+j+t,\frac{1}{2}\gamma\left(-\frac{4}{\overline{\gamma}}+\frac{2(2+k)}{\overline{\gamma}}\right)\right)\right)\right)- \\
& \frac{1}{\left(-\frac{4}{\overline{\gamma}}+\frac{2(2+k)}{\overline{\gamma}}\right)^{3}}16\gamma^{1+f+i+j+t}\overline{\gamma}^{6}\left(\gamma\left(-\frac{4}{\overline{\gamma}}+\frac{2(2+k)}{\overline{\gamma}}\right)\right)^{-f-i-j-t} \\
& \left.\left(\Gamma(3+f+i+j+t)-\Gamma\left(3+f+i+j+t,\frac{1}{2}\gamma\left(-\frac{4}{\overline{\gamma}}+\frac{2(2+k)}{\overline{\gamma}}\right)\right)\right)\right)- \\
& \frac{1}{\left(-\frac{4}{\overline{\gamma}}+\frac{2(2+k)}{\overline{\gamma}}\right)^{3}}8\gamma^{f+i+j+t}\overline{\gamma}^{7}\left(\gamma\left(-\frac{4}{\overline{\gamma}}+\frac{2(2+k)}{\overline{\gamma}}\right)\right)^{-f-i-j-t} \\
& \left.\left(\Gamma(3+f+i+j+t)-\Gamma\left(3+f+i+j+t,\frac{1}{2}\gamma\left(-\frac{4}{\overline{\gamma}}+\frac{2(2+k)}{\overline{\gamma}}\right)\right)\right)\right)+
\end{aligned}
$$

$$\frac{1}{(2+k)^4}32^{-1-f-i-j-t}\gamma^{f+i+j+t}\overline{\gamma}^{10}e^{\frac{2\gamma}{\overline{\gamma}}}\left(\frac{\gamma(2+k)}{\overline{\gamma}}\right)^{-f-i-j-t}$$
$$\left(\Gamma(4+f+i+j+t)-\Gamma\left(4+f+i+j+t,\frac{\gamma(2+k)}{\overline{\gamma}}\right)\right)-$$
$$\frac{1}{\left(-\frac{4}{\overline{\gamma}}+\frac{2(2+k)}{\overline{\gamma}}\right)^4}2\gamma^{4+f+i+j+t}\overline{\gamma}^2\left(\gamma\left(-\frac{4}{\overline{\gamma}}+\frac{2(2+k)}{\overline{\gamma}}\right)\right)^{-f-i-j-t}$$
$$\left(\Gamma(4+f+i+j+t)-\Gamma\left(4+f+i+j+t,\frac{1}{2}\gamma\left(-\frac{4}{\overline{\gamma}}+\frac{2(2+k)}{\overline{\gamma}}\right)\right)\right)+$$
$$\frac{1}{\left(-\frac{4}{\overline{\gamma}}+\frac{2(2+k)}{\overline{\gamma}}\right)^4}8\gamma^{2+f+i+j+t}\overline{\gamma}^4\left(\gamma\left(-\frac{4}{\overline{\gamma}}+\frac{2(2+k)}{\overline{\gamma}}\right)\right)^{-f-i-j-t}$$
$$\left(\Gamma(4+f+i+j+t)-\Gamma\left(4+f+i+j+t,\frac{1}{2}\gamma\left(-\frac{4}{\overline{\gamma}}+\frac{2(2+k)}{\overline{\gamma}}\right)\right)\right)+$$
$$\frac{1}{\left(-\frac{4}{\overline{\gamma}}+\frac{2(2+k)}{b}\right)^4}16\gamma^{1+f+i+j+t}\overline{\gamma}^5\left(\gamma\left(-\frac{4}{\overline{\gamma}}+\frac{2(2+k)}{\overline{\gamma}}\right)\right)^{-f-i-j-t}$$
$$\left(\Gamma(4+f+i+j+t)-\Gamma\left(4+f+i+j+t,\frac{1}{2}\gamma\left(-\frac{4}{\overline{\gamma}}+\frac{2(2+k)}{\overline{\gamma}}\right)\right)\right)+$$
$$\frac{1}{\left(-\frac{4}{\overline{\gamma}}+\frac{2(2+k)}{\overline{\gamma}}\right)^4}8\gamma^{f+i+j+t}\overline{\gamma}^6\left(\gamma\left(-\frac{4}{\overline{\gamma}}+\frac{2(2+k)}{\overline{\gamma}}\right)\right)^{-f-i-j-t}$$
$$\left(\Gamma(4+f+i+j+t)-\Gamma\left(4+f+i+j+t,\frac{1}{2}\gamma\left(-\frac{4}{\overline{\gamma}}+\frac{2(2+k)}{\overline{\gamma}}\right)\right)\right)+$$
$$\frac{1}{(2+k)^5}92^{-3-f-i-j-t}\gamma^{f+i+j+t}\overline{\gamma}^{10}e^{\frac{2\gamma}{\overline{\gamma}}}\left(\frac{\gamma(2+k)}{\overline{\gamma}}\right)^{-f-i-j-t}$$
$$\left(\Gamma(5+f+i+j+t)-\Gamma\left(5+f+i+j+t,\frac{\gamma(2+k)}{\overline{\gamma}}\right)\right)-$$
$$\frac{1}{\left(-\frac{4}{\overline{\gamma}}+\frac{2(2+k)}{\overline{\gamma}}\right)^5}\gamma^{4+f+i+j+t}\overline{\gamma}\left(\gamma\left(-\frac{4}{\overline{\gamma}}+\frac{2(2+k)}{\overline{\gamma}}\right)\right)^{-f-i-j-t}$$
$$\left(\Gamma(5+f+i+j+t)-\Gamma\left(5+f+i+j+t,\frac{1}{2}\gamma\left(-\frac{4}{\overline{\gamma}}+\frac{2(2+k)}{\overline{\gamma}}\right)\right)\right)+$$
$$\frac{1}{\left(-\frac{4}{\overline{\gamma}}+\frac{2(2+k)}{\overline{\gamma}}\right)^5}4\gamma^{3+f+i+j+t}\overline{\gamma}^2\left(\gamma\left(-\frac{4}{\overline{\gamma}}+\frac{2(2+k)}{\overline{\gamma}}\right)\right)^{-f-i-j-t}$$
$$\left(\Gamma(5+f+i+j+t)-\Gamma\left(5+f+i+j+t,\frac{1}{2}\gamma\left(-\frac{4}{\overline{\gamma}}+\frac{2(2+k)}{\overline{\gamma}}\right)\right)\right)+$$
$$\frac{1}{\left(-\frac{4}{\overline{\gamma}}+\frac{2(2+k)}{\overline{\gamma}}\right)^5}4\gamma^{2+f+i+j+t}\overline{\gamma}^3\left(\gamma\left(-\frac{4}{\overline{\gamma}}+\frac{2(2+k)}{\overline{\gamma}}\right)\right)^{-f-i-j-t}$$

$$\left(\Gamma(5+f+i+j+t)-\Gamma\left(5+f+i+j+t,\frac{1}{2}\gamma\left(-\frac{4}{\overline{\gamma}}+\frac{2(2+k)}{\overline{\gamma}}\right)\right)\right)-$$
$$\frac{1}{\left(-\frac{4}{\overline{\gamma}}+\frac{2(2+k)}{\overline{\gamma}}\right)^5}4\gamma^{f+i+j+t}\overline{\gamma}^5\left(\gamma\left(-\frac{4}{\overline{\gamma}}+\frac{2(2+k)}{\overline{\gamma}}\right)\right)^{-f-i-j-t}$$
$$\left(\Gamma(5+f+i+j+t)-\Gamma\left(5+f+i+j+t,\frac{1}{2}\gamma\left(-\frac{4}{\overline{\gamma}}+\frac{2(2+k)}{\overline{\gamma}}\right)\right)\right)+$$
$$\frac{1}{(2+k)^6}2^{-1-f-i-j-t}\gamma^{f+i+j+t}\overline{\gamma}^{10}e^{\frac{2\gamma}{\overline{\gamma}}}\left(\frac{\gamma(2+k)}{\overline{\gamma}}\right)^{-f-i-j-t}$$
$$\left(\Gamma(6+f+i+j+t)-\Gamma\left(6+f+i+j+t,\frac{\gamma(2+k)}{\overline{\gamma}}\right)\right)+$$
$$\frac{1}{\left(-\frac{4}{\overline{\gamma}}+\frac{2(2+k)}{\overline{\gamma}}\right)^6}4\gamma^{3+f+i+j+t}\overline{\gamma}\left(\gamma\left(-\frac{4}{\overline{\gamma}}+\frac{2(2+k)}{\overline{\gamma}}\right)\right)^{-f-i-j-t}$$
$$\left(\Gamma(6+f+i+j+t)-\Gamma\left(6+f+i+j+t,\frac{1}{2}\gamma\left(-\frac{4}{\overline{\gamma}}+\frac{2(2+k)}{\overline{\gamma}}\right)\right)\right)+$$
$$\frac{1}{(2+k)^7}92^{-6-f-i-j-t}\gamma^{f+i+j+t}\overline{\gamma}^{10}e^{\frac{2\gamma}{\overline{\gamma}}}\left(\frac{\gamma(2+k)}{\overline{\gamma}}\right)^{-f-i-j-t}$$
$$\left(\Gamma(7+f+i+j+t)-\Gamma\left(7+f+i+j+t,\frac{\gamma(2+k)}{\overline{\gamma}}\right)\right)-$$
$$\frac{1}{\left(-\frac{4}{\overline{\gamma}}+\frac{2(2+k)}{\overline{\gamma}}\right)^7}6\gamma^{2+f+i+j+t}\overline{\gamma}\left(\gamma\left(-\frac{4}{\overline{\gamma}}+\frac{2(2+k)}{\overline{\gamma}}\right)\right)^{-f-i-j-t}$$
$$\left(\Gamma(7+f+i+j+t)-\Gamma\left(7+f+i+j+t,\frac{1}{2}\gamma\left(-\frac{4}{\overline{\gamma}}+\frac{2(2+k)}{\overline{\gamma}}\right)\right)\right)-$$
$$\frac{1}{\left(-\frac{4}{\overline{\gamma}}+\frac{2(2+k)}{\overline{\gamma}}\right)^7}4\gamma^{1+f+i+j+t}\overline{\gamma}^2\left(\gamma\left(-\frac{4}{\overline{\gamma}}+\frac{2(2+k)}{\overline{\gamma}}\right)\right)^{-f-i-j-t}$$
$$\left(\Gamma(7+f+i+j+t)-\Gamma\left(7+f+i+j+t,\frac{1}{2}\gamma\left(-\frac{4}{\overline{\gamma}}+\frac{2(2+k)}{\overline{\gamma}}\right)\right)\right)-$$
$$\frac{1}{\left(-\frac{4}{\overline{\gamma}}+\frac{2(2+k)}{\overline{\gamma}}\right)^7}2\gamma^{f+i+j+t}\overline{\gamma}^3\left(\gamma\left(-\frac{4}{\overline{\gamma}}+\frac{2(2+k)}{\overline{\gamma}}\right)\right)^{-f-i-j-t}$$
$$\left(\Gamma(7+f+i+j+t)-\Gamma\left(7+f+i+j+t,\frac{1}{2}\gamma\left(-\frac{4}{\overline{\gamma}}+\frac{2(2+k)}{\overline{\gamma}}\right)\right)\right)+$$
$$\frac{1}{(2+k)^8}32^{-7-f-i-j-t}\gamma^{f+i+j+t}\overline{\gamma}^{10}e^{\frac{2\gamma}{\overline{\gamma}}}\left(\frac{\gamma(2+k)}{\overline{\gamma}}\right)^{-f-i-j-t}$$
$$\left(\Gamma(8+f+i+j+t)-\Gamma\left(8+f+i+j+t,\frac{\gamma(2+k)}{\overline{\gamma}}\right)\right)+$$

$$\frac{1}{\left(-\frac{4}{\overline{\gamma}}+\frac{2(2+k)}{\overline{\gamma}}\right)^{8}}4\gamma^{1+f+i+j+t}\overline{\gamma}\left(\gamma\left(-\frac{4}{\overline{\gamma}}+\frac{2(2+k)}{\overline{\gamma}}\right)\right)^{-f-i-j-t}$$
$$\left(\Gamma(8+f+i+j+t)-\Gamma\left(8+f+i+j+t,\frac{1}{2}\gamma\left(-\frac{4}{\overline{\gamma}}+\frac{2(2+k)}{\overline{\gamma}}\right)\right)\right)+$$
$$\frac{1}{\left(-\frac{4}{\overline{\gamma}}+\frac{2(2+k)}{\overline{\gamma}}\right)^{8}}2\gamma^{f+i+j+t}\overline{\gamma}^{2}\left(\gamma\left(-\frac{4}{\overline{\gamma}}+\frac{2(2+k)}{\overline{\gamma}}\right)\right)^{-f-i-j-t}$$
$$\left(\Gamma(8+f+i+j+t)-\Gamma\left(8+f+i+j+t,\frac{1}{2}\gamma\left(-\frac{4}{\overline{\gamma}}+\frac{2(2+k)}{\overline{\gamma}}\right)\right)\right)+$$
$$\frac{1}{(2+k)^{9}}2^{-9-f-i-j-t}\gamma^{f+i+j+t}\overline{\gamma}^{10}e^{\frac{2\gamma}{\overline{\gamma}}}\left(\frac{\gamma(2+k)}{\overline{\gamma}}\right)^{-f-i-j-t}$$
$$\left(\Gamma(9+f+i+j+t)-\Gamma\left(9+f+i+j+t,\frac{\gamma(2+k)}{\overline{\gamma}}\right)\right)-$$
$$\frac{1}{\left(-\frac{4}{\overline{\gamma}}+\frac{2(2+k)}{\overline{\gamma}}\right)^{9}}\gamma^{f+i+j+t}\overline{\gamma}\left(\gamma\left(-\frac{4}{\overline{\gamma}}+\frac{2(2+k)}{\overline{\gamma}}\right)\right)^{-f-i-j-t}$$
$$\left(\Gamma(9+f+i+j+t)-\Gamma\left(9+f+i+j+t,\frac{1}{2}\gamma\left(-\frac{4}{\overline{\gamma}}+\frac{2(2+k)}{\overline{\gamma}}\right)\right)\right)\Bigg)\Bigg]$$

where $\Gamma(L,x)=\int_0^x s^{L-1}e^{-s}ds$ which is an incomplete Gamma function, M the number of relays and $\overline{\gamma}$ is called the scale parameter and is denoted as the average SNR.

References

[1] Y. Yu, S. Keroueden, and J. Yuan, "Closed-loop extended orthogonal space-time block codes for three and four transmit antennas," *Signal Processing Letters, IEEE*, vol. 13, no. 5, pp. 273–276, 2006.

[2] J. Kim, S. Ariyavisitakul, and N. Seshadri, "STBC/SFBC for 4 Transmit Antennas with 1-bit Feedback," in *Communications, 2008. ICC '08. IEEE International Conference on*, pp. 3943–3947, 2008.

[3] Y.-J. Kim, U.-K. Kwon, D.-Y. Seol, and G.-H. Im, "An Effective PAPR Reduction of SFBC-OFDM for Multinode Cooperative Transmission," *Signal Processing Letters, IEEE*, vol. 16, no. 11, pp. 925–928, 2009.

[4] S. Alamouti, "A simple transmit diversity technique for wireless communications," *Selected Areas in Communications, IEEE Journal on*, vol. 16, no. 8, pp. 1451–1458, 1998.

[5] U.-K. Kwon, D. Kim, and G.-H. Im, "Amplitude clipping and iterative reconstruction of MIMO-OFDM signals with optimum equalization," *Wireless Communications, IEEE Transactions on*, vol. 8, no. 1, pp. 268–277, 2009.

[6] J. L. Holsinger, "Digital communication over fixed time-continuous channels with memory-with special application to telephone channels,"

Technical Report No. 366, MIT Lincoln Laboratory, Cambridge, MA, 1964.

[7] J. M. Cioffi, "A multicarrier primer," in *ANSI T1E1.4/91-157*, 1991.

[8] H. Rohling, *OFDM Concepts for Future Communication Systems*. Springer-Verlag Berlin Heidelberg, 2011.

[9] L. Hanzo, J. Akhtman, L. Wang, and M. Jiang, *MIMO-OFDM for LTE,Wi-Fi and WiMAX : coherent versus non-coherent and cooperative turbo-transceivers*. UK: John Wiley and Sons Ltd, 2011.

[10] C. Oestges and B. Clerckx, *MIMO Wireless Communications: From Real-World Propagation to Space-Time Code Design*. Orlando, FL, USA: Academic Press, Inc., 2007.

[11] E. Biglieri, R. Calderbank, A. Constantinides, A. Goldsmith, A. Paulraj, and H. V. Poor, *MIMO Wireless Communications*. New York, NY, USA: Cambridge University Press, 2007.

[12] D. Tse and P. Viswanath, *Fundamentals of Wireless Communications*. Cambridge University Press, 2005.

[13] K. R. Liu, A. K. Sadek, W. Su, and A. Kwasinski, *Cooperative Communications and Networking*. Cambridge University Press, 2009.

[14] Y.-W. P. Hong, W.-J. Huang, and C.-C. J. Kuo, *Cooperative Communications and Networking: Technologies and System Design*. New York, USA: Springer Science and Business Media, LLC, 2010.

[15] J. Laneman, D. Tse, and G. Wornell, "Cooperative diversity in wireless networks: Efficient protocols and outage behavior," *Informa-*

tion Theory, IEEE Transactions on, vol. 50, no. 12, pp. 3062–3080, 2004.

[16] A. Bletsas, A. Khisti, D. Reed, and A. Lippman, "A simple cooperative diversity method based on network path selection," *Selected Areas in Communications, IEEE Journal on*, vol. 24, no. 3, pp. 659–672, 2006.

[17] E. Dahlman, S. Parkvall, and J. Skld, *4G LTE/LTE-Advanced for Mobile Broadband*. Elsevier Ltd, UK, 2011.

[18] M.-O. Pun, M. Morelli, and C.-C. J. Kuo, *Multi-Carrier Techniques For Broadband Wireless Communications: A Signal Processing Perspectives*. London, UK: Imperial College Press, 2007.

[19] G. B. Giannakis, Z. Liu, X. Ma, and S. Zhou, *Space Time Coding for Broadband Wireless Communications*. Wiley-Interscience, 2007.

[20] B. Lu and X. Wang, "Space-time code design in OFDM systems," in *Global Telecommunications Conference, 2000. GLOBECOM '00. IEEE*, vol. 2, pp. 1000–1004, 2000.

[21] H. Bolcskei and A. Paulraj, "Space-frequency coded broadband OFDM systems," in *Wireless Communications and Networking Conference, 2000. WCNC. 2000 IEEE*, vol. 1, pp. 1–6, 2000.

[22] S. Ahson and M. Ilyas, *WiMAX : technologies, performance analysis, and QoS*. Taylor and Francis Group, LLC, 2008.

[23] J. C. Park, T. T. Do, and Y. H. Kim, "Outage Probability of OFDM-Based Relay Networks with Relay Selection," in *Vehicular Technology Conference, 2010 IEEE*, pp. 1–5, 2010.

[24] K. Tourki, M.-S. Alouini, and L. Deneire, "Blind cooperative diversity using distributed space-time coding in block fading channels," *Communications, IEEE Transactions on*, vol. 58, no. 8, pp. 2447–2456, 2010.

[25] K. Tourki, H.-C. Yang, and M.-S. Alouini, "Accurate outage analysis of incremental decode-and-forward opportunistic relaying," *Wireless Communications, IEEE Transactions on*, vol. 10, no. 4, pp. 1021–1025, 2011.

[26] H. Schulze and C. Luders, *Theory and Applications of OFDM and CDMA*. UK: John Wiley and Sons Ltd, The Atrium, Southern Gate, Chichester, West Sussex, 2005.

[27] S. Haykin and M. Sellathurai, *Space Time Layered Information Processing for Wireless Communications*. New Jersey, USA: John Wiley and Sons, Inc, 2009.

[28] R. Prasad, *OFDM for Wireless Communications Systems*. Artech House, Inc, London, 2004.

[29] Y. Cho, J. Kim, W. Yang, and C. G. Kang, *MIMO-OFDM Wireless Communications with MATLAB*. John Wiley and Sons (Asia) Pte Ltd, 2010.

[30] Y. G. Li and G. L. Stiiber, *Orthogonal Frequency Division Multiplexing for Wireless Communications*. Berlin, Heidelberg: Springer-Verlag, 2006.

[31] M. Eddaghel and J. Chambers, "PAPR reduction in distributed closed loop extended orthogonal space frequency block coding with

quantized two-bit group feedback for broadband multi-node cooperative communications," in *Wireless Communications and Mobile Computing Conference (IWCMC), 2011 7th International*, pp. 719 –724, July 2011.

[32] M. Jankiraman, *Space-Time Codes and MIMO Systems*. Norwood, MA, USA: Artech House, Inc., 2004.

[33] T. K. Moon, *Error Correction Coding: Mathematical Methods and Algorithms*. John Wiley and Sons, Inc., 2005.

[34] W. H. Tranter, *Principles of Communication Systems Simulation with Wireless Applications*. Pearson Education, Inc., 2004.

[35] A. Glavieux, *Channel Coding in Communication Networks: From Theory to Turbo Codes (Digital Signal and Image Processing series)*. ISTE, 2006.

[36] A. Neubauer, *Coding Theory: Algorithms, Architectures and Applications*. Wiley-Interscience, 2007.

[37] W. H. Tranter, K. S. Shanmugan, T. S. Rappaport, and K. L. Kosbar, *Principles of communication systems simulation with wireless applications*. Upper Saddle River, NJ, USA: Prentice Hall Press, 2003.

[38] E. Biglieri, *Coding for Wireless Channels*. Springer Science and Business Media, Inc., 2005.

[39] K. Fazel and S. Kaiser, *Multi-Carrier and Spread Spectrum Systems*. New York, NY, USA: John Wiley & Sons, Inc., 2003.

[40] "Using MIMO-OFDM Technology To Boost Wireless LAN Performance Today," *White Paper, Datacomm Research Company, St Louis, USA*, 2005.

[41] M. Eddaghel and J. Chambers, "Comparison of distributed space frequency block coding schemes in broadband multi-node cooperative relay networks with PAPR reduction," in *Digital Signal Processing (DSP), 2011 17th International Conference on*, pp. 1 –5, 2011.

[42] A. Paulraj, R. Nabar, and D. Gore, *Introduction to Space-Time Wireless Communications*. New York, NY, USA: Cambridge University Press, 2008.

[43] M. Dohler and Y. Li, *Cooperative Communications: Hardware, Channel and PHY*. Wiley, NewJersey, 2010.

[44] K. Lee and D. Williams, "A space-frequency transmitter diversity technique for OFDM systems," in *Global Telecommunications Conference, 2000. GLOBECOM '00. IEEE*, vol. 3, pp. 1473–1477, 2000.

[45] W. Zhang, X.-G. Xia, and K. Ben Letaief, "Space-Time/Frequency Coding for MIMO-OFDM in Next Generation Broadband Wireless Systems," *Wireless Communications, IEEE*, vol. 14, no. 3, pp. 32–43, 2007.

[46] G. Bauch, "Space-time block codes versus space-frequency block codes," in *Vehicular Technology Conference, 2003. VTC 2003-Spring. The 57th IEEE Semiannual*, vol. 1, pp. 567–571, April 2003.

[47] N. Eltayeb, S. Kassim, and J. Chambers, "Closed-loop extended orthogonal space frequency block coding techniques for OFDM based broadband wireless access systems," in *Broadband Communications, Networks and Systems, 2008. BROADNETS 2008. 5th International Conference on*, pp. 426–430, 2008.

[48] F. Khan, *LTE for 4G Mobile Broadband: Air Interface Technologies and Performance*. Cambridge University Press, Cambridge, 2009.

[49] Y. Zhang, H.-H. Chen, and M. Guizani, *Cooperative Wireless Communications*. Taylor and Francis Group, LLC, USA, 2009.

[50] S. Haykin and M. Moher, *Modern Wireless Communication*. Upper Saddle River, NJ, USA: Prentice-Hall, Inc., 2004.

[51] Y. Li and G. Stuber, *Orthogonal Frequency Division Multiplexing for Wireless Communications*. Springer Science and Business Media, Inc, USA, 2006.

[52] S. H. Han and J. H. Lee, "An overview of peak-to-average power ratio reduction techniques for multicarrier transmission," *Wireless Communications, IEEE*, vol. 12, no. 2, pp. 56–65, 2005.

[53] M. Senst and G. Ascheid, "Optimal Output Back-Off in OFDM Systems with Nonlinear Power Amplifiers," in *Communications, 2009. ICC '09. IEEE International Conference on*, pp. 1–6, 2009.

[54] H. Ochiai and H. Imai, "Performance of the Deliberate Clipping with Adaptive Symbol Selection for Strictly Band-limited OFDM Systems," *Selected Areas in Communications, IEEE Journal on*, vol. 18, no. 11, pp. 2270–2277, 2000.

[55] J. J. Bussgang, "Crosscorrelation function of amplitude-distorted gaussian signals," in *Research Laboratory of Electronics, Massachusetts Institute of Technology, Cambridge. Technical Report*, no. 216, 1952.

[56] H. E. Rowe, "Memoryless Nonlinearities with Gaussian Inputs: Elementary Results," in *The Bell System Technical Journal*, vol. 61, pp. 1519–1525, 1982.

[57] A. Papoulis, *Probability Random Variables and Stochastic Processes*. McGraw-Hill, 1991.

[58] D. Guel and J. Palicot, "Clipping Formulated As an Adding Signal Technique for OFDM Peak Power Reduction," in *Vehicular Technology Conference, 2009. VTC Spring 2009. IEEE 69th*, pp. 1–5, 2009.

[59] H. Gacanin, S. Takaoka, and F. Adachi, "Reduction of Amplitude Clipping Level with OFDM/TDM," in *Vehicular Technology Conference, 2006. VTC-2006 Fall. 2006 IEEE 64th*, pp. 1–5, 2006.

[60] J. Armstrong, "Peak-to-average power reduction for OFDM by repeated clipping and frequency domain filtering," *Electronics Letters*, vol. 38, no. 5, pp. 246–247, 2002.

[61] K. Seddik and K. Liu, "Distributed space-frequency coding over broadband relay channels," *Wireless Communications, IEEE Transactions on*, vol. 7, no. 11, pp. 4748–4759, 2008.

[62] W. Su, Z. Safar, M. Olfat, and K. Liu, "Obtaining full-diversity space-frequency codes from space-time codes via mapping," *Signal Processing, IEEE Transactions on*, vol. 51, no. 11, pp. 2905–2916, 2003.

[63] V. Tarokh, N. Seshadri, and A. Calderbank, "Space-time codes for high data rate wireless communication: performance criterion and code construction," in *Information Theory, IEEE Transactions on*, vol. 44, pp. 744–765, 1998.

[64] N. Eltayeb, S. Kassim, and J. Chambers, "An Enhanced Feedback Scheme for Extended Orthogonal Space-Frequency Block Coded MISO-OFDM Systems," in *Sarnoff Symposium, 2008 IEEE*, pp. 1–5, 2008.

[65] F. T. Alotaibi and J. Chambers, "Full-rate and full-diversity extended orthogonal space-time block coding in cooperative relay networks with imperfect synchronization," in *Acoustics Speech and Signal Processing (ICASSP), 2010 IEEE International Conference on*, pp. 2882–2885, 2010.

[66] R. Li, Z. Bai, and K. Kwak, "Space frequency codes based amplify-and-forward cooperative system," in *Communications and Information Technology. ISCIT 2009. 9th International Symposium on*, pp. 1185–1188, 2009.

[67] Y. Li, W. Zhang, and X.-G. Xia, "Distributive High-Rate Space Frequency Codes Achieving Full Cooperative and Multipath Diversities for Asynchronous Cooperative Communications," *Vehicular Technology, IEEE Transactions on*, vol. 58, no. 1, pp. 207–217, 2009.

[68] U.-K. Kwon and G.-H. Im, "Iterative amplitude reconstruction of clipped OFDM signals with optimum equalisation," *Electronics Letters*, vol. 42, no. 20, pp. 1189–1190, 2006.

[69] F. Alotaibi and J. Chambers, "Extended orthogonal space time block codes in wireless relay networks," in *Statistical Signal Processing, 2009. SSP '09. IEEE/SP 15th Workshop on*, pp. 745–748, 2009.

[70] W. Zhang, Y. Li, X.-G. Xia, P. Ching, and K. Ben Letaief, "Distributed Space-Frequency Coding for Cooperative Diversity in Broadband Wireless Ad Hoc Networks," *Wireless Communications, IEEE Transactions on*, vol. 7, no. 3, pp. 995–1003, 2008.

[71] U.-K. Kwon, D. Kim, K. Kim, and G.-H. Im, "Amplitude Clipping

and Iterative Reconstruction of STBC/SFBC-OFDM Signals," *Signal Processing Letters, IEEE*, vol. 14, no. 11, pp. 808–811, 2007.

[72] F. Tosato and P. Bisaglia, "Simplified soft-output demapper for binary interleaved COFDM with application to HIPERLAN/2," in *Communications, 2002. ICC 2002. IEEE International Conference on*, vol. 2, pp. 664–668, 2002.

[73] L. Hanzo, T. H. Liew, and B. L. Yeap, *Turbo Coding, Turbo Equalisation and Space-Time Coding for Transmission over Fading Channels*. John Wiley and Sons, Ltd, 2005.

[74] J. Woodard and L. Hanzo, "Comparative study of turbo decoding techniques: an overview," *Vehicular Technology, IEEE Transactions on*, vol. 49, no. 6, pp. 2208–2233, 2000.

[75] N. Eltayeb, S. Lambotharan, and J. Chambers, "A Phase Feedback Based Extended Space-Time Block Code for Enhancement of Diversity," in *Vehicular Technology Conference, 2007. VTC2007-Spring. IEEE 65th*, pp. 2296–2299, 2007.

[76] C. Toker, S. Lambotharan, and J. Chambers, "Space-time block coding for four transmit antennas with closed loop feedback over frequency selective fading channels," in *Information Theory Workshop, 2003. Proceedings. 2003 IEEE*, pp. 195–198, 2003.

[77] Y. Jing and H. Jafarkhani, "Using Orthogonal and Quasi-Orthogonal Designs in Wireless Relay Networks," *Information Theory, IEEE Transactions on*, vol. 53, no. 11, pp. 4106–4118, 2007.

[78] A. Goldsmith, *Wireless Communications*. Cambridge University Press, 2005.

[79] S. S. Ikki and M. H. Ahmed, "Performance of multiple-relay cooperative diversity systems with best relay selection over rayleigh fading channels," *EURASIP J. Adv. Signal Process*, no. 145, 2008.

[80] K. Tourki and M.-S. Alouini, "Toward distributed relay selection for opportunistic amplify-and-forward transmission," in *Vehicular Technology Conference (VTC Spring), 2011 IEEE*, pp. 1–5, 2011.

[81] S. Ikki, M. Uysal, and M. Ahmed, "Performance analysis of incremental-best-relay amplify-and-forward technique," in *Global Telecommunications Conference, 2009. GLOBECOM 2009. IEEE*, pp. 1–6, 2009.

[82] G. Chen and J. Chambers, "Outage probability in distributed transmission based on best relay pair selection," *Communications, IET*, vol. 6, no. 12, pp. 1829–1836, 2012.

[83] V. Krishnan, *Probability and Random Processes*. Wiley, New Jersey, 2006.

[84] P. Anghel and M. Kaveh, "Exact symbol error probability of a Cooperative network in a Rayleigh-fading environment," *Wireless Communications, IEEE Transactions on*, vol. 3, no. 5, pp. 1416–1421, 2004.

[85] I. Gradshteyn and I. Ryzhik, *Table of Integrals, Series and Products*. New York: Academic Press, sixth ed., 2000.

[86] A. Adinoyi, Y. Fan, H. Yanikomeroglu, H. Poor, and F. Al-Shaalan, "Performance of selection relaying and cooperative diversity," *Wireless Communications, IEEE Transactions on*, vol. 8, no. 12, pp. 5790 –5795, 2009.

[87] M. Eddaghel, U. Mannai, and J. Chambers, "Outage probability analysis of a multi-path cooperative communication scheme based on single relay selection," in *Communications, Computers and Applications (MIC-CCA), 2012 Mosharaka International Conference on*, pp. 107–111, IEEE, 2012.

[88] Y. Jing and H. Jafarkhani, "Single and multiple relay selection schemes and their achievable diversity orders," *Wireless Communications, IEEE Transactions on*, vol. 8, no. 3, pp. 1414–1423, 2009.

[89] S. C. Cripps, *RF power amplifiers for wireless communications*. Artech House, Inc, 2006.

[90] J. Pochmara, R. Mierzwiak, and K. Werner, "A combined adaptive predistortion scheme with input back-off," in *Mixed Design of Integrated Circuits Systems, 2009. MIXDES '09. MIXDES-16th International Conference*, pp. 583–587, 2009.

[91] C. Alexandre and R. Fernandes, "Outage performance of cooperative amplify-and-forward OFDM systems with nonlinear power amplifiers," in *Signal Processing Advances in Wireless Communications (SPAWC), 2012 IEEE 13th International Workshop on*, pp. 459–463, 2012.

[92] M. Eddaghel, U. Mannai, G. Chen, and J. Chambers, "Outage probability analysis of an amplify-and-forward cooperative communication system with multi-path channels and max-min relay selection," *Communications, IET*, vol. 7, no. 5, pp. 408–416, 2013.

[93] X. Li and L. J. Cimini, "Effects of Clipping and Filtering on the Per-

formance of OFDM," *IEEE Commun. Letters*, vol. 2, no. 12, pp. 131–133, 1998.

[94] M. Eddaghel, U. Mannai, and J. Chambers, "Outage Probability Analysis of an AF Cooperative Multi-Relay Network with Best Relay Selection and Clipped OFDM Transmission," in *Wireless Communication Systems (ISWCS 2013), Proceedings of the Tenth International Symposium on*, pp. 1–5, 2013.

[95] G. Chen and J. Chambers, "Exact outage probability analysis for cooperative af relay network with relay selection in presence of inter-cell interference," *Electronics Letters*, vol. 48, pp. 1346–1347, October 2012.

[96] M. K. Simon and M.-S. Alouini, *Digital communication over fading channels*. John Wiley and Sons, Inc., 2005.

[97] M. K. Simon, J. K. Omura, R. A. Scholtz, and B. K. Levitt, *Spread Spectrum Communications Handbook*. The McGraw-Hill Companies, Inc., 2004.

[98] L. Yu, W. Hu, C. Liu, and H. Chen, "Cognitive partners in wireless networks," in *Signal Processing Systems (ICSPS), 2010 2nd International Conference on*, vol. 2, pp. 367–371, 2010.

[99] I. Krikidis, Z. Sun, J. Laneman, and J. Thompson, "Cognitive legacy networks via cooperative diversity," *Communications Letters, IEEE*, vol. 13, no. 2, pp. 106–108, 2009.

[100] B. Fette, *Cognitive Radio Technology*. Elsevier Inc., 2006.